Journal of Oncology

Drug Repurposing in Anticancer Therapy

Lead Guest Editor: Paulo Michel Pinheiro Ferreira
Guest Editors: José Roberto de Oliveira Ferreira, Davi Felipe Farias, Gardenia Carmen Gadelha Militão, and Raffaele Capasso

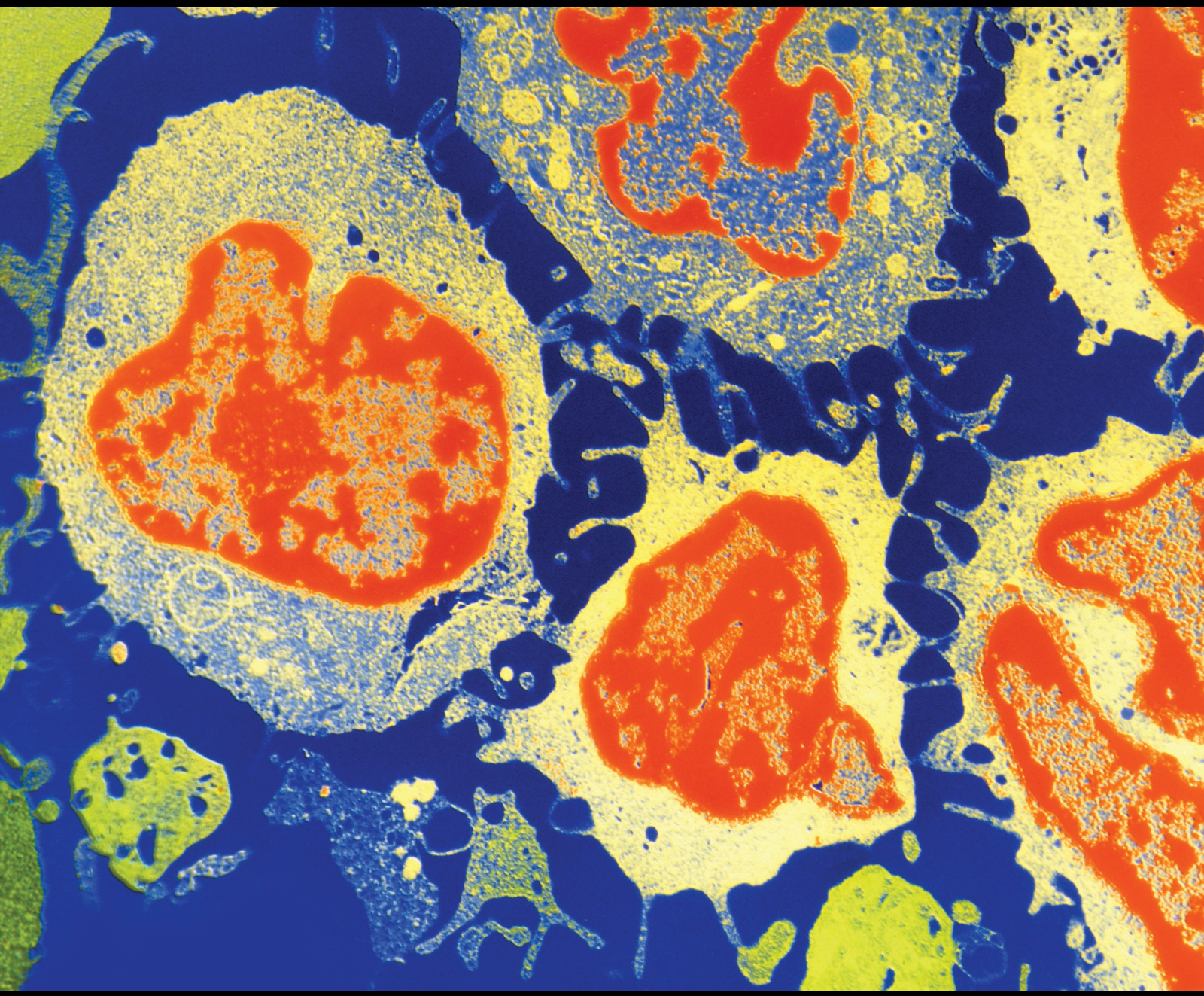

Drug Repurposing in Anticancer Therapy

Journal of Oncology

Drug Repurposing in Anticancer Therapy

Lead Guest Editor: Paulo Michel Pinheiro Ferreira
Guest Editors: José Roberto de Oliveira Ferreira, Davi Felipe Farias, Gardenia Carmen Gadelha Militão, and Raffaele Capasso

Contents

Hindawi
Journal of Oncology
Volume 2021, Article ID 4475192, 15 pages
https://doi.org/10.1155/2021/4475192

Research Article

Low-Dose Albendazole Inhibits Epithelial-Mesenchymal Transition of Melanoma Cells by Enhancing Phosphorylated GSK-3β/Tyr216 Accumulation

Zhiqiang He,[1] **Shun Lei**,[2] **Fucheng Liang**,[1] **Liuchang Tan**,[1] **Weinan Zhang**,[1] **Luoyingzi Xie**,[3] **Hong Zheng**,[4] **and Yuangang Lu**[1]

[1]*Department of Plastic & Cosmetic Surgery, Army Medical Center of PLA, Amy Medical University, Chongqing 400042, China*
[2]*Department of Oncology and Southwest Cancer Center, Southwest Hospital, Army Medical University, Chongqing 400038, China*
[3]*The Institute of Immunology, Army Medical University, Chongqing 400038, China*
[4]*Department of Thoracic Surgery, Xinqiao Hospital, Amy Medical University, Chongqing 400037, China*

Correspondence should be addressed to Hong Zheng; ziecoe@163.com and Yuangang Lu; skin515@163.com

Received 9 August 2021; Accepted 16 November 2021; Published 20 December 2021

Academic Editor: Raffaele Capasso

Albendazole (ABZ) is an effective broad-spectrum anthelmintic agent that has been widely used for humans and animals. Previous studies have reported that ABZ exhibits antitumor effects against melanoma and other different cancer types; however, it is unknown whether ABZ exerts the inhibitory effect against melanoma metastasis. In this study, we aimed to investigate the inhibitory effect of ABZ on melanoma cells. Through in vitro studies, we discovered that low-dose ABZ treatment significantly inhibited the migration and invasion, but not the proliferation, of A375 and B16-F10 cells in a dose-dependent manner. Further analysis revealed that ABZ treatment reduced the expression level of snail family transcriptional repressor 1 (Snail) in the cytoplasm and nucleus by decreasing the levels of phosphorylated AKT (pAKT) Ser473/GSK-3β (pGSK-3β) Ser9 and increasing pGSK-3β/Tyr216, resulting in a significant upregulation of E-cadherin and downregulation of N-cadherin and ultimately reversing the epithelial-mesenchymal transition (EMT) process of melanoma cells. In contrast, the continuous activation of AKT via transfected plasmids elevated the protein levels of pAKT Ser473/pGSK-3β Ser9 and Snail and antagonized the inhibitory action of ABZ. We also confirmed that ABZ treatment effectively inhibited the lung metastasis of melanoma in nude mice in vivo. Subsequent immunohistochemical analysis verified the decreased pAKT Ser473/pGSK-3β Ser9 and increased pGSK-3β/Tyr216 levels in ABZ-treated subcutaneous tumors. Therefore, our findings demonstrate that ABZ treatment can suppress the EMT progress of melanoma by increasing the pGSK-3β/Tyr216-mediated degradation of Snail, which may be used as a potential treatment strategy for metastatic melanoma.

1. Introduction

Melanoma is a highly malignant tumor derived from melanocytes that mostly occurs in the skin but can also be found in the mucous membrane and internal organs. As one of the deadliest skin cancers [1], melanoma incidence continues to increase worldwide [2] at a rate of 3% every year [3]. Furthermore, approximately 230,000 people are diagnosed with primary melanoma worldwide, which causes almost 55,500 deaths annually [4]. Local melanoma can be effectively treated by surgical resection in the early stage, with a five-year survival rate of >90% [5]. In contrast, metastatic melanoma has a poor prognosis, with a five-year survival rate of <10%. Hence, surgical resection is only appropriate for early local melanoma and is almost ineffective after metastases occur [6].

Previous studies have reported that the high mortality rate of malignant melanoma is significantly related to its high metastasis rate [7]. Since melanoma is an epithelial malignant tumor, the epithelial-mesenchymal transition

(EMT) process plays a vital role in melanoma metastasis [8]. EMT is a necessary procedure for normal embryonic development and damage repair [9]; however, it also occurs during malignant tumor progression [10]. The EMT process enables the migration and invasion of epithelial cell-derived malignant tumor cells, which is accompanied by mesenchymal-like changes [11], including loss of cell polarity, decreased intercellular adhesion, and altered expression of cell surface proteins [12]. The abnormal expression of specific markers is a typical feature of the EMT process, such as the upregulation of N-cadherin, snail family transcriptional repressor 1 (Snail), Vimentin, Occludin, and fibronectin 1 (FN1) and the downregulation of E-cadherin [13], which ultimately leads to melanoma metastasis [14]. As an important transcription factor in the EMT process, Snail, which can move into the cell nucleus after phosphorylated at Ser246 and determine the relative expression of downstream N- and E-cadherin proteins [15, 16], is directly regulated by the upstream signaling pathway RAC-alpha serine/threonine-protein kinase (AKT)/Glycogen synthase kinase-3 beta (GSK-3β) during tumor progression [17, 18]. GSK-3β/Tyr216 (active form) can mediate nucleus export and degradation of Snail, while GSK-3β/Ser9 (inactive form) phosphorylated by pAKT can maintain its stability. Therefore, the change in the ratio of Tyr216/Ser9 could be very important for the level of Snail and the ability of tumor cells to invade and metastasize [16, 18, 19]. Although recent advances have been made in cancer medicine, immunotherapy, and targeted drug discovery, the rapid occurrence of drug resistance in cancer patients usually leads to disease recurrence [20]. At present, there is no long-term and effective treatment method for melanoma metastasis. Therefore, identifying the potential inhibitors for EMT is required for the suppression of tumor progression and the development of therapeutic interventions for melanoma [8].

Recently, drug repositioning has become an increasingly attractive option for medical treatments due to the pharmacokinetics and safety of existing drugs, which can reduce the difficulty and risk of clinical trials to a certain extent [21, 22]; in addition, this strategy has economic advantages compared to complete new drug development [23]. One example is albendazole (ABZ), a kind of benzimidazole derivative and antiparasitic drug with known antitumor properties that can be repositioned as an anticancer drug [22, 24]. Despite preexisting researches regarding that ABZ may have an antimelanoma effect by inhibiting proliferation [25] or promoting apoptosis [26], it is still unknown whether ABZ can also exhibit inhibitory effects against the metastasis of melanoma. In this study, we aimed to determine the effects of ABZ treatment on the migration and invasion of A375 and B16-F10 melanoma cells during EMT and to identify associated signaling pathways and potential targets for future studies.

2. Materials and Methods

2.1. Cell Lines and Culture. The A375 human melanoma and B16-F10 mouse melanoma cell lines were obtained from American Type Culture Collection (ATCC; Manassas, VA, USA), while B16-F10-luciferase (B16-F10-luc) cells were purchased from Shanghai Model Organisms Center (Shanghai, China). The A375 and B16-F10-luc cells were cultured in Dulbecco's modified Eagle's medium-high glucose (SH30243.01, HyClone, Logan, UT, USA) containing 10% fetal bovine serum (FBS; SH30084.03, HyClone), 1% penicillin/1% streptomycin (P1400, Solarbio, Beijing, China), 1% L-glutamine (G0200, Solarbio), and 1% nonessential amino acid (N1250, Solarbio). The cells were cultured in an incubator at 37°C with 5% CO_2 (Forma 3111, Thermo Fisher Scientific, Waltham, MA, USA).

2.2. Plasmid Construction. The human AKT1 coding sequence was amplified and cloned into pcDNA3.1 (+) plasmids. The constitutively active AKT plasmid (CA-AKT; T308D/S473D) was obtained by mutating the wild-type human AKT1 using QuikChange® Site-Directed Mutagenesis Kit (Stratagene, La Jolla, CA, USA) and then validated by sequencing. Endotoxin-free CA-AKT plasmids (used for transfection) were extracted using Endo-Free Plasmid Midi Kit-fast (Omega Bio-tek, Norcross, GA, USA). GSK-3β/Tyr216 wild-type (WT) and GSK-3β Y216F mutant pLenti plasmid which encodes WT or Y216F cDNA were purchased from Obio Technology Co. Ltd (Shanghai, China). VSV-G plasmid pMD2.G and psPAX2 packaging plasmids were gifts from Prof. Wenyue Xu (Army Medical University).

2.3. Cell Transfection and Transduction. The A375 and B16-F10 melanoma cells with approximately 80% confluency were selected for transfection. Opti-MEM™ medium (Gibco, Thermo Fisher Scientific Waltham, MA, USA) was used to dilute the Lipofectamine™ 3000 reagent (L3000008, Thermo Fisher Scientific, Waltham, MA, USA) and plasmid master mix containing plasmids and P3000™ reagent, which were subsequently mixed according to the manufacturer's instructions and added to the cell culture medium. HEK293T cells (donated by the Laboratory of Thoracic Surgery, Xinqiao Hospital, Army Medical University) were transfected with the GSK-3β wild-type (WT) or GSK-3β Y216F pLenti plasmid combined with pMD2.G and psPAX2 plasmids for collecting the lentiviruses by using Lipofectamine 3000 (L3000008, Thermo Fisher Scientific, Waltham, MA, USA) according to the manufacturer's instructions. GSK-3β wild-type A375 melanoma cells and GSK-3β/Y216F A375 melanoma cells were generated by using lentiviral transduction and by selection in presence of blasticidin (5ug/ml) (ant-bl-05, InvivoGen, San Diego, USA).

2.4. Cell Viability and Proliferation Assay. ABZ (HY-B0223, MCE, Monmouth Junction, NJ, USA) was dissolved in dimethyl sulfoxide (DMSO; final concentration <0.1%) to a final concentration of 10 mmol/L and stored for subsequent use. The cell counting kit-8 (CCK-8; C0037, Beyotime, Shanghai, China) assay was used to analyze cell viability and proliferation. Melanoma cells in the logarithmic growth phase (5×10^3 cells) were seeded and cultured in 96-well plates containing 100 μL medium. The experimental groups

were treated with DMSO and ABZ at different concentrations (0.1, 0.2, 0.4, 0.8, 1.6, 3.2, 6.4, and 12.8 μM), while the blank groups were untreated. After 24 h, 10 μL CCK-8 reagent was added to each well, and the plates were incubated at 37°C for 2 h. The absorbance values were subsequently measured at 490 nm using a microplate reader (Beckman Coulter, Brea, CA, USA).

2.5. Wound Healing Assay. A wound-healing test was used to detect the effect of ABZ treatment on the migration of melanoma cells. The A375 and B16-F10 cells were inoculated in 6-well plates with a culture medium containing 10% FBS. After the cell coverage reached 95%, a T-1000-B pipette tip was used to scratch a wound on the cells. Then, the plate was washed twice with phosphate-buffered saline (PBS; ZLI-9061, ZSGB-Bio, Beijing, China) to remove the floating cells, and cell images were randomly taken using an inverted microscope (Leica inverted microscope DMi8, Wetzlar, Germany). Finally, the cells were treated with ABZ at different concentrations (0.1, 0.2, and 0.4 μM) for 24 h, and cell images were obtained again using the same microscope. ImageJ software (NIH, Bethesda, MD, USA) was used to quantify the wound healing area on the cell images.

2.6. Transwell Invasion Assay. The bottom of the transwells with 8 μm pores (662638, Greiner Bio-One, Frickenhausen, Germany) was precoated with Matrigel (356234, Corning, Bedford, MA, USA). The A375 and B16-F10 cells were starved using a medium without FBS for 12 h. The cells (6×10^4 per well) were inoculated into a serum-free medium containing different concentrations of ABZ (0.1, 0.2, and 0.4 μM) and allowed to invade through the 8 μm pores into the lower chambers containing medium with 10% FBS. After 24 h, the transwells were fixed with 4% paraformaldehyde (P0099, Beyotime) for 20 min and stained with 0.1% crystal violet (HY-B0324A, MCE) for another 20 min. Images of five randomly selected positions were obtained by using Leica inverted microscope DMi8 and analyzed using ImageJ software (NIH) to determine the number of cells that invaded the lower chambers.

2.7. Western Blotting. A375 and B16F10 cells were treated with 0.4 μM ABZ alone for 24 h or per-transfected with CA-AKT or pcDNA3.1 (+) plasmids and treated with ABZ for 24 h; for proteinase inhibiting, A375 cells were cotreated with ABZ and 10 μM MG132 for 24 h; GSK-3β/WT and GSK-3β/Y216F stable expressing A375 cells were treated with 0.4 μM ABZ alone for 24 h. Then, these cells were lysed in RIPA buffer (89900, Thermo Fisher Scientific, Waltham, MA, USA) to extract the total protein. Nuclear and cytoplasmic proteins were extracted separately using NE-PER™ Nuclear and Cytoplasmic Extraction Reagents (78833, Thermo Fisher Scientific, Waltham, MA, USA) and quantified using BCA Protein Detection Kit (P0012s, Beyotime). The protein samples were resolved by 10% sodium dodecyl sulfate-polyacrylamide gel electrophoresis (1610183, Bio-Rad Laboratories, Hercules, CA, USA) and then transferred to polyvinylidene fluoride (PVDF; IPFL00010, Merck KGaA, Darmstadt, Germany) membranes using electroporation fluid. The membranes were blocked with No protein blocking solution (C510042-0500, Sangon Biotech, Shanghai, China) for 1 h at 25°C. After washing thrice with Tris-buffered saline with Tween®20 (TBST; B548105-0500, Sangon Biotech), the blocked PVDF membranes were cut into appropriate shapes, incubated with the primary antibodies, and kept in a shaker overnight at 4°C. The primary antibodies, namely, anti-phospho-AKT (Ser473) rabbit antibody (44-623G), anti-AKT (44-609G), anti-N-cadherin (13-2100), anti-E-cadherin (14-3249-82), anti-Snail (14-9859-82), anti-Vimentin (MA5-16409), anti-Occludin (33-1500), anti-FN1 (PA5-29578), β-actin (MA5-15452), anti-GSK3B (phospho-Tyr216) rabbit antibody (44-604G), anti-GSK3B (phospho-Ser9) rabbit antibody (MA5-38235), anti-GSK-3β rabbit antibody (PA5-95845), anti-SNAI1 (phospho-Ser246) rabbit antibody (PA5-37739), and proliferating cell nuclear antigen (PCNA; PA5-27214), were purchased from Thermo Fisher Scientific. Subsequently, the PVDF membranes were incubated with the corresponding secondary antibodies (ZB-2306, ZSGB-Bio) for 1 h. After washing thrice with TBST, the protein samples were visualized using Fusion Solo S Chemiluminescence Imaging System (VILBER, Collégien, France). The obtained western blot data were analyzed using ImageJ software (NIH).

2.8. Real-Time Reverse Transcription Quantitative PCR (RT-qPCR). Total RNA was extracted from melanoma cells using TRIzol® reagent (15596026, Thermo Fisher Scientific, Waltham, MA, USA) and reverse-transcribed into cDNA using PrimeScript RT reagent Kit with gDNA Eraser (RR047A, Takara, Kyoto, Japan), according to the manufacturer's instructions. Real-time RT-qPCR analysis was performed to investigate the differences in the mRNA expression of EMT-related genes before and after ABZ treatment. The PCR reaction cocktail (25 μL) contained 0.5 μL each of forward and reverse primers, 12.5 μL SYBR® Pre-mix Ex Taq TM II (RR820A, Takara), 10.5 μL double-distilled water, and 1 μL cDNA. The PCR cycling conditions were as follows: 95°C for 15 s, 60°C for 30 s, and amplification for 40 cycles. Each experiment was performed thrice. The relative expression levels were calculated using the $2^{-\Delta\Delta Ct}$ method, with β-actin as the internal control for normalization. The primers used for E-cadherin, N-cadherin, snail, Vimentin, Occludin, FN1, and β-actin are listed in Supplementary Table 1.

2.9. Animal Experiments. The nude mice (4 weeks old) used for animal experiments were obtained from the Animal Experiment Center of the Army Medical Center of PLA (Chongqing, China) and maintained in the SPF animal house. All studies were conducted in accordance with the experimental protocol approved by the Ethical Review of Experimental Animals of the Army Medical Center of PLA. First, B16-F10-luc cells (5×10^5) were injected through the caudal vein. Second, after 1 week, the mice were anesthetized and injected with Xenolight™ D-Luciferin Potassium Salt

(Perkin Elmer, Boston, MA, USA), 5 min later, they were put on the imaging plate, the exposure time was 20 s, and the unit of measurement is photon flux, and in vivo fluorescence images were obtained using IVIS Lumina III Imaging System (Perkin Elmer). Third, after confirming that the tumor model was successfully constructed, the mice were randomly divided into three groups, namely, 50 mg/kg, 20 mg/kg ABZ, and control, the experimental groups used PBS with different concentrations of ABZ (containing 0.5% sodium carboxymethyl cellulose + 2% DMSO), and the control groups used PBS (containing 0.5% sodium carboxymethyl cellulose + 2% DMSO), the dosage was 100 μL, and they were treated once daily via intragastric administration. Fourth, after continuous intragastric gavage for 10 days, in vivo fluorescence images were obtained again using the same method. Finally, the mice were dissected, and the lungs were taken out and washed with PBS. The melanoma nodules on the lung surfaces were counted and fixed with 4% paraformaldehyde.

2.10. Hematoxylin-Eosin (HE) Staining. Following conventional methods, the lung tissue was embedded in paraffin and cut into 4 μm sections for HE staining. The sections were stained with hematoxylin staining solution for 3 min, washed with distilled water for 15 s, and stained with 1% hydrochloric acid and ethanol for 15 s. After washing with distilled water for 1 min, the sections were stained with eosin for 50 s and washed again with distilled water for 15 s. The sections were dehydrated by gradient ethanol, soaked in xylene, and finally sealed with neutral balsam.

2.11. Immunohistochemistry (IHC) Assay and Scoring. IHC detection of key EMT proteins was performed using the Dako Envision FLEX + system (Dako, Berlin, Germany). Paraffin sections were deparaffinized. Antigen retrieval was performed by heating the samples in citrate buffer (pH 6.0) in the microwave for 15 min, then returning the samples to room temperature, followed by washing with phosphate-buffered saline (PBS). The samples were blocked with the Dako REAL Peroxidase-Blocking Solution for 15 min. The slides were incubated at 4°C overnight with the rabbit antibodies for anti-N-cadherin, Rabbit ant-E-cadherin, anti-phospho-AKT (Ser473), anti-GSK3B (phospho-Tyr216), and anti-GSK3B (phospho-Ser9), followed by incubation (30 min) with the secondary antibody. Slides were stained with 3,3′-diaminobenzidine tetrahydrochloride (DAB) for 2 min. The percentages of cells that were positive for the markers were scored as follows: 0–5%, no positive cells; 1, <25% positive cells; 2, 25–50% positive cells; 3, 50–75% positive cells; 4, 75–100% positive cells. The staining intensity was scored as follows: 0, no positive cells; 1, weak staining; 2, moderate staining; and 3, strong staining. The immunohistochemical staining score was obtained by multiplying the percentage score by the intensity (0, 1, 2, 3, 4, 6, 8, 9, or 12). The X-tile v3.6.1 statistical package [27] was used to analyze the IHC assay results.

2.12. Statistical Analysis. The data were expressed as means ± standard deviation (SD) of three independent experiments. One-way ANOVA was used for comparison of two groups if the data were normally distributed, and if not, the Mann–Whitney *U* test was used. The Tukey-Kramer statistic was used for multiple comparisons in normally distributed; if not, Dunnett's test was used. Statistical Analysis was performed by using SPSS 25.0 statistical software (IBM SPSS).

3. Results

3.1. Low-Dose ABZ Treatment Significantly Inhibits the Migration and Invasion of Melanoma Cells In Vitro. ABZ is a benzimidazole carbamate drug (Figure 1(a)). To determine the effect of ABZ on the migration and invasion abilities of melanoma cells, we performed CCK-8 assays on melanoma cells treated with ABZ at different concentrations and discovered that low-dose ABZ (<0.4 μM/L) treatment had no significant effect on the proliferation of A375 and B16-F10 cells (Figures 1(b) and 1(c)). However, the wound healing assays showed that low-dose ABZ treatment for 24 h significantly inhibited the migration of both A375 (Figure 1(d)) and B16-F10 (Figure 1(e)) cells in a dose-dependent manner. Furthermore, the Matrigel invasion assay revealed that low-dose ABZ treatment markedly suppressed the invasion abilities of the two melanoma cell lines in a dose-dependent manner (Figures 1(f)–1(g)). These findings suggest that low-dose ABZ can significantly inhibit the migration and invasion, but not the proliferation, of melanoma cells in vitro.

3.2. Low-Dose ABZ Treatment Suppresses the Lung Metastasis of Melanoma Cells In Vivo. Since the in vitro experiments demonstrated the inhibitory effects of low-dose ABZ on the migration and invasion of melanoma cells, we then investigated the effects of ABZ treatment on melanoma cells in vivo using a nude mouse model of lung metastasis. After 10 days of continuous intragastric administration of 20 and 50 mg/kg ABZ, which were much lower than the doses used for subcutaneous tumors [28], the in vivo fluorescence images showed that the fluorescence intensity of lung metastatic specimens from ABZ-treated mice was significantly lower than that of the control group (Figures 2(a) and 2(b)), suggesting that the lung metastasis of melanoma cells in the ABZ-treated group was greatly suppressed. In addition, the lung melanoma nodules in the ABZ treatment group were smaller and less tumors formed on the lungs (Figure 2(c)). Moreover, after the number and size of melanoma nodules were counted and scored, the nodule scores in ABZ-treated mice were discovered to be significantly lower than those in control mice (Figure 2(d)), which was confirmed by the HE staining of mice lung sections (Figure 2(e)). These results indicate that, in a dose-dependent manner, ABZ-treated mice had a significantly lower lung metastatic rate than normal. Taken together, our results demonstrate that low-dose ABZ can markedly inhibit the metastasis and invasion of melanoma cells both in vitro and in vivo.

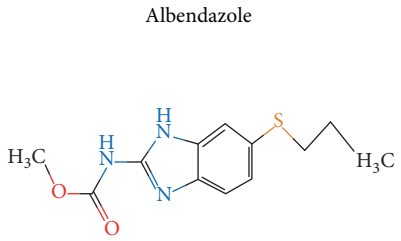

(a)

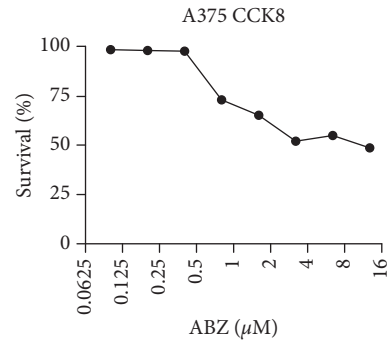

(b)

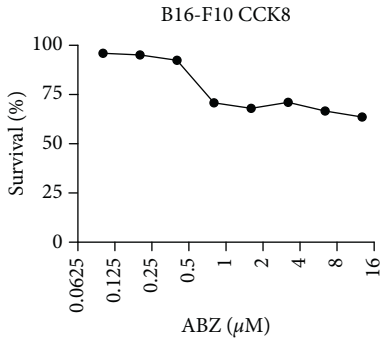

(c)

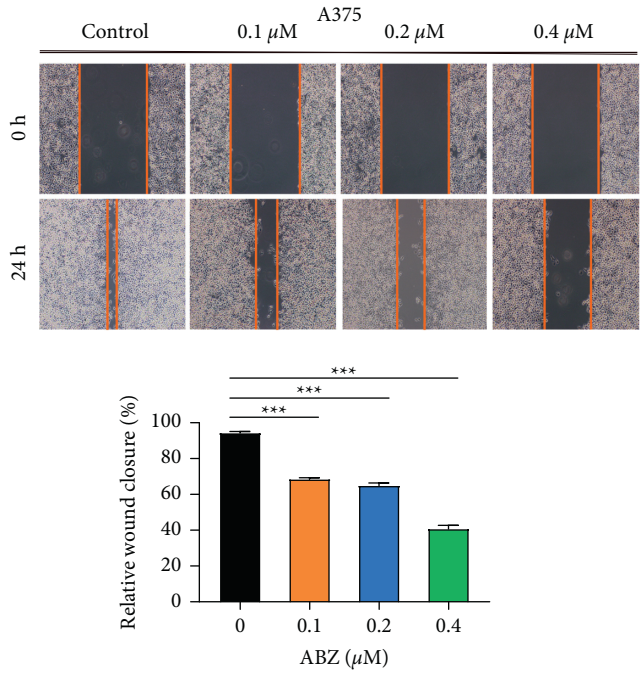

(d)

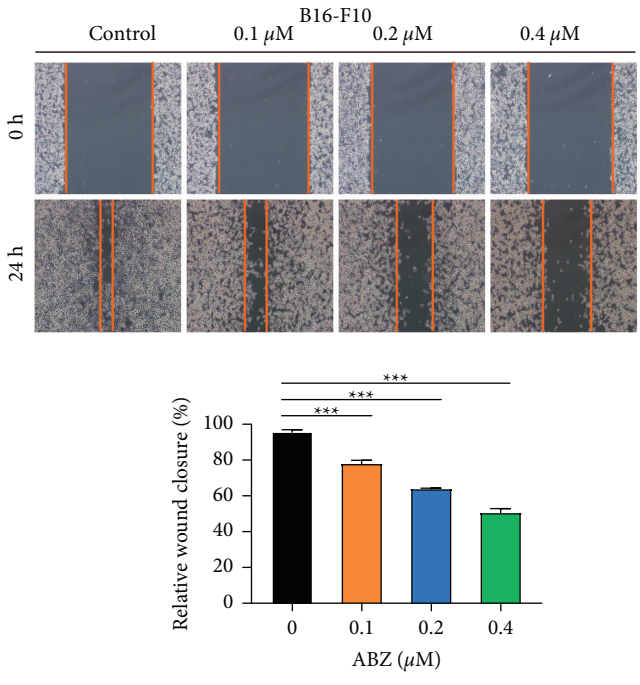

(e)

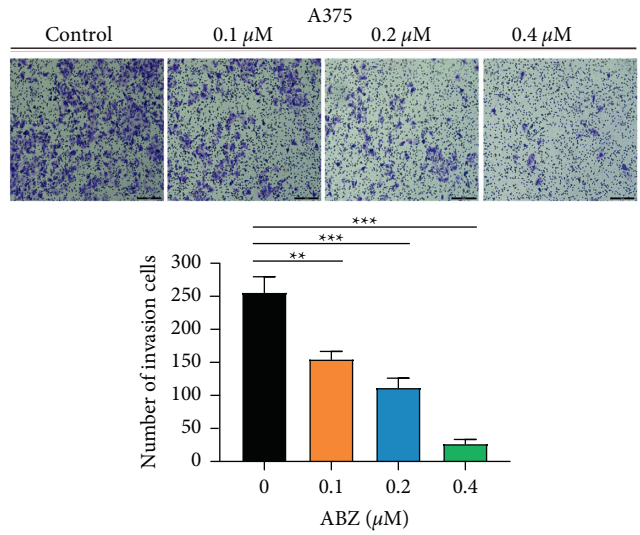

(f)

Figure 1: Continued.

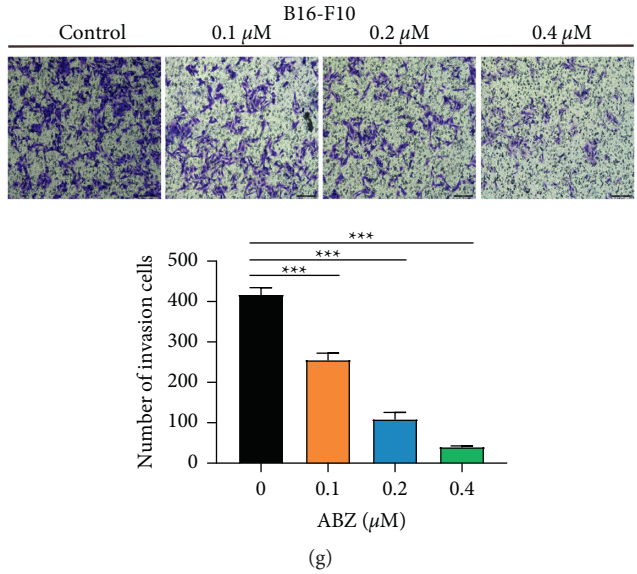

(g)

Figure 1: Low-dose albendazole (ABZ) treatment effectively inhibits the migration and invasion of melanoma cells. (a) The chemical structure of ABZ. (b-c) The A375 and B16-F10 cells were treated with or without different concentrations of ABZ. CCK-8 analysis was performed to detect cell viability and proliferation. (d–e) The A375 and B16-F10 cells were treated with different concentrations of ABZ (0.1, 0.2, and 0.4 μM). The wound healing area and relative wound closure rate (%) in melanoma cells were measured and analyzed 24 h after treatment. (f-g) The inhibitory effect of ABZ on the invasion of A375 and B16-F10 cells was detected using transwell experiments. The data are expressed as means ± SD. All experiments were performed thrice. $^{**}P < 0.01$; $^{***}P < 0.001$.

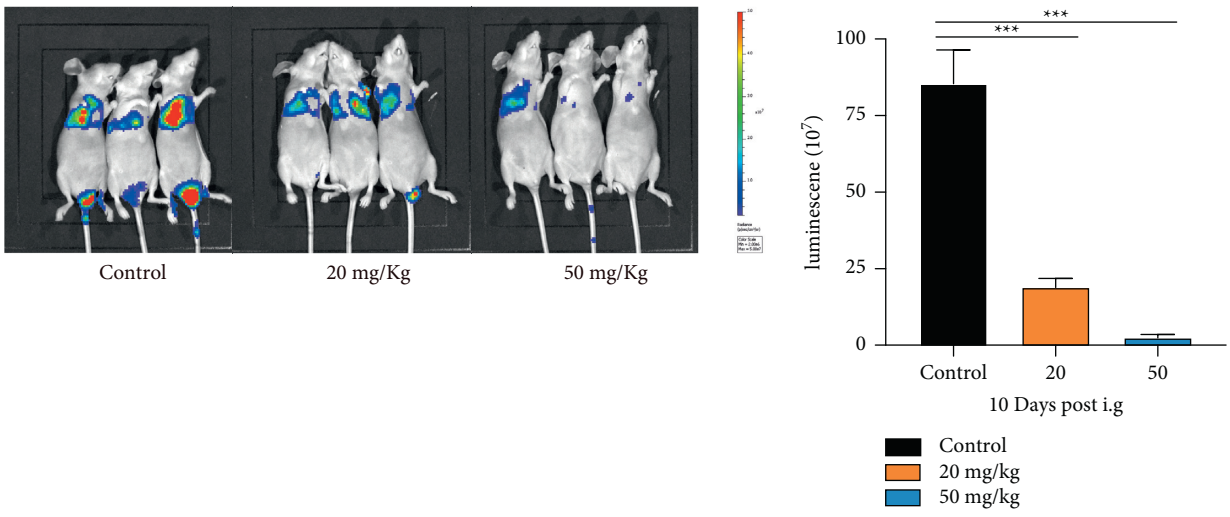

(a) (b)

Figure 2: Continued.

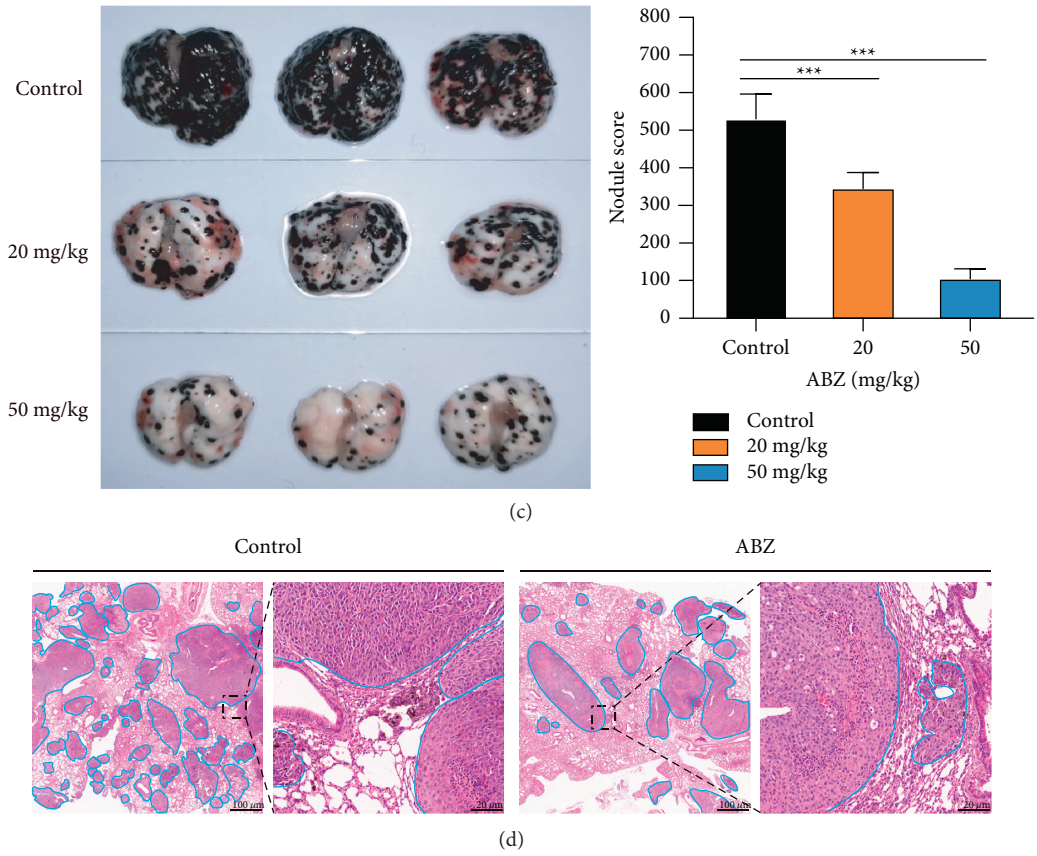

Figure 2: ABZ treatment suppresses lung melanoma metastasis in mice. (a) Representative image and (b) statistical analysis of luminescence intensity in B16-F10-luc tumor-bearing nude mice treated with different concentrations of ABZ ($n = 5$). (c) The upper, middle, and lower panels represent the melanoma nodules on the lung surfaces of mice in the control, 20 mg/kg ABZ, and 50 mg/kg ABZ groups, respectively. (d) Scores of the melanoma nodules in each experimental group. The scoring criteria for tumor nodule diameter were as follows: Level 1: <0.5 mm; Level 2: >0.5 mm, <1.0 mm; Level 3: >1.0 mm, <2.0 mm; and Level 4: >2 mm. (e) Representative images of HE stained mice lung sections from the control and ABZ-treated groups. The circled parts show the lung metastatic nodules. All animal experiments were repeated thrice. $^{***}P < 0.001$.

3.3. ABZ Inhibits the Metastasis of Melanoma Cells by Reversing the EMT Process. Since the EMT process was believed to be responsible for the metastasis and recurrence of melanoma, we also investigated the effects of ABZ treatment on the EMT process of melanoma cells. The mRNA levels of key EMT proteins, namely, N-cad, E-cad, Vimentin, Occludin, and FN1, were detected by real-time RT-qPCR analysis 24 h after ABZ treatment. Compared to the control group, *E-cad* expression was significantly upregulated in the ABZ-treated group, while the relative expression levels of N-cad, Vimentin, FN1, and Occludin were downregulated to varying degrees (Figures 3(a) and 3(b)). Furthermore, these changes were confirmed at the protein level by western blot analysis (Figures 3(c) and 3(d)). To determine the effects of ABZ on the expression of EMT-related proteins in vivo, we also analyzed the E-cad and N-cad levels in the lung sections from ABZ-treated and control mice. The IHC assay results revealed that E-cad and N-cad expression levels in the B16-F10 metastatic foci of ABZ-treated mice lung sections were significantly upregulated and downregulated, respectively, compared to the control mice (Figure 3(e)). These findings suggest that ABZ can inhibit the metastasis of melanoma cells by reversing the EMT process.

3.4. ABZ Downregulates the Snail Expression in Melanoma Cells by Increasing Phosphorylated GSK-3β/Tyr216 Accumulation. To elucidate the molecular mechanism underlying the ABZ-mediated inhibition of the EMT process, we further investigated the expression and distribution of Snail, the main transcription factor that regulates the expression of EMT markers. The qPCR results showed that the relative expression level of Snail was not significantly altered in A375 and B16-F10 cells after ABZ treatment for 24 h (Figure 4(a)). However, ABZ treatment significantly decreased the protein levels of Snail in the cytoplasm of melanoma cells by western blot analysis (Figure 4(b)). These results suggest that ABZ potentially regulates Snail via posttranscriptional rather than translational modification. Since Snail is required to enter the nucleus to initiate transcriptional activity, we subsequently detected the level of Snail in the nucleus after ABZ treatment. As expected, ABZ treatment also reduced the levels of phosphorylated Snail/Ser 246 (pSnail/Ser246) in the nuclei of melanoma cells (Figures 4(c) and 4(d)). We also investigated the phosphorylation levels of GSK-3β, which negatively regulates Snail, and its upstream activator AKT [29]. Interestingly,

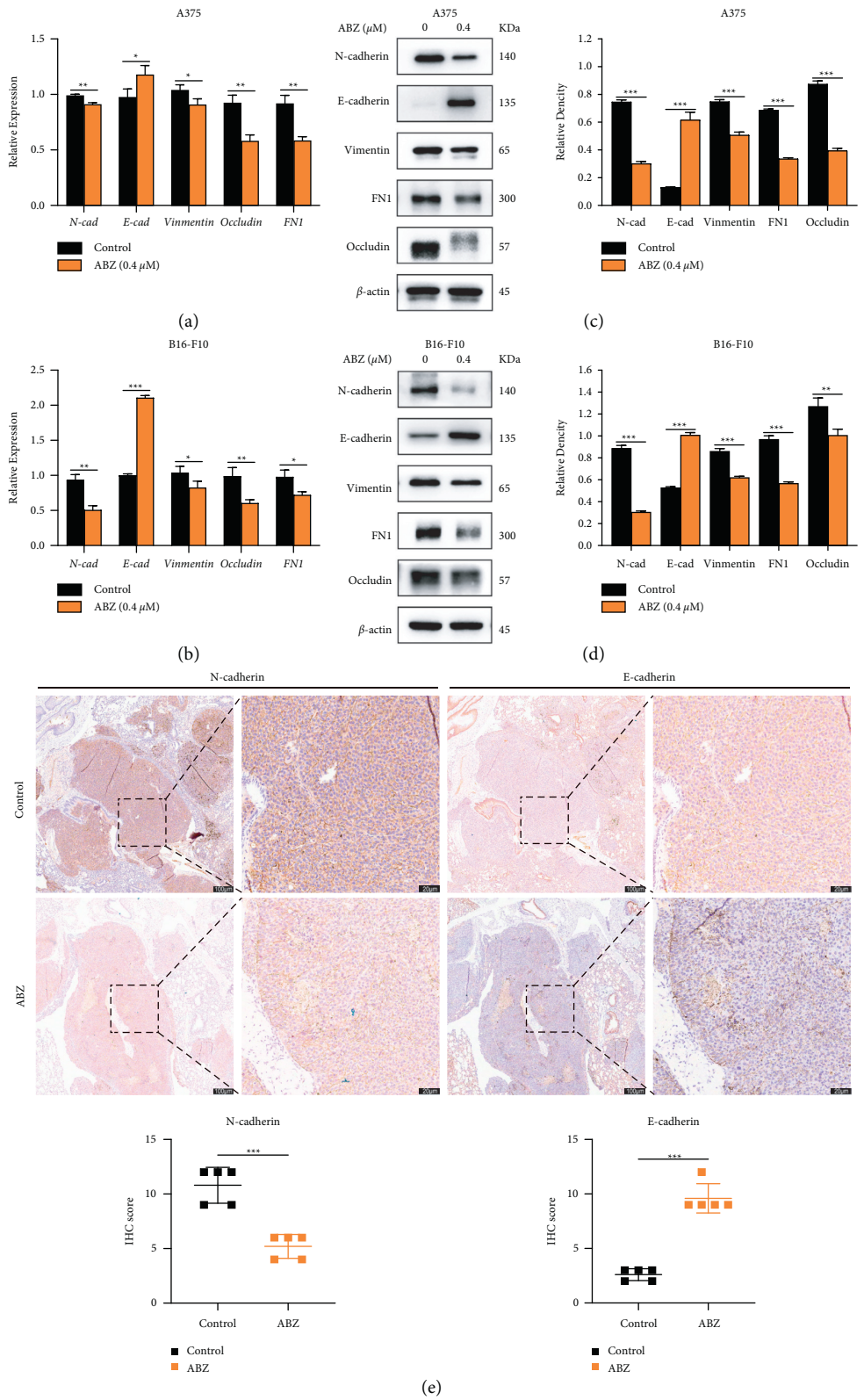

Figure 3: ABZ treatment inhibits the metastasis of melanoma cells by reversing the EMT process. (a-b) The relative expression levels of N-cadherin, E-cadherin, Vimentin, Occludin, and FN1 between the ABZ-treated (0.4 μM) and control groups were measured by RT-qPCR, with β-actin as the reference gene. (c-d) The expression levels of key EMT proteins were detected by western blotting. The histogram shows the relative density of N-cad, E-cad, Vimentin, Occludin, and FN1. (e) The localization and expression levels of N-cad and E-cad in mouse lung cancer tissues were determined using an immunohistochemical (IHC) assay. Image showing the IHC staining specimens (100×; left). The black dotted box is enlarged to the area corresponding to the image (right). Scale bars = 100 and 20 μm. Each point in each group in the statistical graph is calculated as the average score for five selected areas in one lung slice and represents an IHC index of one mouse. The data are expressed as means ± SD. The RT-qPCR and western blot experiments were performed thrice. $^{*}P < 0.05$; $^{**}P < 0.01$; $^{***}P < 0.001$.

ABZ treatment significantly reduced the levels of pGSK-3β/Ser9 (inactive form) and pAKT/Ser473 but greatly enhanced the accumulation of pGSK-3β/Tyr216 (active form) in the cytoplasm of melanoma cells (Figures 4(c) and 4(d)), and the increased ratio of Tyr216/Ser9 indicated ABZ treatment could activate GSK3β kinase (Supplementary Figure 1). To further confirm whether ABZ-mediated increase of pGSK-3β/Tyr216 could promote degradation of Snail protein in melanoma cells, MG132 was used to inhibit proteasome. Western blot analysis showed that MG132 did not affect the protein level of AKT and pGSK-3β/Tyr216 but significantly inhibited the degradation of Snail after ABZ treatment and subsequently resulted in the upregulation of the downstream target gene N-cadherin expression and the downregulation of E-cadherin expression (Figure 4(e)). Furthermore, the IHC results of the B16-F10 metastatic foci in mice lung sections revealed the decreased expression of pGSK-3β/Ser9 and pAKT/Ser473 and increased expression of pGSK-3β/Tyr216 in the ABZ-treated group (Figure 4(f)). Collectively, these findings indicate that ABZ can promote the nuclear export and cytoplasmic degradation of Snail by activating pGSK-3β/Tyr216 and inhibiting pGSK-3β/Ser9, resulting in the suppression of EMT progress in melanoma cells.

3.5. CA-AKT Significantly Reverses the Inhibitory Effects of ABZ on the Migration and Invasion of Melanoma Cells. To determine the relationship between the AKT/GSK-3β signaling pathway and ABZ-mediated reversal of the EMT process, we transiently transfected A375 and B16-F10 cells with the CA-AKT plasmid or pcDNA3.1 (+) plasmid. Western blot analysis demonstrated that the transfection of CA-AKT elevated the protein level of pAKT/Ser473, resulting in increased pGSK-3β/Ser9 expression and decreased pGSK-3β/Tyr216 expression (Figures 5(a) and 5(b)). In contrast, CA-AKT transfection significantly reversed the ABZ-mediated downregulation of Snail in the cytoplasm, which restored the EMT progress in melanoma cells (Figures 5(a) and 5(b)). Furthermore, subsequent wound healing (Figures 5(c) and 5(d)) and transwell invasion experiments (Figures 5(e) and 5(f)) revealed that CA-AKT transfection significantly reversed the inhibitory effect of ABZ treatment on the migration and invasion of melanoma cells. These findings confirm that ABZ can suppress the EMT of melanoma cells by enhancing the pGSK-3β/Tyr216-mediated degradation of Snail.

3.6. Overexpression of GSK-3β/Y216F Could Not Promote the Degradation of Snail after ABZ Treatment. We have demonstrated through previous experiments that ABZ can promote Snail's nuclear export and cytoplasmic degradation by inhibiting pGSK-3β/Ser9, thereby inhibiting the progression of EMT in melanoma cells. However, our study also revealed that ABZ enhanced the accumulation of pGSK-3β/Tyr216 (active form) in the cytoplasm of melanoma cells. In order to further clarify the functional role of pGSK-3β/Tyr216, stable A375 cell expressing wild-type GSK-3β (GSK-3β/WT) and GSK-3β/Y216 phenylalanine (F) mutation (GSK-3β/Y216F) were constructed as previous report [30]. After ABZ treatment for 24 h, the protein levels of the phosphorylation levels of GSK-3β/Tyr216 in the cytoplasm of all three cells were significantly increased compared with the DMSO group. Compared with ABZ-treated control cells, ABZ treatment could facilitate more GSK-3β phosphorylation at Tyr216 after overexpression of GSK-3β/WT, but not in GSK-3β/Y216F overexpressing cells. Meanwhile, we next detected the expression of Snail, N-cadherin, and E-cadherin proteins in three groups after ABZ treatment; as we expected, GSK-3β/Y216F overexpression did not change the protein levels of Snail, N-cadherin, and E-cadherin compared with ABZ-treated control cells. Furthermore, subsequent wound healing (Figure 6(b)) and transwell invasion experiments (Figure 6(c)) demonstrated that the ABZ-mediated inhibitory effect on invasion and migration of A375 cells became more pronounced in GSK-3β/WT overexpression cells; however, GSK-3β/Y216F overexpression cannot improve this effect. These results confirmed the critical role of pGSK-3β/Tyr216 in the EMT process of melanoma cells, suggesting that upregulation of pGSK-3β/Tyr216 inhibits the EMT process of melanoma cells. It was also proved that ABZ can promote the nuclear output and cytoplasmic degradation of Snail by increasing the accumulation of pGSK-3β/Tyr216, thus inhibiting the EMT process of melanoma cells.

4. Discussion

Melanoma is one of the most dangerous skin cancers responsible for >90% of patient mortality [31], especially after metastases occur, which results in the rapidly shortened survival period and very poor prognosis of melanoma patients [32]. Therefore, inhibiting metastasis progression is the main focus of melanoma treatment [31]. There is increasing evidence that benzimidazole can be used as a source of antitumor agents as a repositioned drug for cancer therapeutics [22]. As the most well-studied antiparasitic agent, ABZ has already been validated in a few tumor models [22]. However, no reports are available regarding the effect of ABZ on the EMT process of melanoma. In the present study, our results showed that low-dose ABZ treatment significantly downregulated the expression of N-cadherin, Vimentin, Occludin, and FN1 and upregulated E-cadherin expression, indicating that low-dose ABZ can effectively reverse the EMT process of melanoma cells both in vivo and in vitro.

Previous studies revealed that ABZ promotes the excessive production of reactive oxygen species in tumor cells [24], leading to high oxidative stress, Bax activation, and cell apoptosis [33] and thereby inhibiting the proliferation of tumor cells [34]. Moreover, ABZ inhibits the migration capability of pancreatic cancer cells [28] and HIF-1α-dependent glycolysis in lung cancer cells [35]. Interestingly, the dose of ABZ used in previous in vivo experiments was very high (e.g., 300 mg/kg twice daily [28]), which raised concerns about potential cell toxicity and adverse side effects. In this study, our findings revealed that 20 mg/kg ABZ (orally once daily) remarkably reduced the number of metastatic foci of melanoma cells in the lungs, suggesting that low-dose

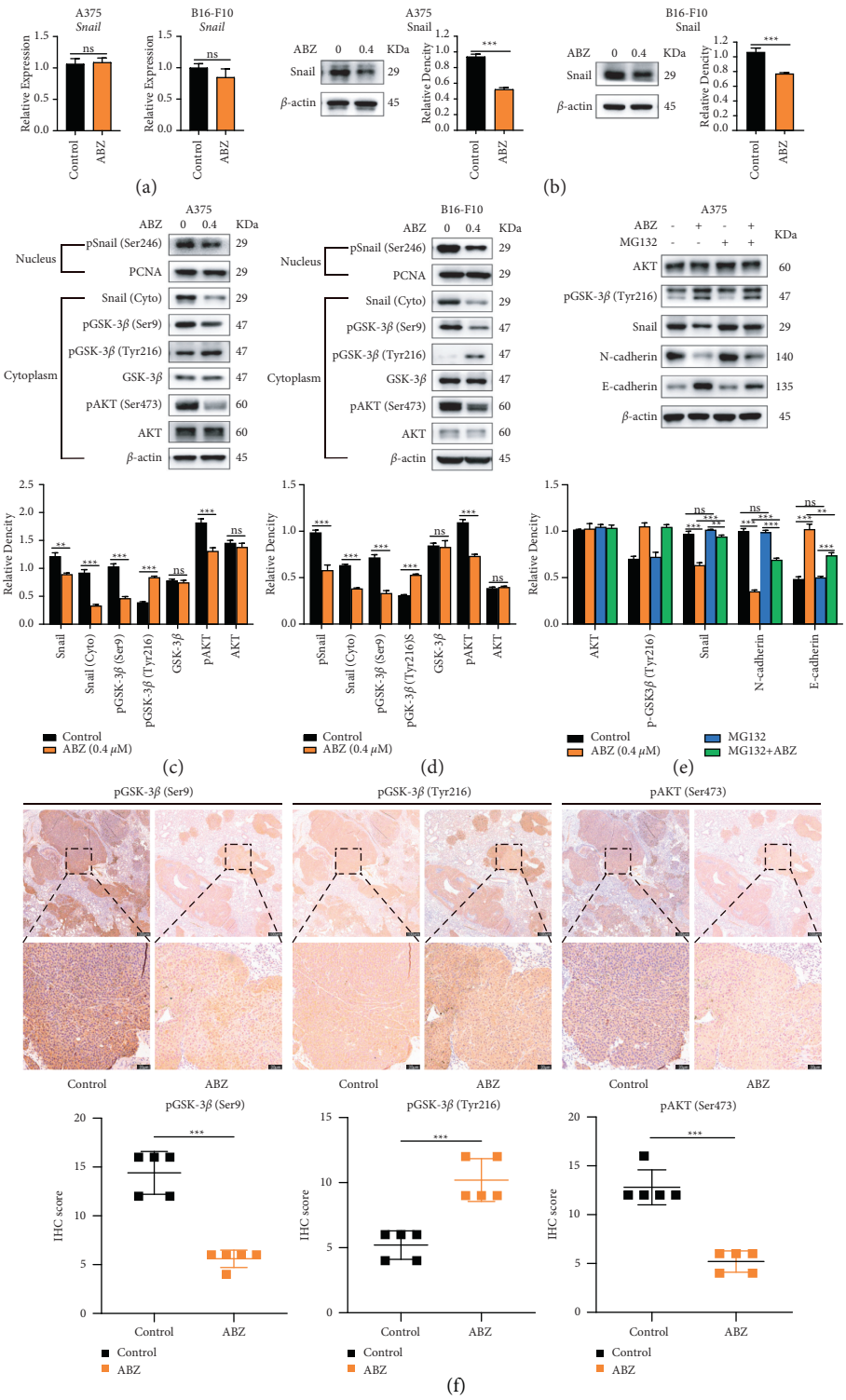

Figure 4: ABZ treatment downregulates the snail expression in melanoma cells by increasing the accumulation of phosphorylated GSK-3β/Tyr216. (a) The relative transcription levels of Snail in the ABZ-treated (0.4 μM) and control groups of A375 (left) and B16-F10 (right) melanoma cells were measured by RT-qPCR, with β-actin as the internal control. (b) The expression of transcription factor Snail in A375 (left) and B16-F10 (right) cells was detected by western blot analysis, with β-actin as the internal reference protein. (c–d) The expression levels of cytoplasmic proteins AKT, pAKT, GSK-3β, pGSK-3β (Ser9/Tyr216) and Snail, and nuclear protein pSnail in A375 and B16-F10 cells were also determined by western blotting, with β-actin and PCNA as the internal controls for the cytoplasmic and nuclear proteins, respectively. The histograms show the relative density of AKT/pAKT, GSK-3β/pGSK-3β (Ser9/Tyr216), and Snail/p-Snail. (e) A375 cells were cotreated with or without MG132 and 0.4 μM ABZ for 24 h western blot (up) was used to detect the expression levels of AKT, pGSK-3β/Tyr216, Snail, N-cadherin, and E-cadherin in the cytoplasm of A375 cells. The histogram (bottom) shows the relative density of AKT, pGSK-3β/Tyr216, Snail, E-cadherin, and N-cadherin. (f) Histogram showing the relative expression intensity of pGSK-3β (Ser9/Tyr216) and pAKT after immunohistochemical staining of mouse metastatic lung cancer tissues. Scale bars = 100 and 20 μm. Each point in each group is calculated as the average score for five randomly selected areas in one lung slice and represents an IHC index of one mouse. All data are expressed as means ± SD. All experiments were performed thrice. $^{**}P < 0.01$; $^{***}P < 0.001$; ns, not significant.

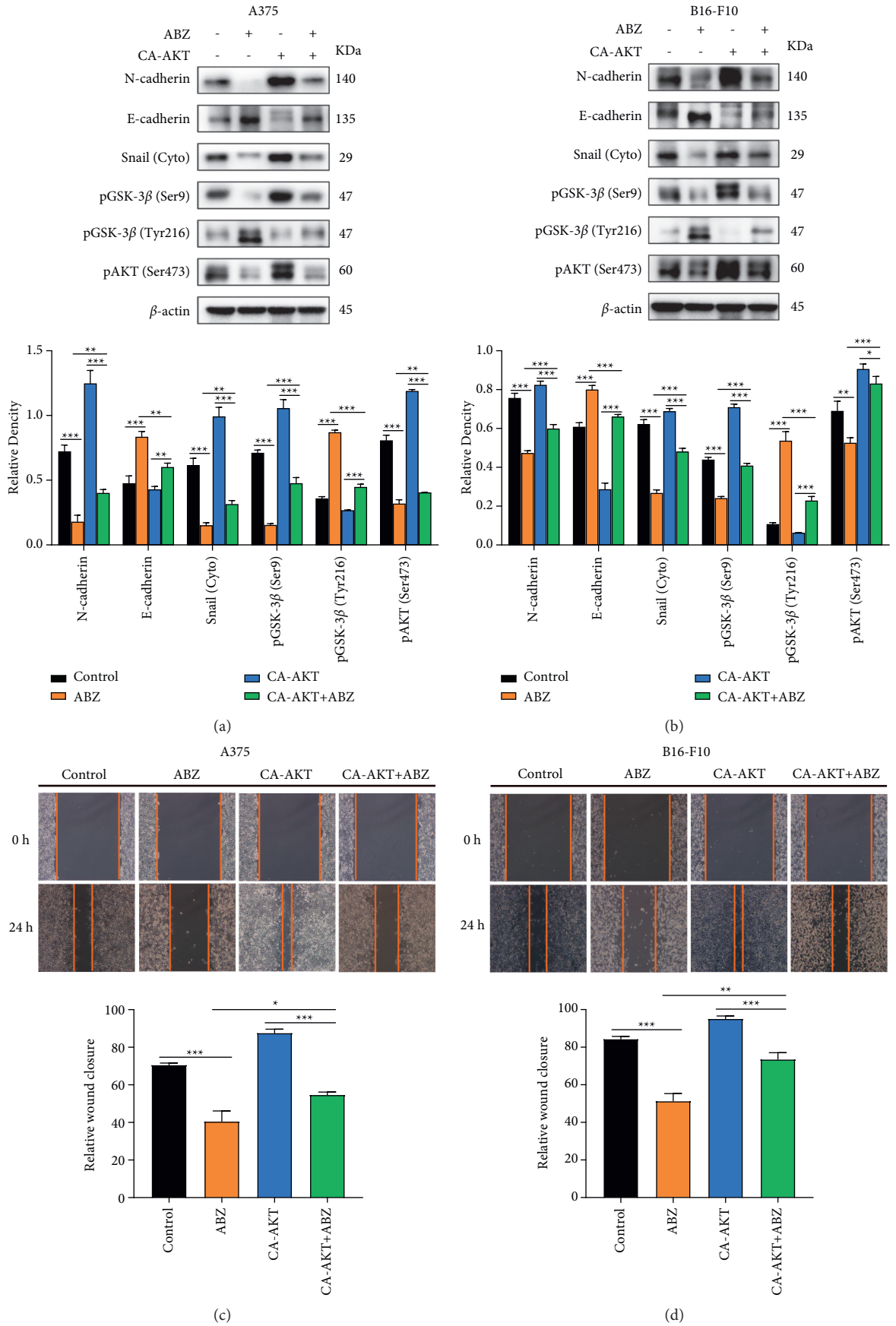

Figure 5: Continued.

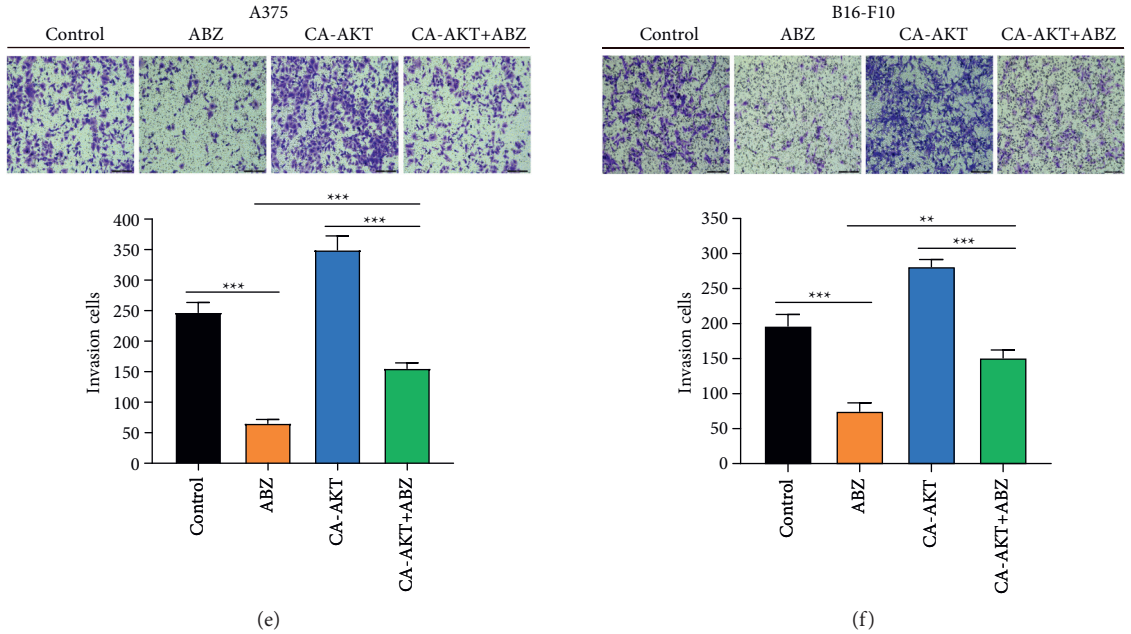

Figure 5: Constitutively active AKT (CA-AKT) significantly reverses the inhibitory effect of ABZ treatment on the migration and invasion of melanoma cells. (a-b) The CA-AKT plasmids were transiently transfected into A375 and B16-F10 cells, while the control group was transfected with the pcDNA3.1 (+) vector only. At 24 h after treatment with 0.4 μM ABZ, western blot analysis was used to detect the expression levels of N-cadherin, E-cadherin, pAKT, pGSK-3β (Ser9/Tyr216), and Snail in the cytoplasm of A375 and B16-F10 cells. The histograms (bottom) show the relative density of the detected proteins. (c-d) The wound healing area and relative wound closure rate (%) in melanoma cells were quantified and analyzed 24 h after treatment with 0.4 μM ABZ. The histograms (bottom) show the relative wound closure rate for each group. (e-f) Results of the transwell invasion experiments for A375 and B16-F10 cells under different conditions. The histograms (bottom) show the number of invasive cells in each group. The data are expressed as means ± SD. All experiments were performed thrice. $^{*}P < 0.05$; $^{**}P < 0.01$; $^{***}P < 0.001$.

ABZ can effectively inhibit tumor metastasis in mice without the expected toxicity and side effects. Furthermore, results of our in vitro experiments indicated that low-dose ABZ (0.4 μM, much lower than 2 μM [33]), which had no effect on proliferation, significantly inhibited the migration and invasion capabilities of melanoma cells. Taken together, our in vitro and in vivo experimental data demonstrate that low-dose ABZ may be a promising intervention strategy for preventing the relapse and metastasis progression of melanoma.

Snail, an important transcription factor in the EMT process, has been observed to be highly expressed during the malignant development and progression of melanoma [36, 37]. Therefore, the regulation of Snail expression was hypothesized to be an effective strategy for controlling and preventing melanoma metastasis. The AKT/GSK-3β signaling pathway is one of the main survival pathways of tumor cells [38] with abnormally high activation in many malignant tumors; specifically, its dysregulation is closely related to the occurrence, migration, and invasion of malignant tumors [39, 40]. Several studies revealed that pGSK-3β/Ser9 (inactive form) is significantly increased in the mouse epidermal carcinogenesis model, while pGSK-3β/Tyr216 (active form) is markedly reduced [41, 42], indicating that the downregulation or inactivation of GSK-3β occurs during skin carcinogenesis [43]. Our findings verified that ABZ treatment suppresses the EMT of melanoma in vitro and in vivo by inhibiting the AKT/GSK-3β pathway, resulting in decreased pGSK-3β/Ser9 (inactive form of GSK-3β) expression. Meanwhile, ABZ increased the accumulation of the active form of GSK-3β (pGSK-3β/Tyr216) in melanoma cells and changed the ratio of Tyr216/Ser9. This change in the ratio may lead to the nuclear export and degradation of Snail. Furthermore, when compared with ABZ-treated control cells, GSK-3β/Y216F overexpression did not change the protein levels of Snail, N-cadherin, and E-cadherin after ABZ-treated; this further confirmed that pGSK-3β/Tyr216 could downregulate Snail protein. However, ABZ-induced inhibitory effect on migration and invasion is not subverted completely by transfection of CA-AKT, indicating that pAKT-mediated phosphorylation of GSK-3β at Ser9 is not the only mechanism for phosphorylated GSK-3β/Tyr216 accumulation after ABZ-treated. We hypothesize that this may be associated with the altered expression of kinases that can phosphorylate GSK-3β at Tyr216 [44]. But the mechanisms underlying the transformation of the two GSK-3β forms are still unknown. Hence, the relationship between ABZ and these specific kinases will be explored in our future work.

Interestingly, GSK-3β appears to play different roles in various cancer types. Similar to melanoma, previous research suggested that GSK-3β may function as a tumor suppressor for breast cancer [45]. In contrast, some studies have suggested that GSK-3β may promote tumorigenesis and tumor development. For example, GSK-3β protein was reportedly overexpressed in human ovarian [46], colon [47],

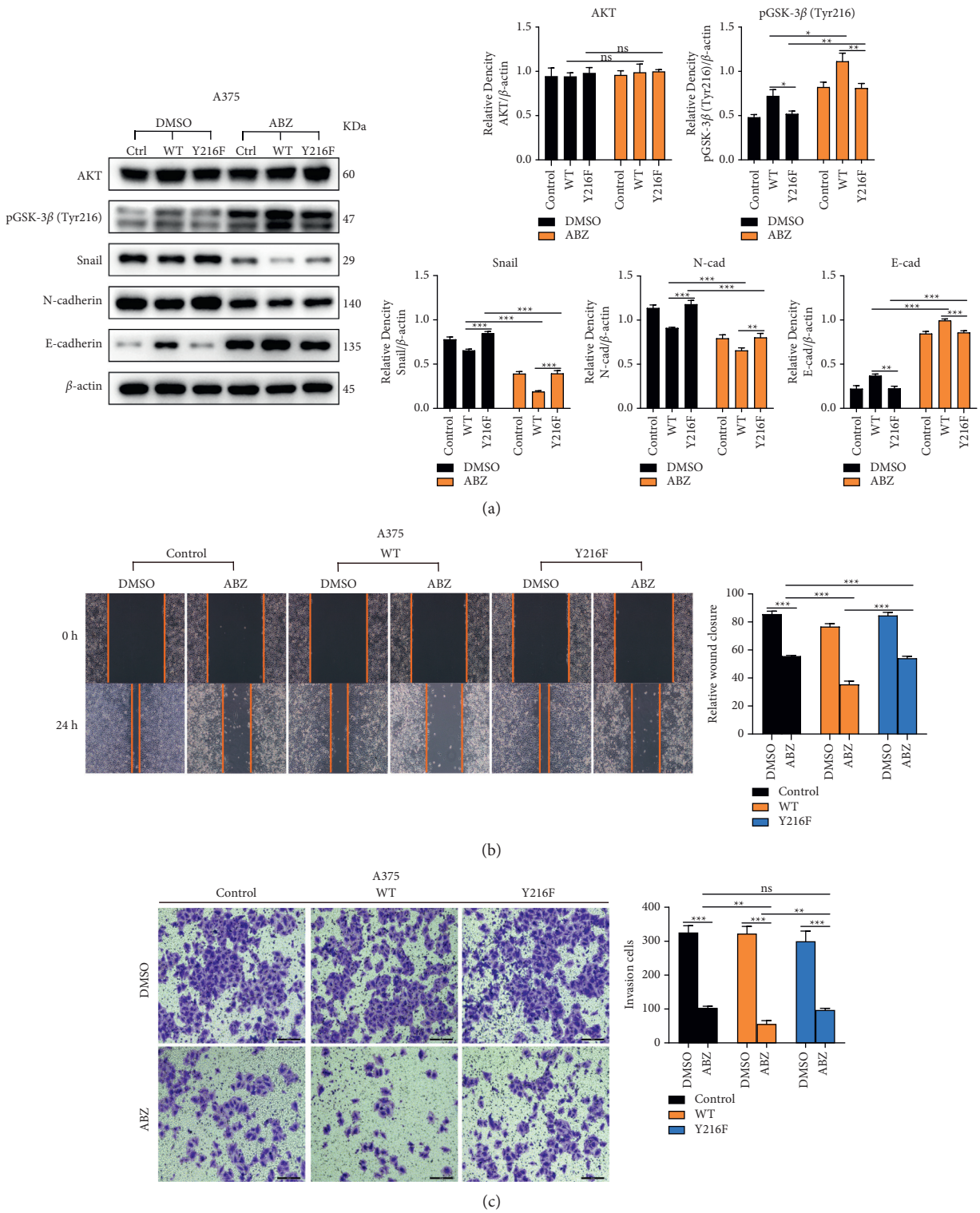

FIGURE 6: Overexpression of GSK-3β/Y216F could not promote the degradation of Snail after ABZ treatment. (a) Control, GSK-3β/WT, and GSK-3β/Y216F A375 cells were treated with 0.4 μM ABZ for 24 h; western blot analysis (left) was used to detect the expression levels of AKT, pGSK-3β /Tyr216, Snail, N-cadherin, and E-cadherin in the cytoplasm. The histograms (right) show the relative density of the detected proteins. (b) The wound healing area and relative wound closure rate (%) in A375 were quantified and analyzed 24 h after treatment with 0.4 μM ABZ. The histograms (right) show the relative wound closure rate for each group. (c) Results of the transwell invasion experiments for A375 cells under different conditions. The histograms (right) show the number of invasive cells in each group. The data are expressed as means ± SD. All experiments were performed thrice. $^{*}P < 0.05$; $^{**}P < 0.01$; $^{***}P < 0.001$; ns, not significant.

and pancreatic [48] cancers. Therefore, the ABZ-mediated inhibition of tumor migration and invasion via the AKT/GSK-3β/Snail pathway may only be applicable to certain types of tumors. Further, the differences in the function of GSK-3β in various cancer types may hinder the study of ABZ as a potentially broad-spectrum cancer metastasis inhibitor. However, for melanoma, the observed inhibitory effect of ABZ on the EMT process was significant data, and the potential clinical application of ABZ still requires further research.

5. Conclusion

In summary, we discovered that low-dose ABZ treatment can significantly inhibit the migration and invasion abilities of melanoma cells. We verified this through in vitro and in vivo experiments and found that ABZ potentially reduces the level of pGSK-3β at Ser9 by downregulating pAKT/pGSK-3β. Furthermore, the protein level of pGSK-3β/Tyr216 was significantly upregulated, which promoted Snail instability and pGSK-3β/Tyr216-mediated degradation, and ultimately reversed the EMT of melanoma cells. Therefore, our findings contribute novel insights on how the antiparasitic drug ABZ can function in inhibiting melanoma metastasis, validating its potential as an antimelanoma metastasis inhibitor for cancer therapeutics.

Data Availability

The raw data supporting the conclusions of this article will be made available by the authors, without undue reservation.

Conflicts of Interest

The authors declare that the research was conducted in the absence of any commercial or financial relationships that could be construed as potential conflicts of interest.

Acknowledgments

The authors would like to thank Prof. Wenyue Xu for providing plasmids and laboratory support and Editage (http://www.editage.cn) for English language editing. This study was supported by the Excellent Talent Program of Army Medical University (B-3253) and National Natural Science Foundation of China No. 81702443.

Supplementary Materials

Supplementary Table 1: the primers list for RT-qPCR. Supplementary Figure 1: relative ratio changes of pGSK-3β/Tyr216 and pGSK-3β/Ser9 in A375 and B16-F10 cells after ABZ treatment. (*Supplementary Materials*)

References

[1] B. Owens, "Melanoma," *Nature*, vol. 515, no. 7527, p. S109, 2014.

[2] M. B. Atkins, C. Curiel-Lewandrowski, D. E. Fisher et al., "The state of melanoma: emergent challenges and opportunities," *Clinical Cancer Research*, vol. 27, no. 10, pp. 2678–2697, 2021.

[3] M. K. Tripp, M. Watson, S. J. Balk, S. M. Swetter, and J. E. Gershenwald, "State of the science on prevention and screening to reduce melanoma incidence and mortality: the time is now," *CA: A Cancer Journal for Clinicians*, vol. 66, no. 6, pp. 460–480, 2016.

[4] D. Schadendorf, A. C. J. van Akkooi, C. Berking et al., "Melanoma," *The Lancet*, vol. 392, no. 10151, pp. 971–984, 2018.

[5] C. Kosnopfel, T. Sinnberg, B. Sauer et al., "YB-1 expression and phosphorylation regulate tumorigenicity and invasiveness in melanoma by influencing EMT," *Molecular Cancer Research*, vol. 16, no. 7, pp. 1149–1160, 2018.

[6] D. G. Coit, J. A. Thompson, M. R. Albertini et al., "Cutaneous melanoma, version 2.2019, NCCN clinical practice guidelines in oncology," *Journal of the National Comprehensive Cancer Network: Journal of the National Comprehensive Cancer Network*, vol. 17, no. 4, pp. 367–402, 2019.

[7] K. D. Miller, L. Nogueira, A. B. Mariotto et al., "Cancer treatment and survivorship statistics, 2019," *CA: A Cancer Journal for Clinicians*, vol. 69, no. 5, pp. 363–385, 2019.

[8] H. H. Vandyck, L. M. Hillen, F. M. Bosisio, J. van den Oord, A. zur Hausen, and V. Winnepenninckx, "Rethinking the biology of metastatic melanoma: a holistic approach," *Cancer and Metastasis Reviews*, vol. 40, no. 2, pp. 603–624, 2021.

[9] J. P. Thiery, H. Acloque, R. Y. J. Huang, and M. A. Nieto, "Epithelial-mesenchymal transitions in development and disease," *Cell*, vol. 139, no. 5, pp. 871–890, 2009.

[10] I. Pastushenko and C. Blanpain, "EMT transition states during tumor progression and metastasis," *Trends in Cell Biology*, vol. 29, no. 3, pp. 212–226, 2019.

[11] K. Woods, A. Pasam, A. Jayachandran, M. C. Andrews, and J. Cebon, "Effects of epithelial to mesenchymal transition on T cell targeting of melanoma cells," *Frontiers in Oncology*, vol. 4, p. 367, 2014.

[12] J. Xu, S. Lamouille, and R. Derynck, "TGF-β-induced epithelial to mesenchymal transition," *Cell Research*, vol. 19, no. 2, pp. 156–172, 2009.

[13] S. J. Serrano-Gomez, M. Maziveyi, and S. K. Alahari, "Regulation of epithelial-mesenchymal transition through epigenetic and post-translational modifications," *Molecular Cancer*, vol. 15, no. 1, p. 18, 2016.

[14] M. Diepenbruck, S. Tiede, M. Saxena et al., "miR-1199-5p and Zeb1 function in a double-negative feedback loop potentially coordinating EMT and tumour metastasis," *Nature Communications*, vol. 8, no. 1, p. 1168, 2017.

[15] W. Huang, J. Zhang, M. Huo et al., "CUL4B promotes breast carcinogenesis by coordinating with transcriptional repressor complexes in response to hypoxia signaling pathway," *Advanced Science*, vol. 8, no. 10, Article ID 2001515, 2021.

[16] K. Skrzypek and M. Majka, "Interplay among SNAIL transcription factor, MicroRNAs, long non-coding RNAs, and circular RNAs in the regulation of tumor growth and metastasis," *Cancers*, vol. 12, no. 1, 2020.

[17] J. Liu, C. Wang, X. Ma et al., "High expression of CCR5 in melanoma enhances epithelial-mesenchymal transition and metastasis via TGFβ1," *The Journal of Pathology*, vol. 247, no. 4, pp. 481–493, 2019.

[18] B. P. Zhou, J. Deng, W. Xia et al., "Dual regulation of Snail by GSK-3β-mediated phosphorylation in control of epithelial-mesenchymal transition," *Nature Cell Biology*, vol. 6, no. 10, pp. 931–940, 2004.

[19] J.-P. Zhang, C. Zeng, L. Xu, J. Gong, J.-H. Fang, and S.-M. Zhuang, "MicroRNA-148a suppresses the epithelial-mesenchymal transition and metastasis of hepatoma cells by

targeting Met/Snail signaling," *Oncogene*, vol. 33, no. 31, pp. 4069–4076, 2014.

[20] S. Wang, K. Xie, and T. Liu, "Cancer immunotherapies: from efficacy to resistance mechanisms–not only checkpoint matters," *Frontiers in Immunology*, vol. 12, 2021.

[21] S. Pushpakom, F. Iorio, P. A. Eyers et al., "Drug repurposing: progress, challenges and recommendations," *Nature Reviews Drug Discovery*, vol. 18, no. 1, pp. 41–58, 2019.

[22] Y.-Q. Li, Z. Zheng, Q.-X. Liu et al., "Repositioning of anti-parasitic drugs for tumor treatment," *Frontiers in Oncology*, vol. 11, Article ID 670804, 2021.

[23] M. F. Adasme, D. Parisi, A. Sveshnikova, and M. Schroeder, "Structure-based drug repositioning: potential and limits," *Seminars in Cancer Biology*, vol. 68, pp. 192–198, 2021.

[24] L. S. E. P. W. Castro, M. R. Kviecinski, F. Ourique et al., "Albendazole as a promising molecule for tumor control," *Redox Biology*, vol. 10, pp. 90–99, 2016.

[25] Z. Mrkvová, S Uldrijan, A Pombinho, P Bartůněk, and I Slaninová, "Benzimidazoles downregulate Mdm2 and MdmX and activate p53 in MdmX overexpressing tumor cells," *Molecules*, vol. 24, no. 11, 2019.

[26] K. Patel, N. A. Doudican, P. B. Schiff, and S. J. Orlow, "Albendazole sensitizes cancer cells to ionizing radiation," *Radiation Oncology*, vol. 6, no. 1, p. 160, 2011.

[27] R. L. Camp, M. Dolled-Filhart, and D. L. Rimm, "X-Tile," *Clinical Cancer Research*, vol. 10, no. 21, pp. 7252–7259, 2004.

[28] H. Chen, Z. Weng, and C. Xu, "Albendazole suppresses cell proliferation and migration and induces apoptosis in human pancreatic cancer cells," *Anti-Cancer Drugs*, vol. 31, no. 5, pp. 431–439, 2020.

[29] S. Li, J. Lu, Y. Chen et al., "MCP-1-induced ERK/GSK-3β/snail signaling facilitates the epithelial-mesenchymal transition and promotes the migration of MCF-7 human breast carcinoma cells," *Cellular and Molecular Immunology*, vol. 14, no. 7, pp. 621–630, 2017.

[30] H. Pan, Y. Song, H. Zhang et al., "Radiation engenders converse migration and invasion in colorectal cancer cells through opposite modulation of ANXA2/AKT/GSK3beta pathway," *American Journal of Cancer Research*, vol. 11, no. 1, pp. 61–78, 2021.

[31] C. Garbe, T. Amaral, K. Peris et al., "European consensus-based interdisciplinary guideline for melanoma. Part 1: diagnostics-update 2019," *European Journal of Cancer*, vol. 126, pp. 141–158, 2020.

[32] M. L. Hawkins, M. J. Rioth, M. M. Eguchi, and M. Cockburn, "Poor prognosis for thin ulcerated melanomas and implications for a more aggressive approach to treatment," *Journal of the American Academy of Dermatology*, vol. 80, no. 6, pp. 1640–1649, 2019.

[33] J. Petersen and S. K. Baird, "Treatment of breast and colon cancer cell lines with anti-helmintic benzimidazoles mebendazole or albendazole results in selective apoptotic cell death," *Journal of Cancer Research and Clinical Oncology*, vol. 147, 2021.

[34] D. S. Son, E. S. Lee, and S. E. Adunyah, "The antitumor potentials of benzimidazole anthelmintics as repurposing drugs," *Immune network*, vol. 20, no. 4, p. e29, 2020.

[35] F. Zhou, J. Du, and J. Wang, "Albendazole inhibits HIF-1alpha-dependent glycolysis and VEGF expression in non-small cell lung cancer cells," *Molecular and Cellular Biochemistry*, vol. 428, no. 1-2, pp. 171–178, 2017.

[36] R. Massoumi, S. Kuphal, C. Hellerbrand et al., "Down-regulation of CYLD expression by snail promotes tumor progression in malignant melanoma," *Journal of Experimental Medicine*, vol. 206, no. 1, pp. 221–232, 2009.

[37] C. Xing, H. Tian, Y. Zhang et al., "DDX39 overexpression predicts a poor prognosis and promotes aggressiveness of melanoma by cooperating with snail," *Frontiers in Oncology*, vol. 10, p. 1261, 2020.

[38] S. Chen, Z. He, C. Zhu et al., "TRIM37 mediates chemoresistance and maintenance of stemness in pancreatic cancer cells via ubiquitination of PTEN and activation of the AKT-GSK-3β-i-catenin signaling pathway," *Frontiers in Oncology*, vol. 10, Article ID 554787, 2020.

[39] R. Fang, G. Zhang, Q. Guo et al., "Nodal promotes aggressive phenotype via Snail-mediated epithelial-mesenchymal transition in murine melanoma," *Cancer Letters*, vol. 333, no. 1, pp. 66–75, 2013.

[40] Z. Q. Cao, X.-X. Wang, L. Lu et al., "Beta-sitosterol and gemcitabine exhibit synergistic anti-pancreatic cancer activity by modulating apoptosis and inhibiting epithelial-mesenchymal transition by deactivating akt/GSK-3beta signaling," *Frontiers in Pharmacology*, vol. 9, p. 1525, 2018.

[41] H. Leis, C. Segrelles, S. Ruiz, M. Santos, and J. S. M. Paramio, "Expression, localization, and activity of glycogen synthase kinase 3? during mouse skin tumorigenesis," *Molecular Carcinogenesis*, vol. 35, no. 4, pp. 180–185, 2002.

[42] C. Ma, J. Wang, Y. Gao et al., "The role of glycogen synthase kinase 3β in the transformation of epidermal cells," *Cancer Research*, vol. 67, no. 16, pp. 7756–7764, 2007.

[43] J. Luo, "Glycogen synthase kinase 3β (GSK3β) in tumorigenesis and cancer chemotherapy," *Cancer Letters*, vol. 273, no. 2, pp. 194–200, 2009.

[44] N. Sharma, A. Tramutola, C. Lanzillotta et al., "Loss of biliverdin reductase-a favors tau hyper-phosphorylation in Alzheimer's disease," *Neurobiology of Disease*, vol. 125, pp. 176–189, 2019.

[45] R. Sun, H.-Y. Xie, J.-X. Qian et al., "FBXO22 possesses both protumorigenic and antimetastatic roles in breast cancer progression," *Cancer Research*, vol. 78, no. 18, pp. 5274–5286, 2018.

[46] K.-J. Ryu, S.-M. Park, S.-H. Park et al., "p38 stabilizes snail by suppressing DYRK2-mediated phosphorylation that is required for GSK3β-βTrCP-induced snail degradation," *Cancer Research*, vol. 79, no. 16, pp. 4135–4148, 2019.

[47] J. Yu, D. Liu, X. Sun et al., "CDX2 inhibits the proliferation and tumor formation of colon cancer cells by suppressing Wnt/β-catenin signaling via transactivation of GSK-3β and Axin2 expression," *Cell Death & Disease*, vol. 10, no. 1, p. 26, 2019.

[48] M. Edderkaoui, C. Chheda, B. Soufi et al., "An inhibitor of GSK3B and HDACs kills pancreatic cancer cells and slows pancreatic tumor growth and metastasis in mice," *Gastroenterology*, vol. 155, no. 6, pp. 1985–1998, 2018.

Hindawi
Journal of Oncology
Volume 2021, Article ID 6141591, 12 pages
https://doi.org/10.1155/2021/6141591

Review Article

Exploring the Pivotal Neurophysiologic and Therapeutic Potentials of Vitamin C in Glioma

Seidu A. Richard,[1] **Marian Sackey**,[2] **and Nii Korley Kortei**[3]

[1]*Department of Medicine, Princefield University, P. O. Box MA-128, Ho, Ghana*
[2]*Department of Pharmacy, Ho Teaching Hospital, P.O. Box MA-374, Ho, Ghana*
[3]*Department of Nutrition and Dietetics, School of Allied Health Sciences, University of Health and Allied Sciences, Ho, Ghana*

Correspondence should be addressed to Seidu A. Richard; gbepoo@gmail.com

Received 20 September 2021; Revised 10 November 2021; Accepted 2 December 2021; Published 14 December 2021

Academic Editor: José Roberto de Oliveira Ferreira

Gliomas represent solely primary brain cancers of glial cell or neuroepithelial origin. Gliomas are still the most lethal human cancers despite modern innovations in both diagnostic techniques as well as therapeutic regimes. Gliomas have the lowest overall survival rate compared to other cancers 5 years after definitive diagnosis. The dietary intake of vitamin C has protective effect on glioma risk. Vitamin C is an essential compound that plays a vital role in the regulation of lysyl and prolyl hydroxylase activity. Neurons store high levels of vitamin C via sodium dependent-vitamin C transporters (SVCTs) to protect them from oxidative ischemia-reperfusion injury. Vitamin C is a water-soluble enzyme, typically seen as a powerful antioxidant in plants as well as animals. The key function of vitamin C is the inhibition of redox imbalance from reactive oxygen species produced via the stimulation of glutamate receptors. Gliomas absorb vitamin C primarily via its oxidized dehydroascorbate form by means of GLUT 1, 3, and 4 and its reduced form, ascorbate, by SVCT2. Vitamin C is able to preserve prosthetic metal ions like Fe^{2+} and Cu^{+} in their reduced forms in several enzymatic reactions as well as scavenge free radicals in order to safeguard tissues from oxidative damage. Therapeutic concentrations of vitamin C are able to trigger H_2O_2 generation in glioma. High-dose combination of vitamin C and radiation has a much more profound cytotoxic effect on primary glioblastoma multiforme cells compared to normal astrocytes. Control trials are needed to validate the use of vitamin C and standardization of the doses of vitamin C in the treatment of patients with glioma.

1. Introduction

Gliomas represent solely primary brain cancers of glial cell or neuroepithelial origin [1–4]. Gliomas are categorized into lowest-grade tumors, lower-grade tumors, higher-grade malignancies, and highest-grade malignancies as stipulated by the American Association of Neurosurgeons [1–4]. World health organization further categorized astrocytoma into four grades [1–4]. Grade I comprises pilocytic astrocytoma; grade II comprises low-grade astrocytoma; grade III comprises anaplastic astrocytoma, whereas grade IV comprises glioblastoma multiforme (GBM) [1–4]. Grade I often has minimal transformation abilities into grades II–IV and mostly seen children. Nevertheless, grade II or III is mostly accompanied with malignant transformations into grade IV [1–4].

Vitamin C, also referred to as L-ascorbic acid/L-ascorbate, is an essential compound that plays a vital role in the regulation of lysyl and prolyl hydroxylase activity [5]. Vitamin C is a general term that describes its oxidized dehydroascorbate (DHA) and its reduced forms (ascorbate) [6]. Vitamin C is a water-soluble enzyme, typically seen as a powerful antioxidant in plants as well as animals [7]. Vitamin C was capable of preserving prosthetic metal ions like Fe^{2+} and Cu^{+} in their reduced forms in several enzymatic reactions as well as scavenge free radicals in order to safeguard tissues from oxidative damage [8, 9]. Also, vitamin C participates in numerous intracellular as well as extracellular

biological processes to efficiently scavenge free radicals [7, 10].

Vitamin C intake as a dietary antioxidant was capable of augmenting growth restriction of cancer cells in general and glioma cells to be specific [11, 12]. Studies have shown that vitamin C was capable of inhibiting cancer via mechanism, such as the argumentation of stromal integrity of normal tissue, activating lymphocytes to a greater level of immunocompetence, stimulating "auspicious modification in the steroid environment," blocking hyaluronidase activity in malignant cells, augmenting antiviral activity, and interfering with the metabolism of malignant cells [13–16].

Studies have demonstrated that vitamin C was selectively concentrated in tumors and may form cytotoxic quantities of hydrogen peroxide (H_2O_2) within the tumor as a byproduct of oxidation [13, 15, 16]. Vitamin C can act as a prodrug to deliver a substantial influx of H_2O_2 to tumors after intravenous (IV) administration [17, 18]. A study established that H_2O_2 was the key mediating factor in cytotoxicity to cancer cells through IV vitamin C [17, 19]. Vitamin C stimulated intracellular oxidation as well as energy generation resulting in total therapeutic potential. Also, vitamin C stimulated of activities like apoptosis and necrosis [17, 20].

Studies have shown that vitamin C precisely eradicated a sizable quantities of cancer cells when plasma concentrations reach 1 mM or more [21–23]. Another study revealed that vitamin C was capable of decreasing the adverse reactions triggered by chemotherapy during the treatment of cancer in patients [24, 25]. Thus, this explicit review explores the pivotal neurophysiologic and therapeutic potentials of vitamin C in glioma. The "Boolean logic" was used to search for article role of vitamin C in glioma. Most of the articles were indexed in PubMed and/or PMC with strict inclusion criteria being the neurophysiologic and therapeutic potentials of vitamin C in glioma. The search terms on PubMed and/or PMC were vitamin C and/or L-ascorbic acid and/or L-ascorbate and glioma.

1.1. Vitamin C Levels in the Blood, Cerebrospinal Fluid, and Brain. The brain, spinal cord, and adrenal glands had the highest vitamin C levels of all the tissues in the body as well as the highest retention capacity of vitamin C [26, 27]. Studies have shown that brain tissue concentration of vitamin C was regionally dependent. Higher concentrations were detected in anterior regions like the cerebral cortex as well as hippocampus, with gradually lower concentrations in more posterior regions like the brainstem as well as spinal cord [28, 29]. Generally, brain tissue vitamin C levels were several millimolars (mM) with the average concentration in neurons likely to be 10 mM and merely 1 mM in glia [28–30]. Under normal circumstances, turnover of vitamin C in brain is approximately 2% per hour [26, 31].

Molecules with low molecular weight as well as passable hydrophilic/hydrophobic balance are allowed to penetrate the central nervous system (CNS) [32, 33]. It was established that endothelial cells of the brain capillaries, which form the blood-brain barrier (BBB), possess selective transport systems for particular nutrients as well as endogenous biomolecules besides unspecific permeation [32]. Thus, they are conscientious for the transport of glucose, neutral, acidic, and basic amino acids like alanine and taurine, monocarboxylic acids, amines, and neuromediators like choline, vitamins, and nucleosides, as well as the peptide transport system for small neurotropic peptides [32, 34, 35].

The epithelium of the choroid plexus, which is a restricted part of the BBB, is implicated for the maintenance of CNS homeostasis for vitamin C [32, 36]. IV administration of vitamin C revealed that vitamin C reached the CSF via the choroid plexus and then gradually penetrates the brain substance from the CSF (Figure 1) [32, 37]. Vitamin C enters the CNS principally via active transport at the choroid plexus (Figure 1). Vitamin C concentration is modulated homeostatically after it diffuses from cerebrospinal fluid (CSF) to brain extracellular fluid (ECF) [32]. Vitamin C was capable of entering the ECF via carrier-mediated uptake and via simple diffusion across brain capillaries at the BBB [26, 38]. Extracellular vitamin C levels are also vigorously regulated via glutamate-mediated activity through glutamate-vitamin C heteroexchange (Figure 1) [26].

It was established that vitamin C from ECF was taken up into brain cells, where its levels augmented up to 20-fold [26]. It was further revealed that, in some neurons, vitamin C levels were up to 200-fold higher than the levels in the bloodstream [26, 32]. Vitamin C is transferred from the blood, where its levels are about 50 μM into the CFS where its levels are maintained at 200 μM via specific physiological mechanisms (Figure 1) [32, 39]. Vitamin C uptake from the blood into CSF involves active stereospecific Na^+-dependent transport at the choroid plexus (Figure 1) [26, 40]. Furthermore, vitamin C serves as a cofactor in several enzymatic activities associated with the processing of neurotransmitters as well as an antioxidant offering neuroprotection within the CNS [32].

Tsukaguchi et al. indicated that the reduced form of vitamin C is absorbed via a mechanism that involves sodium-dependent vitamin C transporters 2 (SVCT2) [8]. SVCT2 RNA was identified in the epithelium of the choroid plexus [7]. Precisely, the neuroepithelial cells of the choroid plexus as well as the retinal pigmented epithelium secreted SVCT2 transporter. It was established that SVCT1 as well as SVCT2 each mediate concentrative, high-affinity vitamin C transport that was stereospecific and was driven by the Na^+ electrochemical gradient (Figure 1) [8]. Higher levels of Na^+-dependent vitamin transporters such as SVCT1 and SVCT2 were detected in the choroid plexus but not in brain capillaries (Figure 1) [8, 26].

In situ hybridization in the rat brain revealed that SVCT2 was more concentrated in neurons than glial cells, which was coherent with higher concentrations of vitamin C in neurons than glia [8, 26]. Thus, neuronal cells take up vitamin C, because these cells secrete SVCT2 [41]. It was affirmed that SVCT2 was present in both glutamatergic as well as GABAergic neurons, including glutamatergic pyramidal cells of the hippocampus, glutamatergic granule cells of the cerebellum, and GABAergic cerebellar Purkinje cells (Figure 1) [8]. It was affirmed that astrocytes were capable of

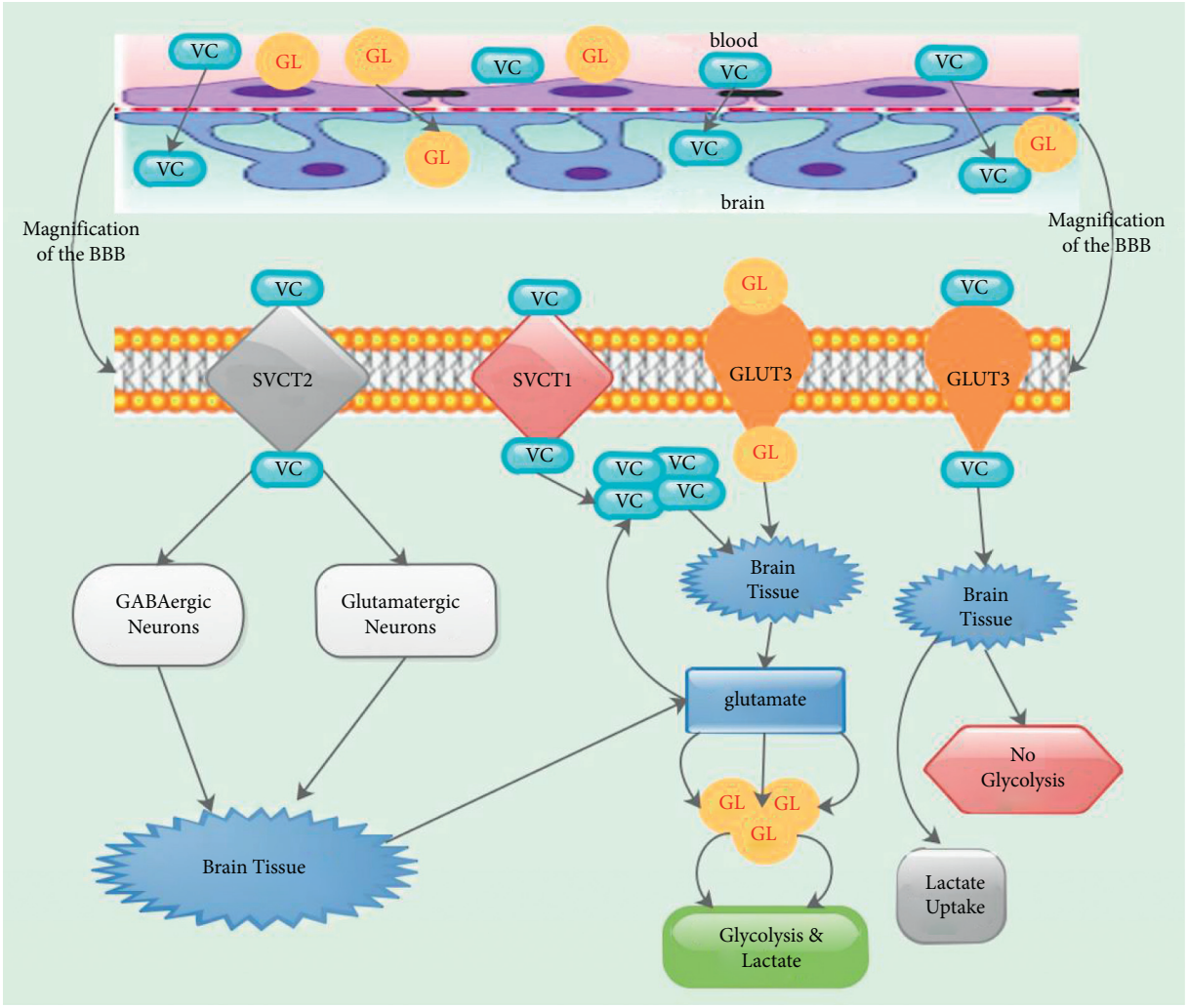

Figure 1: The neurophysiological mechanisms via which vitamin C and glucose cross the blood brain barrier (BBB) to influence normal brain tissues. VC = vitamin C; GL = glucose. All other abbreviations are indicated in the abbreviation list.

removing glutamate from the synaptic cleft when synapses are glutamatergically active [8].

Several studies have demonstrated that glutamate transport in these cells was capable of activating glucose transport, to stimulate glycolysis with lactate and vitamin C release (Figure 1) [42, 43]. Castro et al. demonstrated that intracellular vitamin C blocked glucose transport via direct or indirect blockade of GLUT3 and triggered lactate uptake (Figure 1) [44]. Thus, when GLUT3 was downregulated, glucose utilization was not inhibited by vitamin C and lactate transport was not stimulated (Figure 1) [42].

1.2. Function of Vitamin C in the Normal Brain. Brain vitamin C concentrations are gender dependent, with lower estrogen-modulated levels in the female brain than in the male brain [26, 45]. Neurons store high levels of vitamin C via SVCTs to protect them from oxidative ischemia-reperfusion injury [46, 47]. Studies have demonstrated that the key function of vitamin C was the inhibition of redox imbalance from reactive oxygen species (ROS) produced via the stimulation of glutamate receptors (Figure 2) [48, 49]. Studies have further exhibited that vitamin C was capable of buffering glutamate-generated ROS and inhibited succeeding cell death in cultured neurons [50, 51].

Studies have demonstrated that vitamin C serves as a neuromodulator for both dopamine- and glutamate-mediated neurotransmission besides its functions as an antioxidant in the CNS [52, 53]. It was further established that the main localization of vitamin C in neurons was coherent with such neuromodulatory functions [52, 53]. Furthermore, vitamin C was implicated as a fundamental cofactor for noradrenaline synthesis [26, 54]. Also, vitamin C was essential for the secretion of noradrenaline as well as acetylcholine from synaptic vesicles [26, 55]. In addition, vitamin C was a crucial cofactor in the synthesis of numerous neuropeptides [26, 56]. Moreover, at physiological concentrations, vitamin C augmented the secretion of theses neuropeptides [26, 57].

The accumulate of vitamin C in the basal lamina triggered myelin formation by Schwann cells [26, 58]. Studies have shown that variations in vitamin C concentrations were

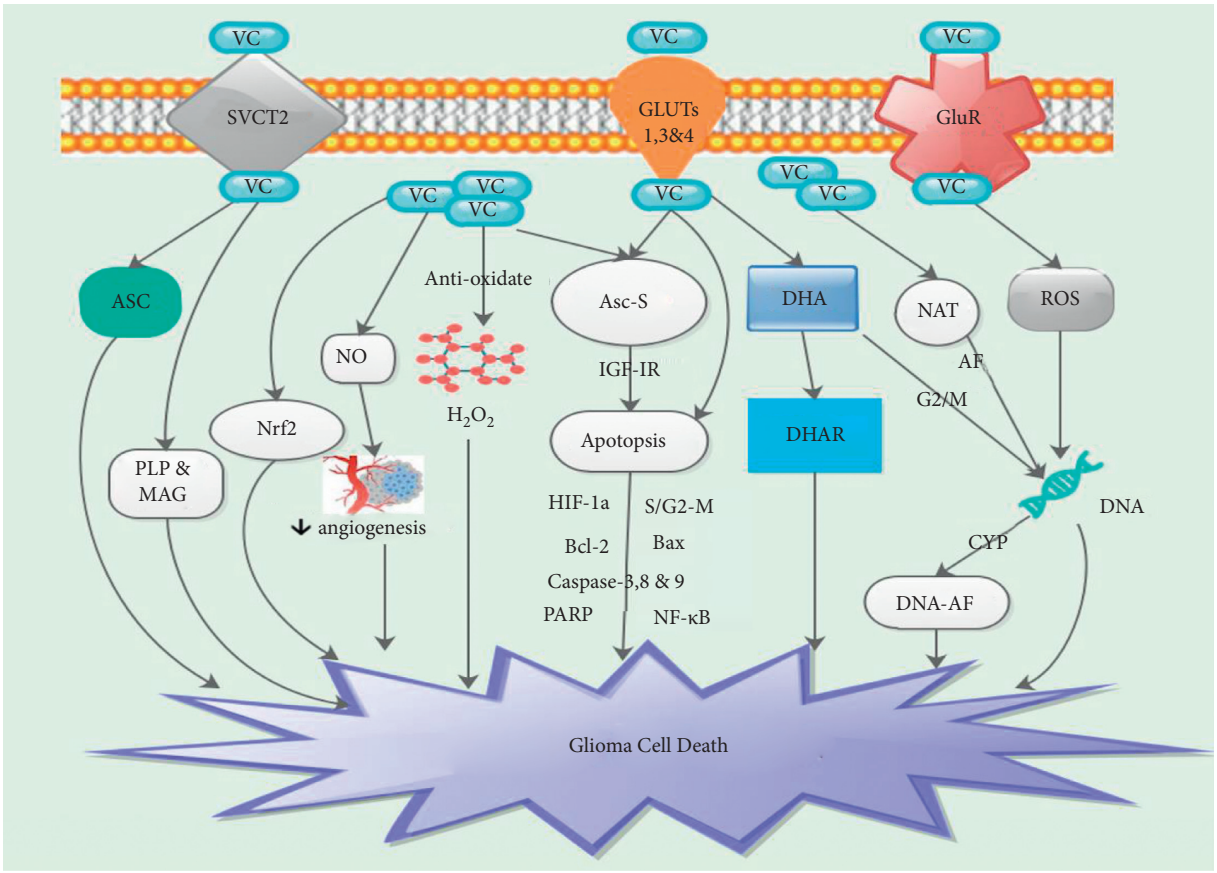

Figure 2: The mechanisms via which vitamin triggers glioma cell death. VC = vitamin C; ASC = ascorbate. All other abbreviations are indicated in the abbreviation list.

associated with brain activity as well as brain energetics [59, 60]. Also, vitamin C servers as a metabolic switch in brain, modulating glucose consumption in neuronal cells via the blockade of neuronal GLUT3 [42]. Owens and Bunge established that vitamin C was a fundamental in the enhancement of axonal ensheathment in Schwann cell-neuronal coculture [61]. They further revealed that vitamin C was crucial for periphery nervous system myelinogenesis because it was capable of stimulating the P0 protein gene in cultured Schwann cells [61].

1.3. Vitamin C and Glioma. Several studies have assessed the outcomes of dietary vitamin C intake on primary brain tumor risk [62–70]. These studies involved both children and adults [62–70]. The studies in children revealed that glioma risk differs inversely with maternal vitamin C intake during pregnancy [62–64]. In studies involving adults, an inverse association between dietary vitamin C intake and glioma risk was also observed [62, 65–67]. Nevertheless, some studies detected a positive relationship between vitamin C intake and glioma risk [62, 68, 69]. Another study found positive relationship for men and a negative relationship for women [70]. Zhou et al. with a meta-analysis observed that the consumption of vitamin C had protective effect on glioma risk [11].

Studies have shown that GLUTs mediate the facilitative transport of the DHA form of vitamin C [6, 71, 72]. Also, studies have demonstrated that ascorbate, the reduced form of vitamin C, is transported by SVCT [6, 8, 73, 74]. Gliomas absorb vitamin C primarily via its oxidized form (DHA) by means of GLUT 1, 3, and 4 and its reduced form, ascorbate, by SVCT2 (Figure 2) [6]. Nevertheless, it was established that SVCT2 had modest capacity in gliomas [75]. DHA was reduced to vitamin C via the GSH-consumption enzyme DHA reductase (DHAR) once it gets into the cells (Figure 2) [6]. Laszkiewicz et al. exhibited that, vitamin C is a potent modulator of the proteolipid protein as well as the secretion of myelin-associated glycoprotein gene in CNS-derived C6 cells [76].

Salmaso et al. established that vitamin C could be utilized as a targeting agent to stimulate the disposition of drug loaded nanosystems in gliomas [32]. Conklin et al. indicated that antioxidants are capable of safeguarding normal brain tissues from radiation damage resulting in better survival, because brain tissues possess oxidative milieus and are thus susceptible to radiation damage [77]. Lawenda et al. demonstrated that antioxidants are capable of rending glioma more resistant to tumor killing by radiation, resulting in poorer patient survival [78]. It was established that, at low doses, vitamin C was capable of protecting cells from oxidative stress, thus inhibiting the advancement of tumors

[5, 79]. Prasad demonstrated that sodium ascorbate triggered a cytotoxic stimulus on normal brain cells in culture [15]. Benade et al. established that the toxicity of ascorbate was as a result of low catalase levels in tumor cells [80].

Vitamin C was able to inhibit DNA damage and the deterioration of subcellular structures like proteins, lipids, and DNA by scavenging of ROS (Figure 2) [5]. Studies have demonstrated that therapeutic concentrations of vitamin C triggered H_2O_2 generation in solid tumors (Figure 2) [22, 81]. Furthermore, studies have demonstrated that H_2O_2 diffuses into cancer cells and overpowers their antioxidant defense system via the depletion of glutathione levels [22, 23]. Espey et al. established that vitamin C stimulated generation of extracellular H_2O_2 was only partly accountable for cell death [82]. Peterkofsky and Prather indicated that H_2O_2 was either formed intracellularly and excreted in the medium or formed at the cell surface on culture medium [83].

It was further established that H_2O_2 was not detectable in growth medium containing Na^+-ascorbate alone [83]. Studies have demonstrated that H_2O_2 was capable of triggering lipid peroxidation, which resulted in cell death [84–86]. It is also revealed that Na^+-ascorbate was capable of triggering the formation of DHA exogenously or intracellularly or both. Also, sodium ascorbate was capable of blocking catalase activity *in vitro* [87]. Furthermore, the blockade of catalase was capable stimulating the accumulation of H_2O_2 in tumor cells resulting in cell death [87].

1.4. Vitamin C Derivatives and Glioma. Ascorbyl esters are nontoxic, synthetic derivative of vitamin C used as antioxidants [88, 89].

These esters can easily cross the BBB because of their lipophilic nature [90]. The breakdown products of ascorbyl stearate are ascorbate and stearic acids, which are nontoxic to biological system [88, 89]. Studies have indicated that ascorbyl esters, such as ascorbyl stearate (Asc-S) and ascorbyl palmitate, block the proliferation of mouse as well as human glioma cells [91, 92]. Furthermore, studies have demonstrated that Asc-S as well as ascorbyl palmitate suppressed the growth of murine (G-26) as well as human glioma (U-373) cells [91, 92]. Makino et al. established that Asc-S, a lipophilic derivative of vitamin C is a potent inhibitor of cell proliferation as compared to vitamin C [93].

Studies have demonstrated that human gliomas are capable of secreting insulin-like growth factor- (IGF-) I as well as IGF-II. It was further established that IGFs autocrine receptor was capable of stimulating glioma cell growth [94, 95]. Naidu et al. established that Asc-S was capable of modulating of secretion of IGF-IR as well as triggering of apoptosis in T98G cells (Figure 2) [96]. They revealed that Asc-S inhibited the growth of human GBM T98G cells via the arrest of cells at late S/G2-M phase of cell cycle as well as trigger cell death via apoptosis (Figure 2) [96]. They further indicated that Na^+-ascorbate was capable of blocking the growth of T98G cells with an IC50 of 6.0 mM [96]. Nevertheless, Asc-S was about 68-fold more potent than Na^+-ascorbate with an IC50 value of 88.5 μM [93].

It was also established that administration of Asc-S led to a substantial augmentation in the proportion of cells in late S/G2-M phase of cell cycle in comparison with untreated control cells [96]. Also, DHA was capable of modulating cell cycle progression as well as trigger cell cycle arrest at G2/M DNA damage checkpoints during oxidative stress (Figure 2) [97]. Furthermore, Asc-S stimulated cell cycle arrest at late S/G2-M phase checkpoints was capable of blocking of cell proliferation as well as apoptosis [96]. Thus, vitamin C derivatives interfere with cell cycle progression [96]. Ryszawy et al. demonstrated that Na^+-ascorbate was capable of triggering significant impairment of GBM cell viability as well as invasiveness [5].

Also, the blockade influence of Na^+-ascorbate on GBM cell motility resulted in heterogeneous viability-associated cell responses [5]. Moreover, a rapid necrotic-like death was detected in a proportion of cells with Na^+-ascorbate, which resulted in cell swelling, membrane break, and their release from cytoplasm [5]. Furthermore, "autoschizis"-associated violent cell responses to elevated Na^+-ascorbate doses substituted apoptosis in "hypersensitive" GBM cells [5]. This cell death mechanism was a self-excision of cytoplasm and was detected only in the coexistence of vitamin C and menadione [98, 99].

1.5. Vitamin C and Glioma Angiogenesis. Angiogenesis is a normal physiological activity, obligatory for normal tissue repair as well as growth [100]. Nevertheless, angiogenesis is depicted by the assiduous proliferation of endothelial cells as well as blood vessel formation in pathological situations [100]. Thus, angiogenesis is very critical in tumor growth, invasion, and metastasis [100]. Studies have implicated the association of circulating endothelial precursor cells (EPCs) to pathologic angiogenesis [101–103]. Several studies have demonstrated that nitric oxide (NO) was associated with tumor angiogenesis [104–106].

Dulak et al. demonstrated that NO was capable of modulating for the secretion of endogenous angiogenic factors like vascular endothelial growth factor (VEGF) as well as basic fibroblast growth factor (bFGF) [107]. Studies established that tumors that produced NO persistently had significantly supplementary vascular network and were more invasive [108, 109]. Thus, angiogenesis is determined by the level of NO, which also influence migration as well as precise motivity of the endothelial cells [100, 110].

Telang et al. analyzed the effect of vitamin C on tumor development in animals after dietary consumption of low levels [111]. Peyman et al. established that the total number of blood vessels were decreased in vitamin C depleted tumors compared to the totally supplemented animals. Contrariwise, high levels of vitamin C administered to cauterized corneas suppressed angiogenesis in a rat prototype [112]. Mikirova et al. evaluated the effect of high levels of vitamin C (100 mg/dl–300 mg/dl) on *in vitro* endothelial cells as well as new blood vessel formation [100]. They observed that IV administration of 25–60 grams of vitamin C affect both endothelial progenitor cells as well as mature endothelial cell functions associated with process of angiogenesis (Figure 2) [100].

Furthermore, the effect of vitamin C on angiogenesis assessed via tube formation assay exhibited blockade of vessel structure after 3–24 h of exposure of the cells to vitamin C (Figure 2) [100]. This appeared as a result of vitamin C ability to block NO in endothelial cells (Figure 2) [100]. Duda et al. established that NO is a key stimulus of new blood vessel formation [113]. Thus, vitamin C was capable of inhibiting NO stimulation resulting in the inhibition of angiogenesis as well as vasculogenesis (Figure 2) [113].

1.6. Signaling Pathways of Vitamin C in Glioma. Vitamin C was implicated in several signal pathways associated with the development of glioma [114–119]. Vitamin C had much a stronger influence on the crucial stages of tumor cell proliferation as well as differentiation by shifting their epigenome and transcriptome. Naidu et al. observed antiproliferative as well as apoptotic effects of vitamin C on T98G glioma cells via modulation of IGF-IR secretion subsequent to the facilitation of programmed cell death [96]. Also, vitamin C was capable of upregulating proteolipid protein (PLP) as well as myelin-associated glycoprotein (MAG) genes in glioma C6 cells of rat models (Figure 2) [76].

Nuclear factor erythroid 2-related factor 2 (Nrf2) is a fundamental constituent of cellular defense against a wide range of endogenous as well as exogenous stresses [114]. It was observed that vitamin C was capable of influencing Nrf2 in GBM (Figure 2) [114]. Hypoxia-inducible factor 1α (HIF-1α) is a transcription factor responsible for the cellular reaction to low O_2 conditions via the modulation of genes regulating various cellular transduction pathways [115]. HIF-1α further modulates growth and apoptosis, cell migration, energy metabolism, angiogenesis, and transport of metal ions and glucose [115]. HIF-1α is often intensely oversecreted in common cancers, cancer cell lines, and metastases [116].

Several studies have demonstrated that therapeutic levels of vitamin C downregulated cell survival pathways in cancer cells via HIF-1α as well as the nuclear transcription factor (NF-κB) [117–119]. Vitamin C was capable of regulating HIF-1α in common cancers including glioma [120]. Also, vitamin C was able to promote prolyl as well as lysyl hydroxylases in the hydroxylation of HIF-1α (Figure 2) [120]. It was established that low vitamin C levels were able to decrease HIF-1α hydroxylation resulting in the promotion of HIF-dependent gene transcription as well as tumor growth [120]. Bi et al. established that over secretion of Bcl-2 and blockade of Bax secretion correlated well with anti-apoptosis/apoptosis imbalance of glioma cells (Figure 2) [121].

Duan et al. demonstrated that Maitake mushroom (MP)/vitamin C was able to inhibit the proliferation of glioma cells, augmented tumor cell apoptosis, and reduced mRNA/protein secretion of Bcl-2 while augmenting Bax mRNA or protein secretion (Figure 2) [7]. They further observed augmentation in the secretion of caspase-3 as well as its endogenous substrate, cleavage of PARP [7]. Moreover, MP/vitamin C was able activate key mediators of the apoptosis pathway, such as caspase-3, caspase-8, and caspase-9 in M059 K cells (Figure 2) [7]. Thus, the combination of MP and VC triggered M059 K cell apoptosis [7]. Holme et al. revealed that vitamin C was capable of decreasing the cytotoxic properties of N-hydroxy-acetylaminofluorene and decrease the covalent binding of N-acetyl-2-aminofluorene (AAF) to cellular protein [122]. Further studies are needed to establish the effect of vitamin C on this protein in glioma.

Hung established that rat glial tumor cells possess N-acetyltransferase (NAT) properties [123]. Furthermore, the rat's brain tissue was able to modulate NAT activity as well as the stimulation of N-acetylation of 2-aminofluorene (AF) (Figure 2) [124]. Hung and Lu demonstrated that vitamin C was able to block NAT activity in C6 glioma cells [125]. They also revealed that vitamin C reduced AF-DNA adduct formation in C6 glioma cells, but vitamin C did not influence DNA to transcript NAT mRNA [125]. Miller and Miller showed that AF is N-acetylated via NAT and subsequently metabolized via cytochrome P450 (CYP) into a reactive metabolite, which binds to DNA to form DNA-AF metabolite adduct (Figure 2) [126].

1.7. Vitamin C in Glioma Treatment. Cameron and Pauling in 1976 suggested that IV vitamin C followed by oral maintenance was a beneficial therapy for patients with cancer [127]. Thus, vitamin C, specifically at high therapeutic levels, has a long and widely been used as cancer treatment in history [127, 128]. IV vitamin C was demonstrated to be toxic to tumor cells, but not to normal cells [129]. Furthermore, IV vitamin C was capable of inhibiting angiogenesis and inflammation, boosts the immune system, causes differentiation of cells, and improves quality of life of patients with cancer [100].

Currently, temozolomide is the drug of choice for the management of patients with glioma [24, 25, 130]. It is an orally bioavailable, methylating agent that is able to pass through the BBB and trigger the death of tumor cells [24, 25]. Nevertheless, some tumor cells are capable of repairing DNA damage triggered by temozolomide and thus lessen the efficiency of the therapy [24, 25]. Laboratory and clinical studies have demonstrated that temozolomide's anticancer efficiency was augmented when combined with etoposide [24, 25].

Gokturk et al. demonstrated that vitamin C alone was capable of triggering oxidative DNA damage in glioma [130]. They revealed that cytotoxic as well as genotoxic effects of temozolomide and etoposide were reduced by vitamin C, but the utmost cytotoxicity with the least genotoxicity was attained with use of the triple therapy [130]. Thus, vitamin C reduced the cytotoxic as well as genotoxic effect of the etoposide and etoposide-temozolomide combination, but it had no significant effect on temozolomide's toxicity [130].

Mikirova et al. were able to treat neurofibromatosis type 1 (NF1) patient with optic pathway glioma (OPG) with a high dose of IV vitamin C [131]. They suggested that vitamin C treatment may be appropriate for young patients' glioma who are not suitable to receive standard treatments regimes due to their toxicity [131]. Studies have demonstrated that

radiotherapy offers a 6-month survival benefit at a median time frame for glioma patients [132, 133]. Herst et al. demonstrated that radiation dose of 2-Gy fractions alone for GBM patients and vitamin C alone at concentrations >1 mM was effective for GBM patients [21].

Herst et al. indicated further that combination therapy using 0.5 mM vitamin C and lower radiation dose of 1-Gy fraction killed considerably more primary GBM cells and astrocytoma cells compared with single therapy [21]. Nevertheless, the combination therapy had a much lesser effect on normal astrocytes, suggesting a certain level of specificity for GBM cells [21]. Thus, they study exhibited that in the clinical situation, combination therapy triggers more specific GBM killing with lower doses of radiation as well as less damage to adjacent, healthy tissues [21].

Herst et al. demonstrated that administration of vitamin C was capable of inhibiting radiation-stimulated G2/M arrest in GBM primary cells, but not in astrocytes, inhibiting homologous recombination and hence DSB repair, which was specifically poor in GBM cells compared with normal astrocytes [21]. Furthermore, both vitamin C and radiation therapy were able to trigger cell death associated with autophagy [134]. Autophagy is a salvaging mechanism that is stimulated in cells under stress [135]. Studies have demonstrated that 5 mM vitamin C, 6-Gy fractions, or combined therapy did not trigger apoptotic cell death in GBM primary cell [134, 136].

Herst et al. postulated that our cells primarily use autophagy as a survival mechanism after exposure to radiation, vitamin C, or combined treatment [21]. They concluded that high-dose combination of vitamin C and radiation has a much more profound cytotoxic effect on primary GBM cells compared to normal astrocytes, and this combination could be a safe as well as clinically viable alternative for treating aggressive radiation-resistant GBMs [21]. Prasad et al. report that vitamin C at nontoxic doses potentiated growth inhibitory capabilities of 5-fluorouracil (5-FUra), bleomycin sulfate, sodium butyrate, cyclic AMP stimulating agents, and X-irradiation on neuroblastoma (NB) cells, but it did not yield analogous capabilities on rat glioma cells in culture [137].

Prasad et al. further postulated that if vitamin C is used arbitrarily in combined therapies, it may reduce the efficiency of some chemotherapeutic agents [137]. They indicated that vitamin C was capable of reducing the cytotoxic effect of methotrexate as well as 5-(3,3-dimethyl-btriazeno)-imidazole-4-carboxamide (DTIC) on NB cells in culture [137]. This was perhaps due to deactivation of these medicines *in vitro* by vitamin C [137]. Prasad et al. in another study demonstrated that vitamin C at nontoxic doses significantly potentiated the effect of methylmercuric chloride (MMC) on NB cells while it did not alter the effect of MMC on glioma cells [137].

The effect of vitamin C was most distinct at a MMC doses of 1 μM [137]. Moreover, vitamin C was similarly effective in potentiating the effect of MMC on NB cells, but glutathione did not exhibit similar effect [137]. Schoenfeld et al. demonstrate that increased labile Fe^{2+} pool levels, triggered by mitochondrial superoxide and H_2O_2, expressively participated in cancer cell-selective toxicity of therapeutic vitamin C combined with standard radio-chemotherapy in GBM models [138]. They postulated that augmented labile Fe^{2+} in cancer cells triggered an upsurge in oxidation of vitamin C to produce H_2O_2 capable of further aggravating the differences in labile Fe^{2+} in cancer compared to normal cells [138].

The above occurred, at least partly, because of H_2O_2-mediated interference of Fe-S cluster-containing proteins [138]. The augmented levels of H_2O_2, in the company of an augmented labile Fe^{2+} pool, triggered an upsurge in Fenton chemistry to produce hydroxyl radicals resulting in oxidative damage [138]. Sharma and Khanna showed that vitamin C inhibited etorphine-stimulated compensatory upsurge in the concentrations of cyclic AMP with slight or no influence on the temporary response of NG108-15 hybrid cells to the effector agents, but it had no effect on the temporary blockade response of the cells to the drug [139].

Sharma and Khanna suggest the potential use of vitamin C in the prevention of the development of tolerance in therapeutic usage of narcotics as analgesics [139]. Vita et al. demonstrated that menadione alone or in combination with vitamin C exhibited similar concentration-response curves as well as IC50 values [140]. They indicated that menadione: vitamin C at a ratio of 1 : 100 exhibited higher antiproliferative activity when compared to each medicine alone and permitted to decrease each medicine concentration between 2.5 and 5-fold [140]. Analogous antiproliferative effects were exhibited in 8 patients derived GBM cell cultures [140].

2. Conclusion

The dietary intake of vitamin C has protective effect on glioma risk. Neurons store high levels of vitamin C via SVCTs to protect them from oxidative ischemia-reperfusion injury. The key function of vitamin C is the inhibition of redox imbalance from ROS produced via the stimulation of glutamate receptors. Vitamin C is able to inhibit DNA damage and the deterioration of subcellular structures like proteins, lipids, and DNA by scavenging of ROS. Also, therapeutic concentrations of vitamin C are capable of triggering H_2O_2 generation in solid tumors including glioma. The total number of blood vessels was decreased in vitamin C depleted tumors compared to the totally supplemented animals, which means that vitamin C is capable of inhibiting tumor angiogenesis. High-dose combination of vitamin C and radiation has a much more profound cytotoxic effect on primary GBM cells compared to normal astrocytes, and this combination could be a safe as well as clinically viable alternative for treating aggressive radiation-resistant GBMs. Control trials are needed to validate the use of vitamin C and standardization of the doses of vitamin C in the treatment of patients with glioma.

Abbreviations

AF: 2-Aminofluorene
5-FUra: 5-Fluorouracil
DTIC: 5-(3,3-Dimethyl-btriazeno)-imidazole-4-carboxamide

Asc-S: Ascorbyl stearate
BBB: Blood-brain barrier
bFGF: Basic fibroblast growth factor
CNS: Central nervous system
CSF: Cerebrospinal fluid
CYP: Cytochrome P450
DHA: Dehydroascorbate
DHAR: DHA reductase
DNA: Deoxyribonucleic acid
ECF: Extracellular fluid
EPCs: Endothelial precursor cells
GBM: Glioblastoma multiforme
H_2O_2: Hydrogen peroxide
HIF-1α: Hypoxia-inducible factor 1α
IV: Intravenous
IGF: Insulin-like growth factor
mM: Millimolar
MAG: Myelin-associated glycoprotein
MMC: Methylmercuric chloride
NO: Nitric oxide
Nrf2: Nuclear factor erythroid 2-related factor 2
NF-κB: Nuclear transcription factor
NAT: N-acetyltransferase
NF1: Neurofibromatosis type 1
NB: Neuroblastoma
OPG: Optic pathway glioma
PLP: Proteolipid protein
ROS: Reactive oxygen species
SVCTs: Sodium-dependent vitamin C transporters
VEGF: Vascular endothelial growth factor.

Data Availability

No data were used in this paper.

Conflicts of Interest

The authors have no conflicts of interest.

Authors' Contributions

All the authors contributed toward literature search, drafting, and critical revision of the paper and agree to be accountable for all aspects of the work.

References

[1] M. Liu, B. Dai, S.-H. Kang et al., "FoxM1B is overexpressed in human glioblastomas and critically regulates the tumorigenicity of glioma cells," *Cancer Research*, vol. 66, no. 7, pp. 3593–3602, 2006.

[2] T. S. Surawicz, F. Davis, S. Freels, E. R. Laws Jr., and H. R. Menck, "Brain tumor survival: results from the national cancer data base," *Journal of Neuro-Oncology*, vol. 40, no. 2, pp. 151–160, 1998.

[3] R. Siegel, D. Naishadham, and A. Jemal, "Cancer statistics, 2013," *CA: A Cancer Journal for Clinicians*, vol. 63, no. 1, pp. 11–30, 2013.

[4] S. A. Richard, "Novel pathogenic, biomarker and therapeutic potentials of Foxm1 in glioma," *NeuroQuantology*, vol. 17, no. 6, 2019.

[5] D. Ryszawy, M. Pudełek, J. Catapano et al., "High doses of sodium ascorbate interfere with the expansion of glioblastoma multiforme cells in vitro and in vivo," *Life Sciences*, vol. 232, Article ID 116657, 2019.

[6] C. G. Garcia, S. A. Kahn, L. H. M. Geraldo et al., "Combination therapy with sulfasalazine and valproic acid promotes human glioblastoma cell death through imbalance of the intracellular oxidative response," *Molecular Neurobiology*, vol. 55, no. 8, pp. 6816–6833, 2018.

[7] L. Duan, X.-L. Wu, F. Zhao, R. Zeng, and K.-H. Yang, "Induction effect to apoptosis by Maitake polysaccharide: synergistic effect of its combination with vitamin C in neuroglioma cell," *Journal of Evidence-Based Complementary & Alternative Medicine*, vol. 22, no. 4, pp. 667–674, 2017.

[8] H. Tsukaguchi, T. Tokui, B. Mackenzie et al., "A family of mammalian Na+-dependent L-ascorbic acid transporters," *Nature*, vol. 399, no. 6731, pp. 70–75, 1999.

[9] R. C. Rose and A. M. Bode, "Biology of free radical scavengers: an evaluation of ascorbate," *The FASEB Journal*, vol. 7, no. 12, pp. 1135–1142, 1993.

[10] A. Sorice, E. Guerriero, F. Capone, G. Colonna, G. Castello, and S. Costantini, "Ascorbic acid: its role in immune system and chronic inflammation diseases," *Mini Reviews in Medicinal Chemistry*, vol. 14, no. 5, pp. 444–452, 2014.

[11] S. Zhou, X. Wang, Y. Tan, L. Qiu, H. Fang, and W. Li, "Association between vitamin C intake and glioma risk: evidence from a meta-analysis," *Neuroepidemiology*, vol. 44, no. 1, pp. 39–44, 2015.

[12] D. Pouliquen, C. Olivier, E. Hervouet et al., "Dietary prevention of malignant glioma aggressiveness, implications in oxidant stress and apoptosis," *International Journal of Cancer*, vol. 123, no. 2, pp. 288–295, 2008.

[13] S. D. Newell Jr., J. Kapp, and J. H. Romfh, "Evaluation of megadose vitamin therapy in an experimental brain tumor," *Surgical Neurology*, vol. 16, no. 2, pp. 161–164, 1981.

[14] E. Cameron and L. Pauling, "The orthomolecular treatment of cancer I. The role of ascorbic acid in host resistance," *Chemico-Biological Interactions*, vol. 9, no. 4, pp. 273–283, 1974.

[15] K. N. Prasad, "Modulation of the effects of tumor therapeutic agents by vitamin C," *Life Sciences*, vol. 27, no. 4, pp. 275–280, 1980.

[16] C. W. M. Wilson, "Clinical pharmacological aspects of ascorbic acid," *Annals of the New York Academy of Sciences*, vol. 258, pp. 355–376, 1975.

[17] I. M. Solís-Nolasco, G. Caraballo, M. J. González, J. Olalde, and R. H. Morales-Borges, "Impact of intravenous vitamin C and endolaser therapies on a pediatric brainstem glioma case," *Global Advances in Health and Medicine*, vol. 9, Article ID 2164956120901489, 2020.

[18] J. Du, J. J. Cullen, and G. R. Buettner, "Ascorbic acid: chemistry, biology and the treatment of cancer," *Biochimica et Biophysica Acta (BBA) - Reviews on Cancer*, vol. 1826, no. 2, pp. 443–457, 2012.

[19] C. M. Doskey, V. Buranasudja, B. A. Wagner et al., "Tumor cells have decreased ability to metabolize H_2O_2: implications for pharmacological ascorbate in cancer therapy," *Redox Biology*, vol. 10, pp. 274–284, 2016.

[20] S. Park, "The effects of high concentrations of vitamin C on cancer cells," *Nutrients*, vol. 5, no. 9, pp. 3496–3505, 2013.

[21] P. M. Herst, K. W. R. Broadley, J. L. Harper, and M. J. McConnell, "Pharmacological concentrations of ascorbate radiosensitize glioblastoma multiforme primary cells by increasing oxidative DNA damage and inhibiting G2/M arrest," *Free Radical Biology and Medicine*, vol. 52, no. 8, pp. 1486–1493, 2012.

[22] Q. Chen, M. G. Espey, A. Y. Sun et al., "Ascorbate in pharmacologic concentrations selectively generates ascorbate radical and hydrogen peroxide in extracellular fluid in vivo," *Proceedings of the National Academy of Sciences*, vol. 104, no. 21, pp. 8749–8754, 2007.

[23] S. L. Cuddihy, A. Parker, D. T. Harwood, M. C. M. Vissers, and C. C. Winterbourn, "Ascorbate interacts with reduced glutathione to scavenge phenoxyl radicals in HL60 cells," *Free Radical Biology and Medicine*, vol. 44, no. 8, pp. 1637–1644, 2008.

[24] B. L. Ebert, E. Niemierko, K. Shaffer, and R. Salgia, "Use of temozolomide with other cytotoxic chemotherapy in the treatment of patients with recurrent brain metastases from lung cancer," *The Oncologist*, vol. 8, no. 1, pp. 69–75, 2003.

[25] D. N. Korones, M. Benita-Weiss, T. E. Coyle et al., "Phase I study of temozolomide and escalating doses of oral etoposide for adults with recurrent malignant glioma," *Cancer*, vol. 97, no. 8, pp. 1963–1968, 2003.

[26] M. E. Rice, "Ascorbate regulation and its neuroprotective role in the brain," *Trends in Neurosciences*, vol. 23, no. 5, pp. 209–216, 2000.

[27] D. Hornig, "Distribution of ascorbic acid, metabolites and analogues in man and animals," *Annals of the New York Academy of Sciences*, vol. 258, pp. 103–118, 1975.

[28] K. Milby, A. Oke, and R. N. Adams, "Detailed mapping of ascorbate distribution in rat brain," *Neuroscience Letters*, vol. 28, no. 1, pp. 15–20, 1982.

[29] M. E. Rice, E. J. Lee, and Y. Choy, "High levels of ascorbic acid, not glutathione, in the CNS of anoxia-tolerant reptiles contrasted with levels in anoxia-intolerant species," *Journal of Neurochemistry*, vol. 64, no. 4, pp. 1790–1799, 1995.

[30] M. E. Rice and I. Russo-Menna, "Differential compartmentalization of brain ascorbate and glutathione between neurons and glia," *Neuroscience*, vol. 82, no. 4, pp. 1213–1223, 1998.

[31] R. Spector, "Vitamin homeostasis in the central nervous system," *New England Journal of Medicine*, vol. 296, no. 24, pp. 1393–1398, 1977.

[32] S. Salmaso, J. S. Pappalardo, R. R. Sawant et al., "Targeting glioma cells in vitro with ascorbate-conjugated pharmaceutical nanocarriers," *Bioconjugate Chemistry*, vol. 20, no. 12, pp. 2348–2355, 2009.

[33] W. M. Pardridge, "Recent advances in blood-brain barrier transport," *Annual Review of Pharmacology and Toxicology*, vol. 28, no. 1, pp. 25–39, 1988.

[34] W. M. Pardridge, "Blood-brain barrier biology and methodology," *Journal of Neurovirology*, vol. 5, no. 6, pp. 556–569, 1999.

[35] D. J. Begley, "The blood-brain barrier: principles for targeting peptides and drugs to the central nervous system," *Journal of Pharmacy and Pharmacology*, vol. 48, no. 2, pp. 136–146, 1996.

[36] R. Spector, "Drug transport in the mammalian central nervous system: multiple complex systems," *Pharmacology*, vol. 60, no. 2, pp. 58–73, 2000.

[37] L. Hammarstrom, "Autoradiographic studies on the distribution of C14-labelled ascrobic acid and dehydroascorbic acid," *Acta Physiologica Scandinavica*, vol. 70, no. Suppl. 289, 1967.

[38] D. K. C. Lam and P. M. Daniel, "The influx of ascorbic acid into the rat's brain," *Quarterly Journal of Experimental Physiology*, vol. 71, no. 3, pp. 483–489, 1986.

[39] H. Reiber, M. Ruff, and M. Uhr, "Ascorbate concentration in human cerebrospinal fluid (CSF) and serum. Intrathecal accumulation and CSF flow rate," *Clinica Chimica Acta*, vol. 217, no. 2, pp. 163–173, 1993.

[40] R. Spector and A. Lorenzo, "Ascorbic acid homeostasis in the central nervous system," *American Journal of Physiology-Legacy Content*, vol. 225, no. 4, pp. 757–763, 1973.

[41] M. Castro, T. Caprile, A. Astuya et al., "High-affinity sodium-vitamin C co-transporters (SVCT) expression in embryonic mouse neurons," *Journal of Neurochemistry*, vol. 78, no. 4, pp. 815–823, 2001.

[42] F. A. Beltrán, A. I. Acuña, M. P. Miró, C. Angulo, Concha II, and M. A. Castro, "Ascorbic acid-dependent GLUT3 inhibition is a critical step for switching neuronal metabolism," *Journal of Cellular Physiology*, vol. 226, no. 12, pp. 3286–3294, 2011.

[43] C. C. Portugal, V. S. Miya, K. d. C. Calaza, R. A. M. Santos, and R. Paes-de-Carvalho, "Glutamate receptors modulate sodium-dependent and calcium-independent vitamin C bidirectional transport in cultured avian retinal cells," *Journal of Neurochemistry*, vol. 108, no. 2, pp. 507–520, 2009.

[44] M. A. Castro, C. Angulo, S. Brauchi, F. Nualart, and Concha II, "Ascorbic acid participates in a general mechanism for concerted glucose transport inhibition and lactate transport stimulation," *Pfluegers Archiv European Journal of Physiology*, vol. 457, no. 2, pp. 519–528, 2008.

[45] J. Kume-Kick and M. E. Rice, "Estrogen-dependent modulation of rat brain ascorbate levels and ischemia-induced ascorbate loss," *Brain Research*, vol. 803, no. 1-2, pp. 105–113, 1998.

[46] M. L. Castro, M. J. McConnell, and P. M. Herst, "Radiosensitisation by pharmacological ascorbate in glioblastoma multiforme cells, human glial cells, and HUVECs depends on their antioxidant and DNA repair capabilities and is not cancer specific," *Free Radical Biology and Medicine*, vol. 74, pp. 200–209, 2014.

[47] J. Mandl, A. Szarka, and G. Bánhegyi, "Vitamin C: update on physiology and pharmacology," *British Journal of Pharmacology*, vol. 157, no. 7, pp. 1097–1110, 2009.

[48] J. A. Dykens, A. Stern, and E. Trenkner, "Mechanism of kainate toxicity to cerebellar neurons in vitro is analogous to reperfusion tissue injury," *Journal of Neurochemistry*, vol. 49, no. 4, pp. 1222–1228, 1987.

[49] J. T. Coyle and P. Puttfarcken, "Oxidative stress, glutamate, and neurodegenerative disorders," *Science*, vol. 262, no. 5134, pp. 689–695, 1993.

[50] E. Ciani, L. Grøneng, M. Voltattorni, V. Rolseth, A. Contestabile, and R. E. Paulsen, "Inhibition of free radical production or free radical scavenging protects from the excitotoxic cell death mediated by glutamate in cultures of cerebellar granule neurons," *Brain Research*, vol. 728, no. 1, pp. 1–6, 1996.

[51] A. Atlante, S. Gagliardi, G. M. Minervini, M. T. Ciotti, E. Marra, and P. Calissano, "Glutamate neurotoxicity in rat cerebellar granule cells: a major role for xanthine oxidase in oxygen radical formation," *Journal of Neurochemistry*, vol. 68, no. 5, pp. 2038–2045, 1997.

[52] R. A. Grünewald, "Ascorbic acid in the brain," *Brain Research Reviews*, vol. 18, no. 1, pp. 123–133, 1993.

[53] G. V. Rebec and R. Christopher Pierce, "A vitamin as neuromodulator: ascorbate release into the extracellular fluid of the brain regulates dopaminergic and glutamatergic transmission," *Progress in Neurobiology*, vol. 43, no. 6, pp. 537–565, 1994.

[54] E. J. Diliberto Jr., F. S. Menniti, J. Knoth, A. J. Daniels, J. S. Kizer, and O. H. Viveros, "Adrenomedullary chromaffin cells as a model to study the neurobiology of ascorbic acid: from monooxygenation to neuromodulation," *Annals of the New York Academy of Sciences*, vol. 498, pp. 28–53, 1987.

[55] C.-H. Kuo, N. Yonehara, F. Hata, and H. Yoshida, "Subcellular distribution of ascorbic acid in rat brain," *The Japanese Journal of Pharmacology*, vol. 28, no. 5, pp. 789–791, 1978.

[56] C. C. Glembotski, "The role of ascorbic acid in the biosynthesis of the neuroendocrine peptides α-MSH and TRH," *Annals of the New York Academy of Sciences*, vol. 498, pp. 54–62, 1987.

[57] B. T. Miller and T. J. Cicero, "Ascorbate-induced release of LHRH: noradrenergic and opioid modulation," *Brain Research Bulletin*, vol. 19, no. 1, pp. 95–99, 1987.

[58] C. F. Eldridge, M. B. Bunge, R. P. Bunge, and P. M. Wood, "Differentiation of axon-related Schwann cells in vitro. I. Ascorbic acid regulates basal lamina assembly and myelin formation," *The Journal of Cell Biology*, vol. 105, no. 2, pp. 1023–1034, 1987.

[59] R. D. O'Neill, M. Fillenz, L. Sundstrom, and J. N. P. Rawlins, "Voltammetrically monitored brain ascorbate as an index of excitatory amino acid release in the unrestrained rat," *Neuroscience Letters*, vol. 52, no. 3, pp. 227–233, 1984.

[60] M. G. Boutelle, L. Svensson, and M. Fillenz, "Rapid changes in striatal ascorbate in response to tail-pinch monitored by constant potential voltammetry," *Neuroscience*, vol. 30, no. 1, pp. 11–17, 1989.

[61] G. C. Owens and R. P. Bunge, "Evidence for an early role for myelin-associated glycoprotein in the process of myelination," *Glia*, vol. 2, no. 2, pp. 119–128, 1989.

[62] J. A. Schwartzbaum and D. G. Cornwell, "Oxidant stress and glioblastoma multiforme risk: serum antioxidants, γ-glutamyl transpeptidase, and ferritin," *Nutrition and Cancer*, vol. 38, no. 1, pp. 40–49, 2000.

[63] G. R. Bunin, R. R. Kuijten, J. D. Buckley, L. B. Rorke, and A. T. Meadows, "Relation between maternal diet and subsequent primitive neuroectodermal brain tumors in young children," *New England Journal of Medicine*, vol. 329, no. 8, pp. 536–541, 1993.

[64] G. R. Bunin, R. R. Kuijten, C. P. Boesel, J. D. Buckley, and A. T. Meadows, "Maternal diet and risk of astrocytic glioma in children: a report from the Childrens Cancer Group (United States and Canada)," *Cancer Causes & Control*, vol. 5, no. 2, pp. 177–187, 1994.

[65] H. Boeing, B. Schlehofer, M. Blettner, and J. Wahrendorf, "Dietary carcinogens and the risk for glioma and meningioma in Germany," *International Journal of Cancer*, vol. 53, no. 4, pp. 561–565, 1993.

[66] M. Lee, M. Wrensch, and R. Miike, "Dietary and tobacco risk factors for adult onset glioma in the San Francisco Bay Area (California, USA)," *Cancer Causes & Control*, vol. 8, no. 1, pp. 13–24, 1997.

[67] J. Hu, C. La Vecchia, E. Negri et al., "Diet and brain cancer in adults: a case-control study in northeast China," *International Journal of Cancer*, vol. 81, no. 1, pp. 20–23, 1999.

[68] L. Blowers, W. Mack, and S. Preston-Martin, "Dietary and other lifestyle factors of women with brain gliomas in Los Angeles County (California, USA)," *Cancer Causes & Control*, vol. 8, no. 1, pp. 5–12, 1997.

[69] S. Kaplan, l. Novikov, and B. Modan, "Nutritional factors in the etiology of brain tumors potential role of nitrosamines, fat, and cholesterol," *American Journal of Epidemiology*, vol. 146, no. 10, pp. 832–841, 1997.

[70] G. G. Giles, J. J. McNeil, G. Donnan et al., "Dietary factors and the risk of glioma in adults: results of a case-control study in Melbourne, Australia," *International Journal of Cancer*, vol. 59, no. 3, pp. 357–362, 1994.

[71] L. Mardones, V. Ormazabal, X. Romo et al., "The glucose transporter-2 (GLUT2) is a low affinity dehydroascorbic acid transporter," *Biochemical and Biophysical Research Communications*, vol. 410, no. 1, pp. 7–12, 2011.

[72] S. C. Rumsey, O. Kwon, G. W. Xu, C. F. Burant, I. Simpson, and M. Levine, "Glucose transporter isoforms GLUT1 and GLUT3 transport dehydroascorbic acid," *Journal of Biological Chemistry*, vol. 272, no. 30, pp. 18982–18989, 1997.

[73] R. Daruwala, J. Song, W. S. Koh, S. C. Rumsey, and M. Levine, "Cloning and functional characterization of the human sodium-dependent vitamin C transporters hSVCT1 and hSVCT2," *FEBS Letters*, vol. 460, no. 3, pp. 480–484, 1999.

[74] Y. Wang, B. Mackenzie, H. Tsukaguchi, S. Weremowicz, C. C. Morton, and M. A. Hediger, "Human vitamin C (L-ascorbic acid) transporter SVCT1," *Biochemical and Biophysical Research Communications*, vol. 267, no. 2, pp. 488–494, 2000.

[75] F. Nualart, L. Mack, A. García et al., "Vitamin C transporters, recycling and the bystander effect in the nervous system: SVCT2 versus gluts," *Journal of Stem Cell Research & Therapy*, vol. 4, no. 5, p. 209, 2014.

[76] I. Laszkiewicz, R. C. Wiggins, and G. Konat, "Ascorbic acid upregulates myelin gene expression in C6 glioma cells," *Metabolic Brain Disease*, vol. 7, no. 3, pp. 157–164, 1992.

[77] K. A. Conklin, "Chemotherapy-associated oxidative stress: impact on chemotherapeutic effectiveness," *Integrative Cancer Therapies*, vol. 3, no. 4, pp. 294–300, 2004.

[78] B. D. Lawenda, K. M. Kelly, E. J. Ladas, S. M. Sagar, A. Vickers, and J. B. Blumberg, "Should supplemental antioxidant administration be avoided during chemotherapy and radiation therapy?" *JNCI Journal of the National Cancer Institute*, vol. 100, no. 11, pp. 773–783, 2008.

[79] G. Waris and H. Ahsan, "Reactive oxygen species: role in the development of cancer and various chronic conditions," *Journal of Carcinogenesis*, vol. 5, no. 1, p. 14, 2006.

[80] L. Benade, T. Howard, and D. Burk, "Synergistic killing of Ehrlich ascites carcinoma cells by ascorbate and 3-amino-1,2,4,-triazole," *Oncology*, vol. 23, no. 1, pp. 33–43, 1969.

[81] Q. Chen, M. G. Espey, M. C. Krishna et al., "Pharmacologic ascorbic acid concentrations selectively kill cancer cells: action as a pro-drug to deliver hydrogen peroxide to tissues," *Proceedings of the National Academy of Sciences*, vol. 102, no. 38, pp. 13604–13609, 2005.

[82] M. G. Espey, P. Chen, B. Chalmers et al., "Pharmacologic ascorbate synergizes with gemcitabine in preclinical models of pancreatic cancer," *Free Radical Biology and Medicine*, vol. 50, no. 11, pp. 1610–1619, 2011.

[83] B. Peterkofsky and W. Prather, "Cytotoxicity of ascorbate and other reducing agents towards cultured fibroblasts as a result of hydrogen peroxide formation," *Journal of Cellular Physiology*, vol. 90, no. 1, pp. 61–70, 1977.

[84] H. S. Jacob and S. E. Lux, "Degradation of membrane phospholipids and thiols in peroxide hemolysis: studies in

vitamin E deficiency," *Blood*, vol. 32, no. 4, pp. 549–568, 1968.

[85] J. E. Smolen and S. B. Shohet, "Permeability changes induced by peroxidation in liposomes prepared from human erythrocyte lipids," *Journal of Lipid Research*, vol. 15, no. 3, pp. 273–280, 1974.

[86] N. M. Payton, M. F. Wempe, Y. Xu, and T. J. Anchordoquy, "Long-term storage of lyophilized liposomal formulations," *Journal of Pharmaceutical Sciences*, vol. 103, no. 12, pp. 3869–3878, 2014.

[87] C. W. M. Orr, "Studies on ascorbic acid. I. Factors influencing the ascorbate-mediated inhibition of catalase*," *Biochemistry*, vol. 6, no. 10, pp. 2995–3000, 1967.

[88] A. Mitra, S. Govindwar, and A. P. Kulkarni, "Inhibition of hepatic glutathione-S-transferases by fatty acids and fatty acid esters," *Toxicology Letters*, vol. 58, no. 2, pp. 135–141, 1991.

[89] A. Mitra, S. Govindwar, P. Joseph, and A. Kulkarni, "Inhibition of human term placental and fetal liver glutathione-S-transferases by fatty acids and fatty acid esters," *Toxicology Letters*, vol. 60, no. 3, pp. 281–288, 1992.

[90] W. A. Banks and A. J. Kastin, "Peptides and the blood-brain barrier: lipophilicity as a predictor of permeability," *Brain Research Bulletin*, vol. 15, no. 3, pp. 287–292, 1985.

[91] A. K. Naidu, M. Wiranowska, S. H. Kori, L. D. Prockop, and A. P. Kulkarni, "Inhibition of human glioma cell proliferation and glutathione S-transferase by ascorbyl esters and interferon," *Anticancer Research*, vol. 13, no. 5a, pp. 1469–1475, 1993.

[92] A. K. Naidu, M. Wiranowska, S. H. Kori, K. C. Roetzheim, and A. P. Kulkarni, "Inhibition of cell proliferation and glutathione S-transferase by ascorbyl esters and interferon in mouse glioma," *Journal of Neuro-Oncology*, vol. 16, no. 1, pp. 1–10, 1993.

[93] Y. Makino, H. Sakagami, and M. Takeda, "Induction of cell death by ascorbic acid derivatives in human renal carcinoma and glioblastoma cell lines," *Anticancer Research*, vol. 19, no. 4b, pp. 3125–3132, 1999.

[94] W. Zumkeller, R. Biernoth, S. Kocialkowski et al., "Expression and synthesis of insulin-like growth factor (IGF)-I, -II and their receptors in human glioma cell lines," *International Journal of Oncology*, vol. 9, no. 5, pp. 983–992, 1996.

[95] A. C. Sandberg-Nordqvist, P. A. Ståhlbom, M. Reinecke, V. P. Collins, H. von Holst, and V. Sara, "Characterization of insulin-like growth factor 1 in human primary brain tumors," *Cancer Research*, vol. 53, no. 11, pp. 2475–2478, 1993.

[96] K. A. Naidu, J. Liu Tang, K. Akhilender Naidu, L. D. Prockop, S. V. Nicosia, and D. Coppola, "Antiproliferative and apoptotic effect of ascorbyl stearate in human glioblastoma multiforme cells: modulation of insulin-like growth factor-I receptor (IGF-IR) expression," *Journal of Neuro-Oncology*, vol. 54, no. 1, pp. 15–22, 2001.

[97] G. N. Bijur, B. Briggs, C. L. Hitchcock, and M. V. Williams, "Ascorbic acid-dehydroascorbate induces cell cycle arrest at G2/M DNA damage checkpoint during oxidative stress," *Environmental and Molecular Mutagenesis*, vol. 33, no. 2, pp. 144–152, 1999.

[98] J. Gilloteaux, J. M. Jamison, D. Arnold et al., "Cancer cell necrosis by autoschizis: synergism of antitumor activity of vitamin C: vitamin K3 on human bladder carcinoma T24 cells," *Scanning*, vol. 20, no. 8, pp. 564–575, 1998.

[99] J. Gilloteaux, J. M. Jamison, D. R. Neal, M. Loukas, T. Doberzstyn, and J. L. Summers, "Cell damage and death by autoschizis in human bladder (RT4) carcinoma cells resulting from treatment with ascorbate and menadione," *Ultrastructural Pathology*, vol. 34, no. 3, pp. 140–160, 2010.

[100] N. A. Mikirova, T. E. Ichim, and N. H. Riordan, "Anti-angiogenic effect of high doses of ascorbic acid," *Journal of Translational Medicine*, vol. 6, no. 1, p. 50, 2008.

[101] R. G. Bagley, J. Walter-Yohrling, X. Cao et al., "Endothelial precursor cells as a model of tumor endothelium: characterization and comparison with mature endothelial cells," *Cancer Research*, vol. 63, no. 18, pp. 5866–5873, 2003.

[102] M. Peichev, A. J. Naiyer, D. Pereira et al., "Expression of VEGFR-2 and AC133 by circulating human CD34+ cells identifies a population of functional endothelial precursors," *Blood*, vol. 95, no. 3, pp. 952–958, 2000.

[103] H. Bompais, J. Chagraoui, X. Canron et al., "Human endothelial cells derived from circulating progenitors display specific functional properties compared with mature vessel wall endothelial cells," *Blood*, vol. 103, no. 7, pp. 2577–2584, 2004.

[104] O. Gallo, I. Fini-Storchi, W. A. Vergari et al., "Role of nitric oxide in angiogenesis and tumor progression in head and neck cancer," *Journal of the National Cancer Institute: Journal of the National Cancer Institute*, vol. 90, no. 8, pp. 587–596, 1998.

[105] L. C. Jadeski and P. K. Lala, "Nitric oxide synthase inhibition by NG-nitro-l-arginine methyl ester inhibits tumor-induced angiogenesis in mammary tumors," *American Journal Of Pathology*, vol. 155, no. 4, pp. 1381–1390, 1999.

[106] P. C. Lee, A. N. Salyapongse, G. A. Bragdon et al., "Impaired wound healing and angiogenesis in eNOS-deficient mice," *American Journal of Physiology - Heart and Circulatory Physiology*, vol. 277, no. 4, pp. H1600–H1608, 1999.

[107] J. Dulak, A. Józkowicz, A. Dembinska-Kiec et al., "Nitric oxide induces the synthesis of vascular endothelial growth factor by rat vascular smooth muscle cells," *Arteriosclerosis, Thrombosis, and Vascular Biology*, vol. 20, no. 3, pp. 659–666, 2000.

[108] V. V. Holotiuk, A. Y. Kryzhanivska, I. K. Churpiy, B. B. Tataryn, and D. Y. Ivasiutyn, "Role of nitric oxide in pathogenesis of tumor growth and its possible application in cancer treatment," *Experimental Oncology*, vol. 41, no. 3, pp. 210–215, 2019.

[109] D. C. Jenkins, I. G. Charles, L. L. Thomsen et al., "Roles of nitric oxide in tumor growth," *Proceedings of the National Academy of Sciences*, vol. 92, no. 10, pp. 4392–4396, 1995.

[110] J.-P. Gratton, M. I. Lin, J. Yu et al., "Selective inhibition of tumor microvascular permeability by cavtratin blocks tumor progression in mice," *Cancer Cell*, vol. 4, no. 1, pp. 31–39, 2003.

[111] S. Telang, A. L. Clem, J. W. Eaton, and J. Chesney, "Depletion of ascorbic acid restricts angiogenesis and retards tumor growth in a mouse model," *Neoplasia*, vol. 9, no. 1, pp. 47–56, 2007.

[112] G. A. Peyman, M. Kivilcim, A. M. Morales, J. T. DellaCroce, and M. D. Conway, "Inhibition of corneal angiogenesis by ascorbic acid in the rat model," *Graefe's Archive for Clinical and Experimental Ophthalmology*, vol. 245, no. 10, pp. 1461–1467, 2007.

[113] D. G. Duda, D. Fukumura, and R. K. Jain, "Role of eNOS in neovascularization: No for endothelial progenitor cells," *Trends in Molecular Medicine*, vol. 10, no. 4, pp. 143–145, 2004.

[114] J. Zhu, H. Wang, Y. Fan et al., "Targeting the NF-E2-related factor 2 pathway: a novel strategy for glioblastoma (review)," *Oncology Reports*, vol. 32, no. 2, pp. 443–450, 2014.

[115] C. J. Schofield and P. J. Ratcliffe, "Oxygen sensing by HIF hydroxylases," *Nature Reviews Molecular Cell Biology*, vol. 5, no. 5, pp. 343–354, 2004.

[116] H. Zhong, A. M. De Marzo, E. Laughner et al., "Overexpression of hypoxia-inducible factor 1alpha in common human cancers and their metastases," *Cancer Research*, vol. 59, no. 22, pp. 5830–5835, 1999.

[117] M. C. M. Vissers, S. P. Gunningham, M. J. Morrison, G. U. Dachs, and M. J. Currie, "Modulation of hypoxia-inducible factor-1 alpha in cultured primary cells by intracellular ascorbate," *Free Radical Biology and Medicine*, vol. 42, no. 6, pp. 765–772, 2007.

[118] M. C. M. Vissers and R. P. Wilkie, "Ascorbate deficiency results in impaired neutrophil apoptosis and clearance and is associated with up-regulation of hypoxia-inducible factor 1α," *Journal of Leukocyte Biology*, vol. 81, no. 5, pp. 1236–1244, 2007.

[119] S.-S. Han, K. Kim, E.-R. Hahm et al., "L-ascorbic acid represses constitutive activation of NF-?B and COX-2 expression in human acute myeloid leukemia, HL-60," *Journal of Cellular Biochemistry*, vol. 93, no. 2, pp. 257–270, 2004.

[120] E. Flashman, S. L. Davies, K. K. Yeoh, and C. J. Schofield, "Investigating the dependence of the hypoxia-inducible factor hydroxylases (factor inhibiting HIF and prolyl hydroxylase domain 2) on ascorbate and other reducing agents," *Biochemical Journal*, vol. 427, no. 1, pp. 135–142, 2010.

[121] D. Bi, M. Yang, X. Zhao, and S. Huang, "Effect of cnidium lactone on serum mutant P53 and BCL-2/BAX expression in human prostate cancer cells PC-3 tumor-bearing BALB/C nude mouse model," *International Medical Journal of Experimental and Clinical Research*, vol. 21, pp. 2421–2427, 2015.

[122] J. r. A. Holme and E. J. Søderlund, "Modulation of genotoxic and cytotoxic effects of aromatic amines in monolayers of rat hepatocytes," *Cell Biology and Toxicology*, vol. 1, no. 1, pp. 95–110, 1984.

[123] C. F. Hung, "Effects of carmustine and lomustine on arylamine N-acetyltransferase activity and 2-aminofluorene-DNA adducts in rat glial tumor cells," *Neurochemical Research*, vol. 25, no. 6, pp. 845–851, 2000.

[124] S. S. Lin, C. F. Hung, C. C. Ho, Y. H. Liu, H. C. Ho, and J. G. Chung, "Effects of ellagic acid by oral administration on N-acetylation and metabolism of 2-aminofluorene in rat brain tissues," *Neurochemical Research*, vol. 25, no. 11, pp. 1503–1508, 2000.

[125] C. F. Hung and K. H. Lu, "Vitamin C inhibited DNA adduct formation and arylamine N-acetyltransferase activity and gene expression in rat glial tumor cells," *Neurochemical Research*, vol. 26, no. 10, pp. 1107–1112, 2001.

[126] E. C. Miller and J. A. Miller, "The carcinogenic activities of certain analogues of 2-acetyl-aminofluorene in the rat," *Cancer Research*, vol. 9, no. 8, pp. 504–509, 1949.

[127] E. Cameron and L. Pauling, "Supplemental ascorbate in the supportive treatment of cancer: prolongation of survival times in terminal human cancer," *Proceedings of the National Academy of Sciences*, vol. 73, no. 10, pp. 3685–3689, 1976.

[128] E. Cameron and A. Campbell, "The orthomolecular treatment of cancer II. Clinical trial of high-dose ascorbic acid supplements in advanced human cancer," *Chemico-Biological Interactions*, vol. 9, no. 4, pp. 285–315, 1974.

[129] N. H. Riordan, H. D. Riordan, X. Meng, Y. Li, and J. A. Jackson, "Intravenous ascorbate as a tumor cytotoxic chemotherapeutic agent," *Medical Hypotheses*, vol. 44, no. 3, pp. 207–213, 1995.

[130] D. Gokturk, H. Kelebek, S. Ceylan, and D. M. Yilmaz, "The effect of ascorbic acid over the etoposide- and temozolomide-mediated cytotoxicity in glioblastoma cell culture: a molecular study," *Turkish neurosurgery*, vol. 28, no. 1, pp. 13–18, 2018.

[131] N. Mikirova, R. Hunnunghake, R. C. Scimeca et al., "High-dose intravenous vitamin C treatment of a child with neurofibromatosis type 1 and optic pathway glioma: a case report," *American Journal of Case Reports*, vol. 17, pp. 774–781, 2016.

[132] M. Brada, "Radiotherapy in malignant glioma," *Annals of Oncology*, vol. 17, no. Suppl 10, pp. x183–x185, 2006.

[133] M. D. Walker, E. Alexander Jr., W. E. Hunt et al., "Evaluation of BCNU and/or radiotherapy in the treatment of anaplastic gliomas," *Journal of Neurosurgery*, vol. 49, no. 3, pp. 333–343, 1978.

[134] K. C. Yao, T. Komata, Y. Kondo, T. Kanzawa, S. Kondo, and I. M. Germano, "Molecular response of human glioblastoma multiforme cells to ionizing radiation: cell cycle arrest, modulation of cyclin-dependent kinase inhibitors, and autophagy," *Journal of Neurosurgery*, vol. 98, no. 2, pp. 378–384, 2003.

[135] B. Levine, "Autophagy and cancer," *Nature*, vol. 446, no. 7137, pp. 745–747, 2007.

[136] A. H. Stegh, L. Chin, D. N. Louis, and R. A. DePinho, "What drives intense apoptosis resistance and propensity for necrosis in glioblastoma? A role for Bcl2L12 as a multifunctional cell death regulator," *Cell Cycle*, vol. 7, no. 18, pp. 2833–2839, 2008.

[137] K. N. Prasad, P. K. Sinha, M. Ramanujam, and A. Sakamoto, "Sodium ascorbate potentiates the growth inhibitory effect of certain agents on neuroblastoma cells in culture," *Proceedings of the National Academy of Sciences*, vol. 76, no. 2, pp. 829–832, 1979.

[138] J. D. Schoenfeld, Z. A. Sibenaller, K. A. Mapuskar et al., "O_2–and H_2O_2 -mediated disruption of Fe metabolism causes the differential susceptibility of NSCLC and GBM cancer cells to pharmacological ascorbate," *Cancer Cell*, vol. 31, no. 4, pp. 487–500, 2017.

[139] S. K. Sharma and N. C. Khanna, "Ascorbate suppresses the opiate-induced compensatory increase in cyclic AMP in neuroblastoma × glioma hybrid cells," *Biochemical Journal*, vol. 208, no. 1, pp. 43–46, 1982.

[140] M. F. Vita, N. Nagachar, D. Avramidis et al., "Pankiller effect of prolonged exposure to menadione on glioma cells: potentiation by vitamin C," *Investigational New Drugs*, vol. 29, no. 6, pp. 1314–1320, 2011.

Hindawi
Journal of Oncology
Volume 2021, Article ID 9031975, 12 pages
https://doi.org/10.1155/2021/9031975

Research Article

Chemotherapeutic and Safety Profile of a Fraction from *Mimosa caesalpiniifolia* Stem Bark

Paulo Michel Pinheiro Ferreira,[1,2] **Renata Rosado Drumond**,[1,2] **Jurandy do Nascimento Silva**,[1,2] **Ian Jhemes Oliveira Sousa**,[1] **Marcus Vinicius Oliveira Barros de Alencar**,[2,3] **Ana Maria Oliveira Ferreira da Mata**,[2,3] **Nayana Bruna Nery Monção**,[4] **Antonia Maria das Graças Lopes Citó**,[4] **Ana Fontenele Urano Carvalho**,[5] **Davi Felipe Farias**,[6] **Patrícia Marçal da Costa**,[7] **Adriana Maria Viana Nunes**,[1] **João Marcelo de Castro e Sousa**,[2,3] **and Ana Amélia de Carvalho Melo-Cavalcante**[2,3]

[1]*Laboratory of Experimental Cancerology (LabCancer), Department of Biophysics and Physiology, Federal University of Piauí, Teresina, Brazil*
[2]*Postgraduate Program in Pharmaceutical Sciences, Federal University of Piauí, Teresina, Brazil*
[3]*Laboratory of Genetic Toxicology (Lapgenic), Department of Biochemistry and Pharmacology, Federal University of Piauí, Teresina, Brazil*
[4]*Department of Chemistry, Federal University of Piauí, Teresina, Brazil*
[5]*Department of Biology, Federal University of Ceará, Fortaleza, Brazil*
[6]*Department of Molecular Biology, Federal University of Paraíba, João Pessoa, Brazil*
[7]*Faculty of Medicine, State University of Ceará, Fortaleza, Brazil*

Correspondence should be addressed to Paulo Michel Pinheiro Ferreira; pmpf@ufpi.edu.br

Received 23 July 2021; Revised 22 October 2021; Accepted 17 November 2021; Published 7 December 2021

Academic Editor: Liren Qian

Mimosa caesalpiniifolia (Fabaceae) is used by Brazilian people to treat hypertension, bronchitis, and skin infections. Herein, we evaluated the antiproliferative action of the dichloromethane fraction from *M. caesalpiniifolia* (DFMC) stem bark on murine tumor cells and the *in vivo* toxicogenetic profile. Initially, the cytotoxic activity of DFMC on primary cultures of Sarcoma 180 (S180) cells by Alamar Blue, trypan, and cytokinesis block micronucleus (CBMN) assays was assessed after 72 h of exposure, followed by the treatment of S180-bearing Swiss mice for 7 days, physiological investigations, and DNA/chromosomal damage. DFMC and betulinic acid revealed similar *in vitro* antiproliferative action on S180 cells and induced a reduction in viable cells, induced a reduction in viable cells and caused the emergence of bridges, buds, and morphological features of apoptosis and necrosis. S180-transplanted mice treated with DFMC (50 and 100 mg/kg/day), a betulinic acid-rich dichloromethane, showed for the first time *in vivo* tumor growth reduction (64.8 and 80.0%) and poorer peri- and intratumor quantities of vessels. Such antiproliferative action was associated with detectible side effects (loss of weight, reduction of spleen, lymphocytopenia, and neutrophilia and increasing of GOT and micronucleus in bone marrow), but preclinical general anticancer properties of the DFMC were not threatened by toxicological effects, and these biomedical discoveries validate the ethnopharmacological reputation of *Mimosa* species as emerging phytotherapy sources of lead molecules.

1. Introduction

The history of anticancer drugs is closely related to natural products, since at least 60% of clinical drugs naturally or chemically resemble ones [1]. In this context, Brazil remains at the top of 17 megadiverse countries and the home of around 20% of the world species [2], mainly because approximately 700 new animal species have been discovered each year [3]; it has the greatest number of endemic species on a global scale and about 55,000 plant species (22% of the world total) [4, 5]. Moreover, it is a great producer of medicinal plants for internal consumption as well as for international markets. This invaluable biodiversity encourages biotechnological and pharmacological studies about effective therapy and health recovery [6–8].

A Brazilian dry region named "Caatinga" dominates 7% of the Brazilian territory and is an exclusive biome. It generates particular environmental conditions for steppe climate-adapted flora and fauna and a high number of rare and endemic taxa [9, 10], exhibiting many vegetal families, such as Fabaceae, Anarcadiaceae, Caryocaraceae, Rhamnaceae, Chrysobalanaceae, Clusiaceae, Connaraceae, Sapindaceae, Annonaceae, Combretaceae, and Bignoniaceae [11–15]. Among them, inflorescences from *Mimosa caesalpiniifolia* Benth. (synonym: *Mimosa caesalpiniaefolia*, family Fabaceae), known as "unha de gato," "sabiá," and sansão-do-campo," have been traditionally used by Brazilian people as hedges and windbreaks. Dried fruits and leaves are given as fodder for cattle, goats, and sheep (crude protein ranging from 13.4 to 17.1%) [16] and to treat hypertension [17]. Its bark is popularly used as a coagulant to stop or avoid bleeding and as wound washing to prevent inflammation and skin infections. Moreover, the ingestion of bark infusion alleviates symptoms of bronchitis [16, 18, 19]. Recently, a bioassay-guided phytochemical study found 28 compounds in *M. caesalpiniifolia* leaf extract, and four of them revealed potent antifungal properties against *Candida glabrata* and *Candida krusei* [20]; the latter was often associated with the prior use of azoles and corticosteroids, bone marrow transplantation, malignant hematological diseases, and neutropenia [21].

An expert Brazilian research group about pharmacology of natural products confirmed bioactivity usages for cardiovascular diseases. They reported that ethanolic extracts of different parts of *M. caesalpiniifolia* (leaves, bark, fruit, and inflorescences) cause vasorelaxation, the tea of flowers promotes hypotension and tachycardia, and the ethanolic extract causes hypotension and bradycardia [22]. Based on these ethnopharmacological properties, this work evaluated the antiproliferative action of the dichloromethane fraction from *M. caesalpiniifolia* (DFMC) stem bark on murine tumor cells and the *in vivo* toxicogenetic profile.

2. Materials and Methods

2.1. Plant Collection and Extract/Fraction Preparation. Plant specimens were collected in May 2010 in Teresina (Piauí, Brazil). A voucher sample (26.824) was deposited at Graziela Barroso Herbarium at Federal University of Piauí (Teresina, Piauí, Brazil). Air-dried plant material was pulverized, extracted with ethanol, concentrated under reduced pressure, and subjected to successive partitioning with dichloromethane as described by Silva et al. [15]. Previously, we isolated betulinic acid [3β-hydroxy-lup-20(29)-en-28-oic acid] and verified it as the main compound in the dichloromethane fraction (~70.3%), as demonstrated by TLC (thin-layer chromatography), GC-qMS (gas chromatograph quadrupole mass spectrometer), HRAPCIMS (high-resolution atmospheric pressure chemical ionization mass spectrometer), ^{1}H- and ^{13}C-nuclear magnetic resonance, and DEPT analysis [15, 23]. Plant samplings were authorized by the System of Authorization and Information on Biodiversity (SISBIO/BAMA #50090-3) and registered in SisGen (*Sistema Nacional de Gestão do Patrimônio Genético e do Conhecimento Tradicional Associado* #ABC4AC2) according to Brazilian legislation (Federal Law No 13,123/2015). These investigations were performed using the fraction composed of a mixture of molecules because such preparations represent the main folk approach of consumption by the Brazilian population [15].

2.2. Animal's Facilities. Adult female Swiss mice (*Mus musculus* Linnaeus, 1758) weighing 20–25 g were obtained from the animal facilities at Universidade Federal do Piauí (UFPI), Teresina, Brazil. All animals were maintained in well-ventilated cages under standard conditions of light (12 h with alternate day and night cycles) and temperature ($25 \pm 2^{\circ}$C) with free access to food (Nutrilabor™, Campinas, Brazil) and drinkable water. After the tests, mice were euthanized with sodium thiopental (100 mg/kg) (i.p.). All protocols were approved by the Ethical Committee on Animal Experimentation at UFPI (CEUA #034/2014) and followed Brazilian (*Sociedade Brasileira de Ciência em Animais de Laboratório*–SBCAL) and international (Directive 2010/63/EU of the European Parliament and of the Council on the protection of animals used for scientific purposes) rules on the care and use of experimental animals.

2.3. In vitro Antiproliferative Studies on Sarcoma 180 Cells

2.3.1. Ex vivo Cytotoxic Action. Mice with 9 to 10 days of S180 ascitic tumors were euthanized with an overdose of sodium thiopental, and a suspension of S180 cells was taken from the intraperitoneal cavity under aseptic conditions. The cell suspension was centrifuged at 2,000 rpm for 5 min to obtain a pellet, which was washed three times with sterile RPMI medium. The cell concentration was adjusted to 0.5×10^{6} cells/mL in RPMI-1640 medium supplemented with 20% fetal bovine serum, 2 mM glutamine, 100 U/mL penicillin, and 100 μg/mL streptomycin (Cultilab™, Brazil), plated in 96-well plates with increasing concentrations (0.8–50 μg/mL) of DFMC and betulinic acid, and incubated at 37°C in a 5% CO_2 atmosphere (Shel Lab CO_2 Incubator, USA).

Cell proliferation was assessed by the Alamar Blue™ assay after 72 h. At 48 h of incubation, 20 μL of stock solution (0.156 mg/mL) of Alamar Blue™ (Resazurin, Sigma

Aldrich™, USA) was added to each well. Cell proliferation was determined spectrophotometrically using a multiplate reader (T80+ UV/VIS Spectrometer, PG Instruments™, United Kingdom) at 570 and 595 nm. The antiproliferative effect was expressed as the percentage of the control according to Ferreira et al. [12].

2.3.2. Trypan Blue Exclusion Assay. Sarcoma 180 cells (0.5×10^6 cells/mL) plated in 24-well plates were exposed to DFMC at 5, 10, and 25 μg/mL. Doxorubicin (Dox, 0.3 μg/mL) was used as a positive control. Cell viability was examined by the exclusion of trypan blue [24]. Briefly, aliquots of 10 μL were collected from DFMC-treated S180 cultures after 72 h of exposure, and viability was separated into viable blue-marked and nonviable blue-coloured cells in a Neubauer chamber under light microscopy (Biosystems™, USA).

2.3.3. Cytokinesis-Block Micronucleus (CBMN) Assay. Sarcoma 180 cells were plated in 24-well plates (0.5×10^6 cells/mL) and treated with DFMC at 5, 25, and 50 μg/mL. After 44 h at 37°C, cytochalasin B (Sigma Aldrich, USA, 6 μg/mL) was added, and the cells were reincubated for an additional 28 h. At 72 h, the cultures were transferred to tubes and centrifuged at 800 rpm for 5 minutes. Then, the supernatant was removed, and the body of the cell bottom was enlarged and centrifuged again before the addition of 2 mL of fixing solution (methanol and acetic acid, ratio 5 : 1) and 3 drops of formaldehyde 37% (Vetec™, Brazil). This procedure was repeated 3x using fixing solution 3 : 1 without formaldehyde. Supernatants were discarded, and 2-3 drops of cell suspension were dripped onto slides and stained with Giemsa for 5 min [25]. Considering blind examination, a total of 2000 cells by concentration were counted by optical microscopy at 1000x (1000 cells/slide) to count buds, bridges, and micronuclei.

2.4. In vivo Assays

2.4.1. Assessment of Antitumor Capacity, Physiological Parameters, and Histological Aspects. Ten-day-old S180 ascites tumor cells were removed from the peritoneal cavity, counted (6×10^6 cells/mL) and subcutaneously implanted into the right hind axillary of healthy Swiss animals. On the next day, they were randomly divided into four groups ($n = 10$ each). DFMC dissolved in dimethylsulfoxide (DMSO 5%, Vetec™, Brazil) was intraperitoneally injected at 50 or 100 mg/kg/day for 7 days. Negative and positive controls received DMSO 5% and 5-fluoruracil (5-FU, 25 mg/kg/day, Sigma Aldrich™, USA), respectively [26].

All animals were anaesthetized on day 8 with ketamine (90 mg/kg)-xylazine (4.5 mg/kg) for cardiac puncture blood collection [27] using sterile tubes and heparinize pipettes to determine hematological parameters (erythrocytes, leukocytes, platelets, hemoglobin, and hematocrit) in peripheral blood samples using an automatic analyzer of hematologic cells (SDH-3 Vet Labtest™, Brazil). The absolute count of white cellular subtypes was calculated as the product of its respective differential percentage and total leukocyte count. For biochemical analysis, blood samples were centrifuged at 2,000 rpm for 5 minutes. Physiological markers of the liver [blood urea nitrogen (BUN), glutamate oxaloacetate transaminase (GOT), glutamate pyruvate transaminase (GPT), alkaline phosphatase (ALP)] and kidneys (creatinine) were evaluated according to Labmax Plenno Labtest™. Subsequently, all animals were euthanized to dissect out the liver, kidneys, spleen, stomach, heart, and lungs to estimate wet relative weights and for macroscopic analysis. Next, organs were fixed with 10% buffered formalin, processed, and cut into small pieces to prepare histological sections (4–7 μm). Staining was carried out with hematoxylin and eosin (H&E, Vetec™, Brazil). Morphological blind analyses were performed under light microscopy (Olympus™, Japan) by an expert pathologist.

2.4.2. Determination of Chromosomal Damages. The femurs were removed and carefully cleaned, and proximal epiphyses were sectioned. Bone marrow samples were collected using 5 mL syringes filled with 0.5 mL of sterile fetal bovine serum (Cultilab™, Brazil), centrifuged, and homogenized. Drops of cell suspension were transferred to slides to prepare smears (two slides/animal), fixed and stained by the Leishman method. All analyses were blindly performed under light microscopy (Olympus™, Japan) with magnifications of 200x and 400x. We considered micronuclei to be rounded structures, with a diameter of 1/5 to 1/20 found in young erythrocytes and identified by bluish staining. A total of 1,000 polychromatic erythrocytes (PCEs) was quantified per slide (two slides/animal) [28–30].

2.5. Statistical Analysis. Half maximal inhibitory concentration (IC_{50}) and their 95% confidence intervals were calculated by nonlinear regression (GraphPad Prisma 9.0, Intuitive Software for Science, USA). Statistical differences were evaluated comparing data [mean ± standard error of mean (S.E.M.)] by one-way analysis of variance (ANOVA) and Newman–Keuls test as *post hoc* test ($p < 0.05$). All *in vitro* studies were carried out in duplicate ($n = 3$/concentration) and represent independent biological evaluations.

3. Results

3.1. In vitro Antiproliferative Action on Sarcoma 180 Cells: Cytotoxicity, Chromosomal Changes, and Cell Death Pattern. DFMC and betulinic acid revealed similar *in vitro* antiproliferative activity against S180 cells after 72 h of incubation, with IC_{50} values of 29.0 (24.9–33.6) μg/mL and 33.7 (30.1–37.6) μg/mL, respectively ($p > 0.05$, Table 1). Afterwards, this action was confirmed by trypan blue assay (Figure 1), a direct method to detect cytotoxicity, which showed that all concentrations of DFMC (5, 25, and 50 μg/mL) reduced the number of viable cells (48.2 ± 7.1, 87.6 ± 1.4, and 98.7 ± 0.5%, respectively) when compared to the negative control ($p < 0.05$).

Morphological analysis of DFMC-treated Sarcoma 180 cells did not show significant micronucleus induction

Table 1: Cytotoxic activity of the dichloromethane fraction and betulinic acid from *Mimosa caesalpiniifolia* (DFMC) stem bark on primary culture of sarcoma 180 cells after 72 h of exposure evaluated by alamar blue assay.

Sample	IC_{50} (μg/mL)	
	Sarcoma 180 cells	R^2
DFMC	29.0 (24.9–33.6)	0.9278
Betulinic acid	33.7 (30.1–37.6)	0.9292
Doxorubicin	1.9 (1.4–2.4)	0.9801

Data are presented as IC_{50} values and 95% confidence intervals. Doxorubicin was used as positive control. Experiments were performed in duplicate.

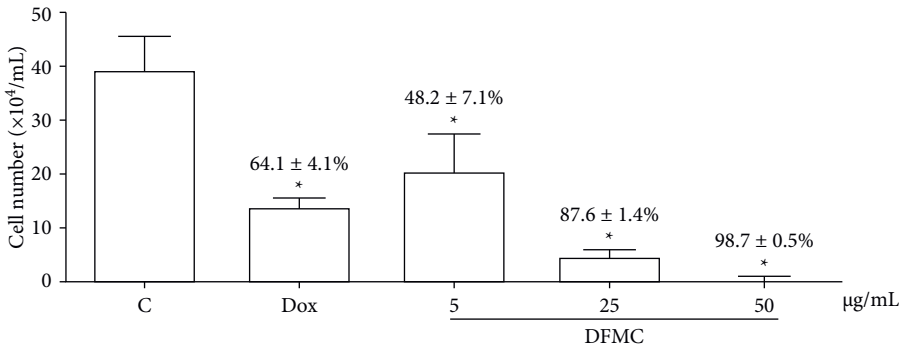

Figure 1: The cell number of viable cells was determined by trypan blue staining and analyzed by light microscopy after 72 h of exposure to the dichloromethane fraction from *Mimosa caesalpiniifolia* (DFMC) stem bark. The percentage of viability reduction in relation to the negative control is described above. The negative control (C) was treated with the vehicle used to dilute the tested substance. Doxorubicin (Dox, 0.3 μg/mL) was used as a positive control. The results are expressed as mean ± standard error of measurement (S.E.M.) from two independent experiments. $^*p < 0.05$ compared to the control by ANOVA followed by student Newman–Keuls test.

(4.5 ± 0.7, 5.5 ± 2.1, and 4.5 ± 2.1 for 5, 25, and 50 μg/mL, respectively) in relation to the negative control (3.5 ± 0.7, $p > 0.05$, Figure 2(a)). On the other hand, bridges (14.6 ± 3.9 and $27.0 \pm (2)$ and buds (13.8 ± 3.3) were observed at 25 and 50 μg/mL and 50 μg/mL ($p < 0.05$) when compared to the negative control (2.0 ± 1.4 and 5.5 ± 3.5), respectively. Such chromosomal damage was corroborated by morphological features of apoptosis (213.0 ± 73.5 and 337.0 ± 57.9) and necrosis (162.5 ± 60.1 and 189.5 ± 40.3) at 25 and 50 μg/mL ($p < 0.05$, Figure 2(b)) in the presence of cell rarefaction and vacuolization. As expected, Dox increased buds (15.5 ± 3.5) and micronuclei (18.5 ± 4.9) and caused typical findings of apoptosis (466.0 ± 101.8) and necrosis (177.5 ± 3.5) ($p < 0.05$).

3.2. In vivo Antitumoral Activity. Experimentally transplanted mice with Sarcoma 180 cells and treated with DFMC (50 and 100 mg/kg/day) for 7 days revealed a significant reduction in tumor growth [(0.28 ± 0.04 g ($64.8 \pm 5.3\%$) and 0.16 ± 0.07 g ($80.0 \pm 8.4\%$)] when compared to the negative control (0.80 ± 0.13 g, respectively). Tumor reduction was also noted in the positive control group treated with 5-FU [0.11 ± 0.03 g ($82.8 \pm 4.2\%$)] ($p < 0.05$, Table 2).

The negative control group showed characteristics of malignant neoplasms consisting of round and polyhedral cells, anisocariosis, binucleation, mitoses, and different degrees of cell and nuclear pleomorphism, chromatin condensation, and extensive areas of muscle invasion (Figures 3(a)–3(d)). Tumor samples from 5-FU 25 mg/kg/day and FDCM 50 and 100 mg/kg/day also revealed the typical morphology of neoplastic cells, although rare mitoses were observed, which indicated a reduction in proliferation (Figures 3(e)–3(l)). 5-FU-treated tumors showed larger blood vessels and well vascularized sarcomas, similar to those noted in negative control tumors (Figure 3(e)). On the other hand, DFMC-treated Sarcoma 180 tumors treated with 50 and 100 mg/kg/day exhibited poorer peri- and intratumor quantities of vessels. In such tumors, vascularization was partially restricted to the adipose tissue surrounding the tumor (Figures 3(i)–3(j)).

3.3. Physiological Parameters. In the next step, we assessed macroscopic and microscopic parameters of key organs and the hematological profile of Sarcoma 180-bearing mice after treatment with DFMC. First, we found a reduction in body weight gain in DFMC-treated animals (20.6 ± 0.8 and 21.4 ± 1.6 g, for 50 and 1000 mg/kg/day) in a similar way to the 5-FU group (20.1 ± 0.9 g) when compared to the negative control (26.3 ± 2.2 g, $p < 0.05$, Table 1). Wet relative weight reduction of spleens was noted in both doses of DFMC (0.2 ± 0.08 and 0.2 ± 0.03 g/100 g of body weight) and in 5-FU-treated animals (0.2 ± 0.04 g), but liver decrease was observed in 5-FU-treated animals only (4.7 ± 0.1 g) in comparison with the negative group (0.4 ± 0.04 g and 6.0 ± 0.4 g, respectively, $p < 0.05$).

Hematological analysis of DFMC-treated animals showed neutrophilia ($33.8 \pm 3.2\%$), lymphocytopenia ($61.5 \pm 3.6\%$), a reduction in eosinophils ($0.4 \pm 0.2\%$), and a slight increase in GOT levels (315.3 ± 8.9 U/mL) ($p < 0.05$, Table 3). Animals exposed to 5-FU showed intense leukopenia ($1.6 \pm 0.3/mm^3$) due to declines in neutrophils ($12.9 \pm 1.3\%$), monocytes

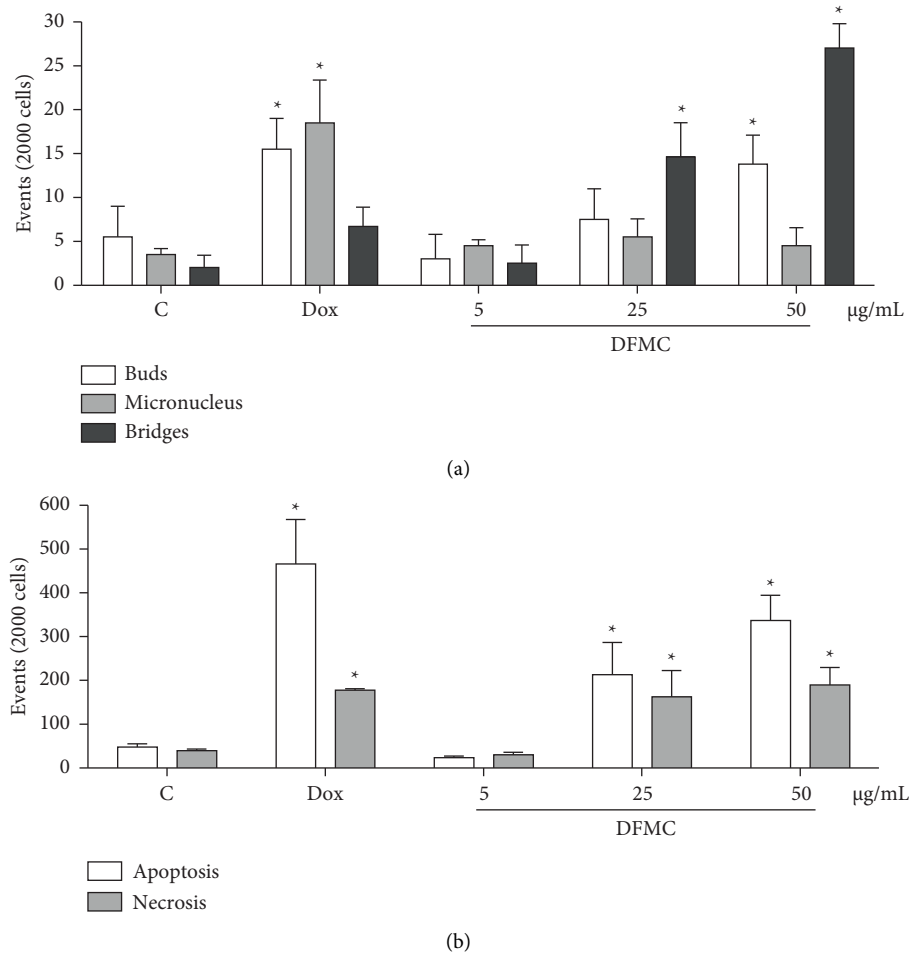

Figure 2: *Ex vivo* chromosomal changes and cell death pattern in sarcoma 180 cells determined by micronucleus assay with cytokinesis block after 72 h exposure to the dichloromethane fraction from *Mimosa caesalpiniifolia* (DFMC) stem bark. The negative control (C) was treated with the vehicle used to dilute the tested substance (DMSO 0.1%). Doxorubicin (Dox, 0.3 μg/mL) was used as a positive control. The results are expressed as mean ± standard error of measurement (S.E.M.) from two independent experiments. $^*p < 0.05$ compared to the control by ANOVA followed by student Newman–Keuls test.

Table 2: Effect of the dichloromethane fraction from *Mimosa caesalpiniifolia* (DFMC) stem bark on the relative weight of key organs and on the tumor growth of sarcoma 180-bearing swiss mice after 7 days of intraperitoneal treatment.

Substance	Dose (mg/kg/day)	Mice weight (g)	Liver	Kidney	Spleen	Stomach	Lungs	Tumor (g)	Tumor inhibition (%)
			g/100 g body weight						
Negative control	—	26.3 ± 2.2	6.0 ± 0.4	1.1 ± 0.1	0.4 ± 0.04	1.0 ± 0.1	0.8 ± 0.1	0.80 ± 0.13	—
5-FU	25	20.1 ± 0.9*	4.7 ± 0.1*	1.2 ± 0.1	0.2 ± 0.04*	1.1 ± 0.1	0.8 ± 0.1	0.11 ± 0.03*	82.8 ± 4.2*
DFMC	50	20.6 ± 0.8*	5.8 ± 0.2	1.2 ± 0.1	0.2 ± 0.08*	1.1 ± 0.1	1.0 ± 0.2	0.28 ± 0.04*	64.8 ± 5.3*
	100	21.4 ± 1.0*	5.9 ± 0.2	1.3 ± 0.1	0.2 ± 0.03*	1.2 ± 0.5	0.8 ± 0.1	0.16 ± 0.07*	80.0 ± 8.4*

Values are means ± S.E.M. ($n = 10$ animals/group). The negative control was treated with the vehicle used to dilute the drug (DMSO 5%). 5-Fluorouracil (5-FU) was used as positive control. $^*p < 0.05$ compared with the negative control by ANOVA followed by Newman–Keuls test.

(0.6 ± 0.2%) and eosinophils (0.6 ± 0.3%) compared to the animals from the negative group (5.1 ± 0.4/mm^3, 18.8 ± 2.8%, 1.8 ± 0.3% and 1.8 ± 0.4%, respectively, $p < 0.05$).

3.4. Histological Alterations. Animals from the negative control group and treated with DFMC (50 and 100 mg/kg/day) did not show signs of toxicity, with similarity among organs from these groups. Livers did not exhibit hyperplasia, hemosiderin pigments, infiltration of leukocytes, cell swelling, portal congestion, or areas of necrosis, although microesteatosis was detected in all groups (Figure 4(a)). Kidneys present no swelling, tubular degeneration, vascular congestion, or necrosis focus (Figure 4(b)); in hearts, there were no areas of degeneration or fibroblasts proliferation and striations were clearly visible (Figure 4(c)); lungs showed bronchioles and

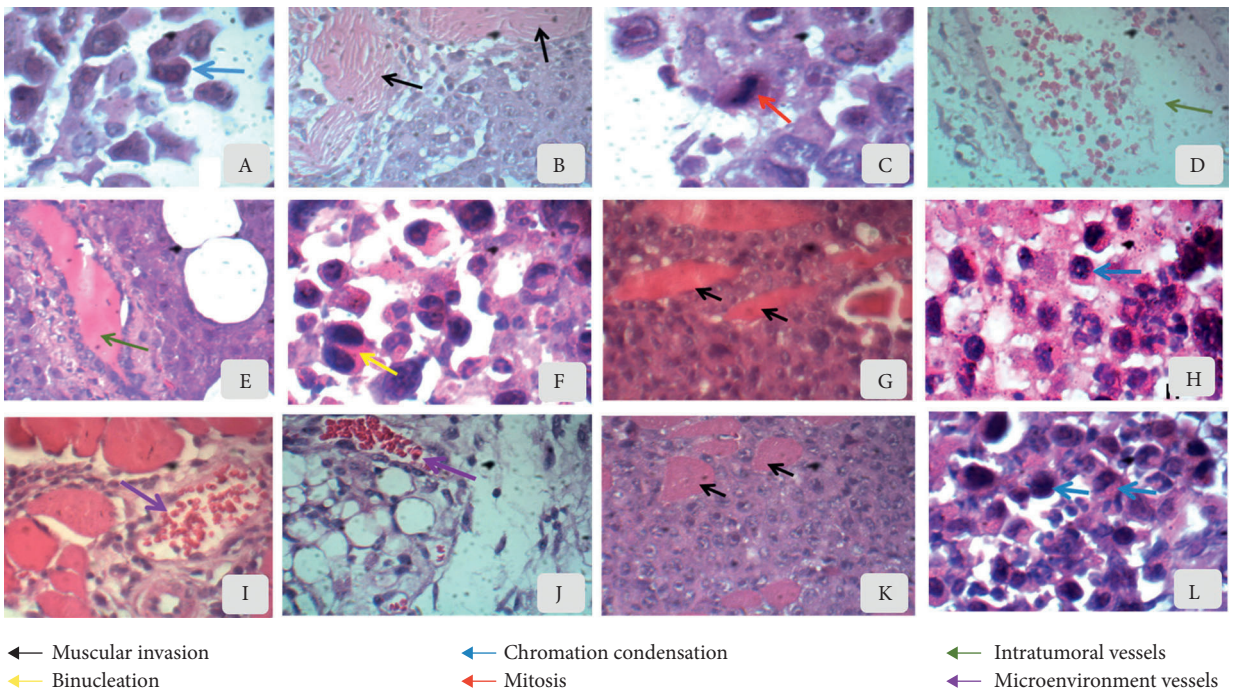

Figure 3: Morphology of sarcoma 180 tumor cells from swiss mice after 7 days of treatment with dichloromethane fraction from *Mimosa caesalpiniifolia* stem bark. Animals were treated by intraperitoneal injection (50 mg/kg/day: g, h, and i; 100 mg/kg/day: j, k, and l). The negative control was treated with the vehicle used to dilute the substance (DMSO 5%: a–d). 5-Fluorouracil was used as a positive control (e and f). Hematoxylin-eosin staining. Light microscopy magnification, 100x-400x.

Table 3: Hematological and biochemical parameters of mice intraperitoneally treated with dichloromethane fraction from *Mimosa caesalpiniifolia* stem bark for 7 days.

Parameters	Negative control	5-FU 25 mg/kg/day	Dichloromethane fraction from *Mimosa caesalpiniifolia*	
			50 mg/kg/day	100 mg/kg/day
Erythrocytes (mm^3)	4.5 ± 0.2	4.4 ± 0.2	5.0 ± 0.1	4.9 ± 0.2
Hemoglobin (g/dL)	13.6 ± 0.7	13.3 ± 0.8	15.4 ± 0.4	15.0 ± 0.7
Hematocrit (%)	40.7 ± 2.3	40.1 ± 2.3	46.3 ± 1.1	44.9 ± 2.2
VCM (fL)	90.8 ± 0.5	90.6 ± 0.6	91.8 ± 0.3	91.6 ± 0.5
HCM (pg)	30.2 ± 0.2	30.2 ± 0.2	30.5 ± 0.1	30.5 ± 0.2
CHCM (g/dL)	33.3 ± 0.1	33.1 ± 0.1	33.2 ± 0.1	33.3 ± 0.1
Platelets (mm^3)	3.6 ± 0.5	2.9 ± 0.2	3.4 ± 0.2	3.4 ± 0.2
Total leukocytes (mm^3)	5.1 ± 0.4	1.6 ± 0.3*	5.4 ± 0.6	4.9 ± 0.7
Neutrophils (%)	18.8 ± 2.8	12.9 ± 1.3*	23.3 ± 4.1	33.8 ± 3.2*
Rods (%)	0.4 ± 0.2	0.4 ± 0.3	0.6 ± 0.2	1.8 ± 0.7
Lymphocytes (%)	77.3 ± 3.0	85.6 ± 1.8	73.7 ± 4.1	61.5 ± 3.6*
Monocytes (%)	1.8 ± 0.3	0.6 ± 0.2*	1.7 ± 0.6	2.6 ± 0.8
Eosinophils (%)	1.8 ± 0.4	0.6 ± 0.3*	0.7 ± 0.3*	0.4 ± 0.2*
Basophils (%)	0.0	0.0	0.0	0.0
GOT (U/mL)	286.9 ± 5.8	303.2 ± 7.6	280.8 ± 9.1	315.3 ± 8.9*
GTP (U/mL)	158.8 ± 2.6	157.5 ± 4.3	161.6 ± 5.0	156.3 ± 1.1
ALP (U/L)	112.3 ± 5.5	131.2 ± 9.8	101.2 ± 3.4	93.8 ± 6.6
Creatinine (mg/dL)	0.5 ± 0.05	0.5 ± 0.08	0.4 ± 0.01	0.4 ± 0.04
BUN (mg/dL)	48.9 ± 4.2	37.7 ± 2.4	41.3 ± 6.6	42.8 ± 3.1

MCH, mean corpuscular hemoglobin; MCV, mean corpuscular volume; MCHC, mean corpuscular hemoglobin concentration; BUN, blood urea nitrogen; GOT, glutamate oxaloacetate transaminase; GPT, glutamate pyruvate transaminase; ALP, alkaline phosphatase. Values are means ± S.E.M. ($n = 10$ animals/group). The negative control was treated with the vehicle used to dilute the drug (DMSO 5%). 5-Fluorouracil (5-FU) was used as positive control. *$P < 0.05$ compared with the negative control by ANOVA followed by Newman–Keuls test.

visible alveolar spaces, absence of mono and polymorphonuclear cells or areas of necrosis (Figure 4(d)); stomachs showed normal mucosa and submucosa, absence of hemorrhagic streaks, a cardiac region with a keratinized squamous lining, no changes in chorion and easy visualization of parietal and main cells (Figure 4(e)). Spleens showed

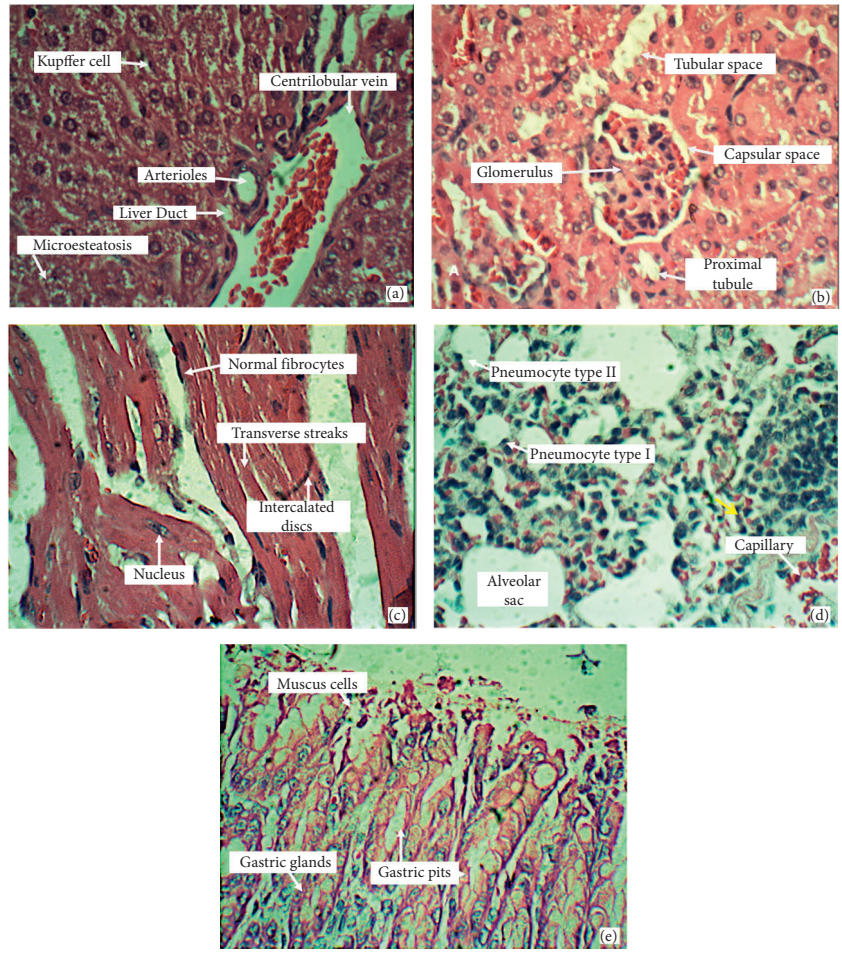

Figure 4: General morphology of livers (a), kidneys (b), hearts (c), lungs (d), and stomachs (e) from Swiss mice after 7 days of treatment with dichloromethane fraction from *Mimosa caesalpiniifolia* stem bark (50 or 100 mg/kg/day) or vehicle used to dilute the substance (DMSO 5%). Important changes among these groups were not observed. Hematoxylin-eosin staining. Light microscopy magnification, 400x.

megakaryocytes and hemosiderin pigments in all groups. Disorganization of lymphoid follicles and relative reduction of the white pulp were observed in the 5-FU (Figure 5(b)) and DFMC-treated animals (Figures 5(c) and 5(d)). On the other hand, 5-FU-treated animals showed slight hepatocyte swelling and suggestion of mild changes in fatty metabolism since macroesteatosis was noted, and kidneys presented swelling of tubular cells and foci of atrophic glomeruli (results not shown).

3.5. In vivo Chromosomal Damage. DFMC increased micronucleated polychromatic erythrocytes in the bone marrow of mice in a dose-dependent manner (50 and 100 mg/kg/day: 11.5 ± 0.2 and 26.0 ± 2.1, respectively) compared to the vehicle group (2.8 ± 0.2, $p < 0.05$). As expected, 25 mg/kg/day 5-FU caused clastogenic effects (14.0 ± 0.1, $p < 0.05$).

4. Discussion

In the last century, the development of cytotoxic agents has revolutionized anticancer therapy. Adjuvant treatments with antiproliferative substances have demonstrated an indisputable advantage when compared to traditional treatments based on surgery and monochemotherapy, making it possible to cure neoplasms such as acute childhood leukemia, Hodgkin and non-Hodgkin's lymphomas, and germ cell tumors [31, 32]. However, the great heterogeneity of tumor cells makes treatment difficult and facilitates the manifestation of resistance [33], which stimulates the search for new chemotherapeutic agents.

Initially, the antiproliferative action of DFMC was evaluated in primary cultures of Sarcoma 180 cells. *In vitro* cytotoxicity tests in cell cultures are important for the evaluation of antitumor agents, and at least during the screening phase, they have reduced *in vivo* tests on animals. In addition, they are widely used as alternative methods to pharmacological tests on isolated organs [26, 34]. Herein, DFMC and its majority compound betulinic acid revealed similar cytotoxic capacity on S180 cells by Alamar blue assay, whose action was confirmed by cell viability reduction in trypan blue exclusion tests. Some reports, including the American National Cancer Institute (NCI-USA) [35], suggest that IC_{50} values around 30 μg/mL are a suitable outcome to consider extracts and fractions promising substances for further purification and biological studies [12, 15]. Recently, we reported that DFMC

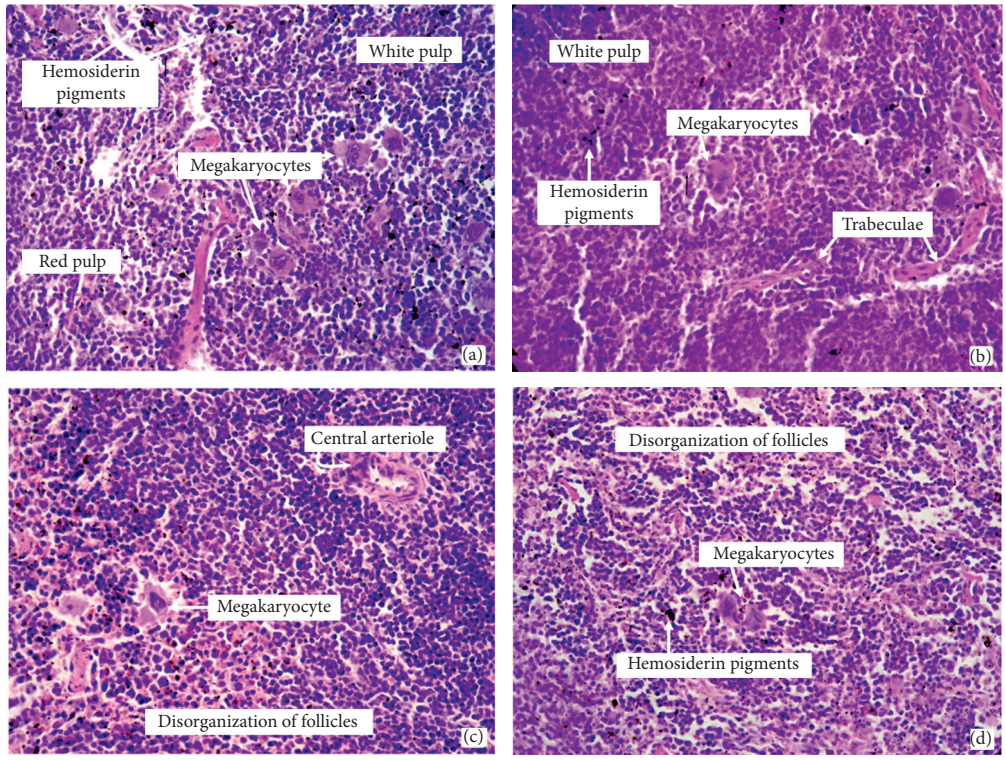

Figure 5: Spleen morphology of Swiss mice after 7 days of treatment with dichloromethane fraction from *Mimosa caesalpiniifolia* stem bark (50 mg/kg/day (c); 100 mg/kg/day (d)), vehicle used to dilute the substance DMSO 5% (a) or 5-fluorouracil 25 mg/kg/day (b). Hematoxylin-eosin staining. Light microscopy magnification, 400x.

has higher cytotoxic action against different types of tumor tissues (promyelocytic leukemia, HL-60; glioblastoma, SF-295; ovarian, OVCAR-8; colon, HCT-116) than hexane and water extracts. DFMC did not produce hemolysis and showed higher potential as a cytotoxic agent than betulinic acid for the SF-295 and HL-60 lines [20, 36], corroborating the findings described here for S180 cells.

Phytochemical investigation of extracts from *Mimosa* species revealed the existence of terpenes, flavonoids, steroids, phenols (especially tannins), and fatty acid derivatives in different parts of the plant (leaves, fruits, flowers, branches, and stem bark) [36–40], mainly betulinic acid, lupeol, phytol, lactic acid, α-tocopherol, stigmasterol, β-sitosterol, sitostenone, and stigmasta-4,22-dien-3-one, which had been identified in dichloromethane, ethanolic, and hexane fractions of leaves and barks from *M. caesalpiniifolia* [15, 36, 40], suggesting that the antiproliferative potential of DFMC may be attributed, at least in part, to its chemopreventive action. In this context, Silva et al. [15] stated the scavenger activity of *M. caesalpiniifolia* extracts, whose presence of phenolic compounds was confirmed by ultraviolet-visible spectroscopy and thin-layer chromatography.

Betulinic acid, a naturally occurring pentacyclic triterpenoid, is the main compound in the fraction (~70.3%) [15, 23], and both samples (DFMC and isolated molecule) have similar bioactivity on S180 cells ($p > 0.05$), confirming reports about the antiproliferative action of betulinic acid in many types of cancers [41–50].

To complement the *ex vivo* cytotoxic analysis on S180 tumor cells and *in vivo* pharmacological safety, cytokinesis-block micronucleus (CBMN) assays were performed to measure micronuclei quantification and DNA damage in mammalian cell cultures [28]. Apart from the evaluation of micronuclei, the CBMN cytome assay allows the assessment of other relevant biodosimetric markers: nucleoplasmic bridges, nuclear buds, proportion of dividing cells (parameter of cytostasis), and cells undergoing apoptosis and necrosis (parameters of cytotoxicity). Therefore, this technique was updated to detect chromosomal breaks, DNA rearrangements, chromosomal losses, cytostasis, and to separate types of cell death [25, 28, 51, 52]. Therefore, for the first time, an increase in chromosomal damage represented by (i) nucleoplasm bridges: a biomarker of dicentric chromosomes, resulting from the fusion of the final telomeres after DNA double-strand breaks or DNA misrepair/rearrangements; (ii) buds: a biomarker of gene amplification and originating from interstitial or terminal acentric fragments; and (iii) morphological features of apoptosis and necrosis in S180 cells at higher concentrations of DFMC was noted. Meanwhile, both doses of DFMC also induced the emergence of micronucleated polychromatic erythrocytes in bone marrow. Previously, Silva et al. [23] reported an ethanolic extract from *M. caesalpiniifolia* leaves with maximum cytotoxicity on breast carcinoma MCF-7 cells at 320 μg/mL and morphological changes suggestive of apoptosis, including DNA fragmentation and nuclear chromatin condensation.

Recently, we also showed that micronuclei formation and changes indicating mutagenic index in DFMC-treated roots were not detected, although this fraction has inhibited

growth of *Allium cepa* roots and increase amount of bridges in dividing meristematic cells, which indicates capacity for mitotic index reduction as seen as dropping of cells at metaphase, anaphase, and telophase phases and cycle arrest at prophase [15]. Regardless, it is likely that DNA/chromosomal damage is a sign of nonselective mechanism(s) in tumor or normal dividing cells. Therefore, *in vitro* (bridges and buds) and *in vivo* (micronucleus) clastogenic findings led to cell cycle arrest as a "cellular escape" from death, mainly if we consider the antiproliferative action of DFMC on human normal leukocytes well [15].

Indeed, antineoplastic agents induce DNA strand breaks in mammalian cells, as seen with inhibitors of topoisomerase I (camptothecin) and topoisomerase II (etoposide) [53] and 5-FU. 5-FU is a widely used antimetabolite to treat breast adenocarcinomas and cancers of the gastrointestinal tract and head and neck due to its inhibitory action on the enzyme thymidylate synthase [54], among other mechanisms, despite its unblemished *in vivo* clastogenic activity [55]. However, genotoxicity does not mean mutagenicity because some genome injuries are biochemically fixed, which indicates that antineoplastic acute toxic consequences (e.g., inhibition of growth and cell division) are not automatically linked to chromosomal loss/impairments [56].

The cytotoxic activity on cancer cells using *in vitro* models may not reflect *in vivo* findings, since the latter considers pharmacokinetic and pharmacodynamic variables, such as ligand binding to specific receptors, downstream cascade, involvement of second messengers, water/lipid solubility, bioavailability, first-pass metabolism, and renal excretion [57, 58]. Therefore, combining these two types of scientific tools is appropriate for a more complete assessment of a substance with antiproliferative action. For the first time, the amazing antitumor action of a dichloromethane fraction from *M. caesalpiniifolia* stem bark on *in vivo* proliferating Sarcoma 180 cells was demonstrated. *In vivo* studies have already shown that betulinic acid inhibits the growth of human ovarian IGROV-1 carcinoma xenographic tumors at 100 mg/kg/day and increases the survival rate of mice [46].

No specific changes were noted during histopathological analysis of the Sarcoma 180 tumors [34], but it is important to emphasize that local vascularization from DFMC-treated animals was predominantly confined to the adipose tissue surrounding the tumors. These unexpected findings were not described before and suggest that the fraction interferes with the cell cycle of Sarcoma 180 cells and inhibits angiogenesis, which obviously alters the stromal environment, such as the local pH, partial pressure of oxygen and carbon dioxide, input of nutrients/growth factors, and cleaning of metabolic residues [57], all essential primary conditions for cellular division and tumor growth. Molecular studies are underway to confirm such antiangiogenic potential. These data corroborate our findings about the biomedical potential of *M. caesalpiniifolia* and inspired us to assess the pharmacological safety profile of the fraction, taking into consideration its promising phytotherapy properties.

The development of new (phyto)pharmaceutical products includes not only pharmacodynamic discoveries but also essential data about the pharmacokinetics profile, therapeutic window, and pharmacological safety, including systemic and genetic toxicology [58, 59]. These assessments allow the exclusion of undesirable drug candidates and save time, material and human resources. In the case of plant toxicity/poisoning, its harmful action must be proven experimentally. For humans, this experimental reproduction should be carried out in the same animal species, naturally affected, or related species (e.g., mice and rats), although different susceptibilities to the effects of toxic herbals among species are a common mark [60, 61].

Acute signs of systemic toxicity are loss of body mass and expansion or involution of key organs in mammals exposed to an investigational drug [62]. Weight loss is one of the most common side effects after chemotherapy cycles with 5-FU or doxorubicin, since the gastrointestinal system is one of the main nonspecific targets of nontarget antiproliferative agents, causing seasickness, suppression of appetite, vomiting, and diarrhea [63]. Loss of body weight and reduction of spleens were macroscopic manifestations found in the 5-FU- and DFMC-treated groups, but signs of diarrhea were not seen in the DFMC-treated groups. Spleen diminution is another very common side effect found in S180-bearing mice under experimental treatment with promising antitumoral substances [26, 64] and reflects lymphocytopenia seen in 5-FU- and DFMC-treated groups and strong leukopenia in 5-FU-treated mice, which was confirmed by disorganization of lymphoid follicles and size reduction of white pulps.

In vivo toxicological studies with DFMC were not found in the literature, but oral subacute treatment of rats for 32 days with 750 mg/kg/day ethanolic extract from *M. caesalpiniifolia* leaves caused weight loss, hepatomegaly, and an increase in adrenal and pituitary glands [40], but serum biochemical evaluation (alkaline phosphatase, GOT, urea, and creatinine) did not identify renal or liver changes. On the other hand, we noted that the 100 mg/kg/day DFMC-treated group revealed a slight but significant increase in GOT.

Transaminases (GOT and GTP) are found in all human systems and many organs, but they are more present in the cytoplasm (100% GTP/20% GOT) or mitochondria (80% GOT) of hepatocytes, since they catalyze transamination reactions, working central providers of secondary metabolites to the citric acid cycle. Any type of liver injury may sensibly increase serum GTP concentrations, a classic biomarker to assess acute or chronic hepatic damage, but its origin can have kidney, heart, or muscle reasons because these organs also possess higher GTP concentrations in comparison with other tissues [65]. On the other hand, GOT is more abundant in heart, skeletal muscle, kidneys, brain, and red blood cells [66], with lower concentrations in skeletal muscle and kidney. Although GTP is more specific for detecting liver damage, ischemic or toxic damage to zone 3 of the hepatic acinus may change GOT levels since this region has greater GOT concentrations [65].

Histological changes were not found in livers from DFMC-treated animals. Thus, it is probable that higher levels of GOT may be associated with muscle damage and/

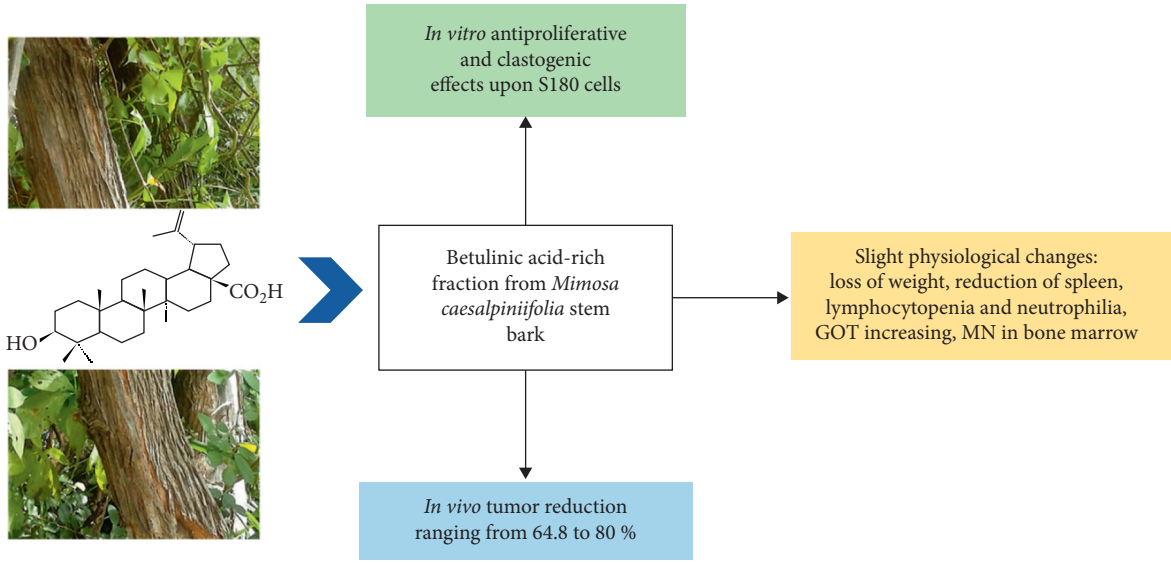

Figure 6: Summary of the antiproliferative, genotoxic, antitumoral, and toxicological effects of a betulinic acid-rich fraction from *Mimosa caesalpiniifolia* stem bark.

or trauma after continual intraperitoneal injections because this procedure can result in aminotransferase release, and an increase in GOT is common in such situations [66].

The majority of clinically available anticancer medications provoke strong side effects, especially suppression of bone marrow and immune response, toxicity on hepatocytes, cardiac myocytes and enterocytes, mucositis, weight and hair loss (incidence of 65%), opportunistic infections, seasickness, vomiting, chemotherapy-related anorexia, peripheral neuropatia, and tiredness [33, 63, 67–69], whose types and intensity depend on the mechanism(s) of action and idiosyncratic reactions. Based on nonsevere organic findings, we believe that the preclinical general anticancer properties of DFMC are not threatened by toxicological effects (Figure 6).

5. Conclusions

A betulinic acid-rich fraction from *Mimosa caesalpiniifolia* stem bark showed, for the first time, *in vitro* and *in vivo* antiproliferative capacity on Sarcoma 180 tumors and induction of nonselective chromosomal damage (bridges, buds, and micronucleus) to dividing murine cells. Such antimitotic action was associated with detectible physiological changes, indicating side effects (loss of weight, reduction of spleen, lymphocytopenia, and neutrophilia and increasing of GOT and micronucleus in bone marrow). These biomedical discoveries validate the ethnopharmacological reputation of *Mimosa* species as emerging phytotherapy sources of lead molecules.

Data Availability

The data sets used and/or analyzed during the present study are available from the corresponding author on reasonable request.

Conflicts of Interest

The authors declare that there are no conflicts of interest regarding the publication of this paper.

Acknowledgments

Paulo Michel Pinheiro Ferreira is grateful to the public Brazilian agency "Conselho Nacional de Desenvolvimento Científico e Tecnológico" [CNPq (#303247/2019-3)] for his personal scholarship. The authors also thank Leane Brunelle dos Santos Alves for technical assistance and the Postgraduate Program in Pharmaceutical Sciences (PPGCF, Teresina, Piauí, Brazil) for structural support.

References

[1] D. J. Newman and G. M. Cragg, "Natural products as sources of new drugs over the 30 years from 1981 to 2010," *Journal of Natural Products*, vol. 75, no. 3, pp. 311–335, 2012.

[2] Fundação de Amparo à Pesquisa do Estado de São Paulo, *Biota Program, Brazilian Biodiversity Research, A Promising Future*, FAPESP, São Paulo, Brazil, 2020, https://fapesp.br/biota/.

[3] Biodiversity Finance Initiative (BIOFIN), Brazil, September 2020, https://biodiversityfinance.net/brazil.

[4] Brazil, Ministry of Health, Health Care Secretariat, Department of Primary Care, "Food guide for the Brazilian population," Brasília, Ministry of Health, September 2020, https://bvsms.saude.gov.br/bvs/publicacoes/guia_alimentar_populacao_brasileira_2ed.pdf.

[5] Brazil, Ministry of Environment, "The Status of Brazilian Biological Diversity," First National Report for the Convention on Biological Diversity – Brazil, September 2020, https://www.mma.gov.br/component/k2/item/7927.html.

[6] M. Valli, M. Pivatto, A. Danuello et al., "Tropical biodiversity: has it been a potential source of secondary metabolites useful for medicinal chemistry?" *Química Nova*, vol. 35, no. 11, pp. 2278–2287, 2012.

[7] J. B. A. Pereira, M. M. Rodrigues, I. R. Morais et al., "The therapeutic role of the program farmacia viva and the medicinal plants in the center-south of Piauí," *Revista Brasileira de Plantas Medicinais*, vol. 17, no. 4, pp. 550–561, 2015.

[8] M. Valli and V. S. Bolzani, "Natural products: perspectives and challenges for use of Brazilian plant species in the bioeconomy," *Anais da Academia Brasileira de Ciências*, vol. 91, no. 3, Article ID e20190208, 2019.

[9] L. P. Queiroz, A. Rapini, and A. M. Giulietti, *Rumo ao Amplo Conhecimento da Biodiversidade do Semi-árido Brasileiro*, Ministério da Ciência e Tecnologia, Brasília, Distrito Federal, 2020, http://www.terrabrasilis.org.br/ecotecadigital/pdf/rumo-ao-amplo-conhecimento-da-biodiversidade-do-semi-arido-brasileiro.pdf.

[10] Brasil, Ministério da Integração Nacional, "Resolução N° 107/2017," Superintendência do Desenvolvimento do Nordeste, 2019, http://sudene.gov.br/images/2017/arquivos/Resolucao-107-2017.pdf.

[11] M. I. G. Silva, C. T. V. d. Melo, L. F. Vasconcelos, A. M. R. d. Carvalho, and F. C. F. Sousa, "Bioactivity and potential therapeutic benefits of some medicinal plants from the Caatinga (semi-arid) vegetation of Northeast Brazil: a review of the literature," *Revista Brasileira de Farmacognosia*, vol. 22, no. 1, pp. 193–207, 2012.

[12] P. M. P. Ferreira, D. F. Farias, M. P. Viana et al., "Study of the antiproliferative potential of seed extracts from Northeastern Brazilian plants," *Anais da Academia Brasileira de Ciências*, vol. 83, no. 3, pp. 1045–1058, 2011.

[13] D. F. Farias, T. M. Souza, M. P. Viana et al., "Antibacterial, antioxidant, and anticholinesterase activities of plant seed extracts from Brazilian semiarid region," *BioMed Research International*, vol. 2013, Article ID 510736, 9 pages, 2013.

[14] N. M. Lima, V. A. La Porta, and F. A. La Porta, "Chemodiversity, bioactivity and chemosystematics of the genus Inga (Fabaceae): a brief review," *Revista Virtual de Química*, vol. 10, no. 3, pp. 459–473, 2018.

[15] J. N. Silva, N. B. N. Monção, R. R. S. Farias et al., "Toxicological, chemopreventive, and cytotoxic potentialities of rare vegetal species and supporting findings for the Brazilian Unified Health System (SUS)," *Journal of Toxicology and Environmental Health, Part A*, vol. 83, no. 13-14, pp. 525–545, 2020.

[16] P. E. R. Carvalho, "Sabiá, *Mimosa caesalpiniifolia*," Edited by C. Técnica and E. Florestas, Eds., Embrapa, Colombo, Brasil, 2007.

[17] U. P. de Albuquerque, P. M. de Medeiros, A. L. S. de Almeida et al., "Medicinal plants of the Caatinga (semi-arid) vegetation of NE Brazil: a quantitative approach," *Journal of Ethnopharmacology*, vol. 114, no. 3, pp. 325–354, 2007.

[18] S. M. de Sousa, A. C. Reis, and L. F. Viccini, "Polyploidy, B chromosomes, and heterochromatin characterization of Mimosa caesalpiniifolia Benth. (Fabaceae-Mimosoideae)," *Tree Genetics & Genomes*, vol. 9, no. 2, pp. 613–619, 2013.

[19] J. B. S. Araújo and J. B. Paes, "Natural wood resistance of *Mimosa caesalpiniifolia* in field testing," *Floresta e Ambiente*, vol. 25, no. 2, 2018.

[20] M. J. Dias Silva, A. M. Simonet, N. C. Silva, A. L. T. Dias, W. Vilegas, and F. A. Macías, "Bioassay-guided isolation of fungistatic compounds from *Mimosa caesalpiniifolia* leaves," *Journal of Natural Products*, vol. 82, no. 6, pp. 1496–1502, 2019.

[21] D. L. Horn, D. Neofytos, E. J. Anaissie et al., "Epidemiology and outcomes of candidemia in 2019 patients: data from the prospective antifungal therapy alliance registry," *Clinical Infectious Diseases*, vol. 48, no. 12, pp. 1695–1703, 2009.

[22] M. E. P. Santos, L. H. P. Moura, M. B. Mendes et al., "Hypotensive and vasorelaxant effects induced by the ethanolic extract of the *Mimosa caesalpiniifolia* Benth. (Mimosaceae) inflorescences in normotensive rats," *Journal of Ethnopharmacology*, vol. 164, pp. 120–128, 2015.

[23] M. J. D. Silva, A. J. S. Carvalho, C. Q. Rocha, W. Vilegas, M. A. Silva, and C. M. C. P. Gouvêa, "Ethanolic extract of *Mimosa caesalpiniifolia* leaves: chemical characterization and cytotoxic effect on human breast cancer MCF-7 cell line," *South African Journal of Botany*, vol. 93, pp. 64–69, 2014.

[24] D. Renzi, M. Valtolina, and R. Forster, "The evaluation of a multi-endpoint cytotoxicity assay system," *Alternatives to Laboratory Animals*, vol. 21, no. 1, pp. 89–96, 1993.

[25] M. Fenech, "Cytokinesis-block micronucleus cytome assay," *Nature Protocols*, vol. 2, no. 5, pp. 1084–1104, 2007.

[26] P. M. P. Ferreira, D. P. Bezerra, J. N. Silva et al., "Preclinical anticancer effectiveness of a fraction from *Casearia sylvestris* and its component Casearin X: *in vivo* and *ex vivo* methods and microscopy examinations," *Journal of Ethnopharmacology*, vol. 186, pp. 270–279, 2016.

[27] B. H. Waynforth, *Injection Techniques: Experimental and Surgical Techniques in the Rat*, Academic Press, London, UK, 1980.

[28] W. Schmid, "The micronucleus test," *Mutation Research: Environmental Mutagenesis & Related Subjects*, vol. 31, no. 1, pp. 9–15, 1975.

[29] J. Heddle, "A rapid in vivo test for chromosomal damage," *Mutation Research: Fundamental and Molecular Mechanisms of Mutagenesis*, vol. 18, no. 2, pp. 187–190, 1973.

[30] Organisation for Economic Co-operation and Development, "Test No. 487: *in vitro* mammalian cell micronucleus test," in *Guidelines for the Testing of Chemicals, Section 4*OECD, Paris, France, 2020, https://www.oecd.org/chemicalsafety/test-no-487-in vitro-mammalian-cell-micronucleus-test-9789264264861-en.htm.

[31] M. V. N. Souza, A. C. Pinheiro, M. L. Ferreira, R. S. B. Gonçalves, and C. H. C. Lima, "Natural products in advance clinical trials applied to cancer," *Revista Fitos*, vol. 3, pp. 25–41, 2007.

[32] G. F. V. Ismael, D. D. Rosa, M. S. Mano, and A. Awada, "Novel cytotoxic drugs: old challenges, new solutions," *Cancer Treatment Reviews*, vol. 34, no. 1, pp. 81–91, 2008.

[33] P. M. P. Ferreira and C. Pessoa, "Molecular biology of human epidermal receptors, signaling pathways and targeted therapy against cancers: new evidences and old challenges," *Brazilian Journal of Pharmaceutical Sciences*, vol. 53, no. 2, Article ID e16076, 2017.

[34] P. M. P. Ferreira, R. R. Drumond, C. L. S. Ramos et al., "Biologia e aplicações pré-clínicas do modelo experimental Sarcoma 180," in *Análise Crítica das Ciências Biológicas e da Natureza*, J. M. B. Oliveira Junior, Ed., Atena Editora, Ponta Grossa, Brazil, pp. 270–287, 2019.

[35] M. Suffness and J. M. Pezzuto, "Assays related to cancer drug discovery," in *Methods in Plant Biochemistry: Assays for Bioactivity*, K. Hostettmann, Ed., p. 376, Academic Press, London, UK, 1991.

[36] N. B. Monção, B. Q. Araújo, J. N. Silva et al., "Assessing chemical constituents of *Mimosa caesalpiniifolia* stem bark: possible bioactive components accountable for the cytotoxic effect of M. caesalpiniifolia on human tumour cell lines," *Molecules (Basel, Switzerland)*, vol. 20, no. 3, pp. 4204–4224, 2015.

[37] C. A. Gonçalves and R. C. C. Lelis, "Tannin content of the bark and wood of five Leguminosae species," *Floresta e Ambiente*, vol. 18, no. 1, pp. 1–8, 2011.

[38] A. Ohsaki, R. Yokoyama, H. Miyatake, and Y. Fukuyama, "Two diterpene rhamnosides, Mimosasides B and C, from *Mimosa hostilis*," *Chemical and Pharmaceutical Bulletin*, vol. 54, no. 12, pp. 1728-1729, 2006.

[39] I. A. d. Nascimento, R. Braz-Filho, M. G. d. Carvalho, L. Mathias, and F. d. A. Fonseca, "Flavonoides e outros compostos isolados de Mimosa artemisiana Heringer e Paula," *Química Nova*, vol. 35, no. 11, pp. 2159–2164, 2012.

[40] N. B. Monção, L. M. Costa, D. D. Arcanjo et al., "Chemical constituents and toxicological studies of leaves from *Mimosa caesalpiniifolia* Benth., a Brazilian honey plant," *Pharmacognosy Magazine*, vol. 10, no. 3, pp. S456–S462, 2014.

[41] E. Pisha, H. Chai, I.-S. Lee et al., "Discovery of betulinic acid as a selective inhibitor of human melanoma that functions by induction of apoptosis," *Nature Medicine*, vol. 1, no. 10, pp. 1046–1051, 1995.

[42] S. Fulda, C. Friesen, M. Los et al., "Betulin acid triggers CD95 (APO-1/Fas) and p53-independent apoptosis via activation of caspases in neuroectodermal tumors," *Cancer Research*, vol. 57, no. 21, pp. 4956–4964, 1997.

[43] S. Fulda, I. Jeremias, H. H. Steiner, T. Pietsch, and K.-M. Debatin, "Betulinic acid: a new cytotoxic agent against malignant brain-tumor cells," *International Journal of Cancer*, vol. 82, no. 3, pp. 435–441, 1999.

[44] S. Fulda and K.-M. Debatin, "Betulinic acid induces apoptosis through a direct effect on mitochondria in neuroectodermal tumors," *Medical and Pediatric Oncology*, vol. 35, no. 6, pp. 616–618, 2000.

[45] S. Fulda and K.-M. Debatin, "Sensitization for anticancer drug-induced apoptosis by betulinic acid," *Neoplasia*, vol. 7, no. 2, pp. 162–170, 2005.

[46] V. Zuco, R. Supino, S. C. Righetti et al., "Selective cytotoxicity of betulinic acid on tumor cell lines, but not on normal cells," *Cancer Letters*, vol. 175, no. 1, pp. 17–25, 2002.

[47] D. Thurnher, D. Turhani, M. Pelzmann et al., "Betulinic acid: a new cytotoxic compound against malignant head and neck cancer cells," *Head & Neck*, vol. 25, no. 9, pp. 732–740, 2003.

[48] H. Ehrhardt, S. Fulda, M. Führer, K. M. Debatin, and I. Jeremias, "Betulinic acid-induced apoptosis in leukemia cells," *Leukemia*, vol. 18, no. 8, pp. 1406–1412, 2004.

[49] S. Fulda, "Betulinic acid for cancer treatment and prevention," *International Journal of Molecular Sciences*, vol. 9, no. 6, pp. 1096–1107, 2008.

[50] J. B. Foo, L. Saiful Yazan, Y. S. Tor et al., "Induction of cell cycle arrest and apoptosis by betulinic acid-rich fraction from *Dillenia suffruticosa* root in MCF-7 cells involved p53/p21 and mitochondrial signalling pathway," *Journal of Ethnopharmacology*, vol. 166, pp. 270–278, 2015.

[51] M. Fenech, "The *in vitro* micronucleus technique," *Mutation Research*, vol. 455, no. 1-2, pp. 81–95, 2000.

[52] M. Fenech, "Cytokinesis-block micronucleus assay evolves into a "cytome" assay of chromosomal instability, mitotic dysfunction and cell death," *Mutation Research*, vol. 600, no. 1-2, pp. 58–66, 2006.

[53] A. N. C. Sortibrán, M. G. O. Téllez, and R. R. Rodríguez-Arnaiz, "Gentotoxic profile of inhibitors of topoisomerase I (camptothecin) and II (etoposide) in a mitotic recombination and sex-chromosome loss somatic eye assay of *Drosophila melanogaster*," *Mutation Research*, vol. 604, no. 1-2, pp. 83–90, 2006.

[54] P. Noordhuis, U. Holwerda, C. L. Van Der Wilt et al., "5-fluorouracil incorporation into RNA and DNA in relation to thymidylate synthase inhibition of human colorectal cancers," *Annals of Oncology*, vol. 15, no. 7, pp. 1025–1032, 2004.

[55] G. M. Zúñiga-González, O. Torres-Bugarín, A. L. Zamora-Perez et al., "Induction of micronucleated erythrocytes in mouse peripheral blood after cutaneous application of 5-fluorouracil," *Archives of Medical Research*, vol. 34, no. 2, pp. 141–144, 2003.

[56] M. Misik, C. Pichler, B. Rainer, M. Filipic, A. Nersesyan, and S. Knasmueller, "Acute toxic and genotoxic activities of widely used cytostatic drugs in higher plants: possible impact on the environment," *Environmental Research*, vol. 135, pp. 196–203, 2014.

[57] A. I. Minchinton and I. F. Tannock, "Drug penetration in solid tumours," *Nature Reviews Cancer*, vol. 6, no. 8, pp. 583–592, 2006.

[58] N. Muhamad and K. Na-Bangchang, "Metabolite profiling in anticancer drug development: a systematic review," *Drug Design, Development and Therapy*, vol. 14, pp. 1401–1444, 2020.

[59] A. S. Bass, M. E. Cartwright, C. Mahon et al., "Exploratory drug safety: a discovery strategy to reduce attrition in development," *Journal of Pharmacological and Toxicological Methods*, vol. 60, no. 1, pp. 69–78, 2009.

[60] D. Williams, N. Kitteringham, D. Naisbitt, M. Pirmohamed, D. Smith, and B. Park, "Are chemically reactive metabolites responsible for adverse reactions to drugs?" *Current Drug Metabolism*, vol. 3, no. 4, pp. 351–366, 2002.

[61] P. M. P. Ferreira, D. B. Santos, and J. D. N. Silva, "Toxicological findings about an anticancer fraction with casearins described by traditional and alternative techniques as support to the Brazilian Unified Health System (SUS)," *Journal of Ethnopharmacology*, vol. 241, Article ID 112004, 2019.

[62] L. Hou, C. Fan, C. Liu, Q. Qu, C. Wang, and Y. Shi, "Evaluation of repeated exposure systemic toxicity test of PVC with new plasticizer on rats via dual parenteral routes," *Regenerative Biomaterials*, vol. 5, no. 1, pp. 9–14, 2018.

[63] B. L. Rapoport, "Delayed chemotherapy-induced nausea and vomiting: pathogenesis, incidence, and current management," *Frontiers in Pharmacology*, vol. 8, pp. 1–10, 2017.

[64] G. C. G. Militão, I. N. Dantas, P. M. P. Ferreira et al., "*In vitro* and *in vivo* anticancer properties of cucurbitacin isolated from *Cayaponia racemosa*," *Pharmaceutical Biology*, vol. 50, no. 12, pp. 1479–1487, 2012.

[65] E. G. Giannini, R. Testa, and V. Savarino, "Liver enzyme alteration: a guide for clinicians," *Canadian Medical Association Journal*, vol. 172, no. 3, pp. 367–379, 2005.

[66] S. K. Ramaiah, "A toxicologist guide to the diagnostic interpretation of hepatic biochemical parameters," *Food and Chemical Toxicology*, vol. 45, no. 9, pp. 1551–1557, 2007.

[67] R. M. Trüeb, "Chemotherapy-induced alopecia," *Current Opinion in Supportive and Palliative Care*, vol. 4, no. 4, pp. 281–284, 2010.

[68] K. Nurgali, R. T. Jagoe, and R. Abalo, "Editorial: adverse effects of cancer chemotherapy: anything new to improve tolerance and reduce sequelae?" *Frontiers in Pharmacology*, vol. 9, pp. 245–247, 2018.

[69] J. D. Sara, J. Kaur, R. Khodadadi et al., "5-fluorouracil and cardiotoxicity: a review," *Therapeutic Advances in Medical Oncology*, vol. 10, pp. 1758835918780140–18, 2018.

Hindawi
Journal of Oncology
Volume 2021, Article ID 3569349, 18 pages
https://doi.org/10.1155/2021/3569349

Review Article

Aminoquinolines as Translational Models for Drug Repurposing: Anticancer Adjuvant Properties and Toxicokinetic-Related Features

Paulo Michel Pinheiro Ferreira,[1] **José Roberto de Oliveira Ferreira**,[2] **Rayran Walter Ramos de Sousa**,[1] **Daniel Pereira Bezerra**,[3] **and Gardenia Carmen Gadelha Militão**[4]

[1]*Department of Biophysics and Physiology, Laboratory of Experimental Cancerology (LabCancer), Federal University of Piauí, Teresina 64049-550, Brazil*
[2]*Center for Integrative Sciences, State University of Health Sciences of Alagoas, Maceió 57010-382, Brazil*
[3]*Gonçalo Moniz Institute, Oswaldo Cruz Foundation (IGM-FIOCRUZ-BA), Salvador 40296-710, Brazil*
[4]*Department of Physiology and Pharmacology, Federal University of Pernambuco, Recife 50670-901, Brazil*

Correspondence should be addressed to Paulo Michel Pinheiro Ferreira; pmpf@ufpi.edu.br

Received 21 June 2021; Accepted 21 August 2021; Published 6 September 2021

Academic Editor: Tian Li

The indiscriminate consumption of antimalarials against coronavirus disease-2019 emphasizes the longstanding clinical weapons of medicines. In this work, we conducted a review on the antitumor mechanisms of aminoquinolines, focusing on the responses and differences of tumor histological tissues and toxicity related to pharmacokinetics. This well-defined analysis shows similar mechanistic forms triggered by aminoquinolines in different histological tumor tissues and under coexposure conditions, although different pharmacological potencies also occur. These molecules are lysosomotropic amines that increase the antiproliferative action of chemotherapeutic agents, mainly by cell cycle arrest, histone acetylation, physiological changes in tyrosine kinase metabolism, inhibition of PI3K/Akt/mTOR pathways, cyclin D1, E2F1, angiogenesis, ribosome biogenesis, triggering of ATM-ATR/p53/p21 signaling, apoptosis, and presentation of tumor peptides. Their chemo/radiotherapy sensitization effects may be an adjuvant option against solid tumors, since 4-aminoquinolines induce lysosomal-mediated programmed cytotoxicity of cancer cells and accumulation of key markers, predominantly, LAMP1, p62/SQSTM1, LC3 members, GAPDH, beclin-1/Atg6, α-synuclein, and granules of lipofuscin. Adverse effects are dose-dependent, though most common with chloroquine, hydroxychloroquine, amodiaquine, and other aminoquinolines are gastrointestinal changes, blurred vision ventricular arrhythmias, cardiac arrest, QTc prolongation, severe hypoglycemia with loss of consciousness, and retinopathy, and they are more common with chloroquine than with hydroxychloroquine and amodiaquine due to pharmacokinetic features. Additionally, psychological/neurological effects were also detected during acute or chronic use, but aminoquinolines do not cross the placenta easily and low quantity is found in breast milk despite their long mean residence times, which depends on the coexistence of hepatic diseases (cancer-related or not), first pass metabolism, and comedications. The low cost and availability on the world market have converted aminoquinolines into "star drugs" for pharmaceutical repurposing, but a continuous pharmacovigilance is necessary because these antimalarials have multiple modes of action/unwanted targets, relatively narrow therapeutic windows, recurrent adverse effects, and related poisoning self-treatment. Therefore, their use must obey strict rules, ethical and medical prescriptions, and clinical and laboratory monitoring.

1. Introduction

Globally, about 1 in 6 deaths is due to cancer and about 70% of cancer deaths occur in low- and middle-income countries. Approximately, one third of these deaths are associated with high body mass index, low consumption of fruits and vegetables, lack of physical activity, and use of tobacco and alcohol. Tobacco use is the most important risk factor for cancer and accounts for approximately 22% of the total deaths. On the other hand, infections such as hepatitis and human papilloma virus (HPV) are responsible for up to 25% of cancer cases in poor and developing countries. In 2018 alone, approximately 9.6 million deaths were related to cancer [1–3].

Determining treatment and palliative care goals are critical steps for cancer therapy with integrated and people-centered health services [3]. Even with a variety of options to treat sarcomas, carcinomas, and adenocarcinomas, such as antimetabolites, microtubule inhibitors, DNA intercalators [4], and monoclonal antibodies [5], resistance remains the cause central to therapeutic failures as well as adverse side effects [6].

In this context, the synthesis and identification of strategic molecules is essential if we want low cost, efficiency, and speed in the production of valuable chemotherapy molecules. Here, we can include aminoquinoline compounds that have the amino group at position 4 of the quinoline ring system. These compounds include molecules used in the treatment of first line (amodiaquine and chloroquine), recurrence (tafenoquine), uncomplicated (hydroxychloroquine) and prevention (chloroquine, hydroxychloroquine and tafenoquine) of malaria infections by *Plasmodium vivax*, *P. malariae*, *P. ovale*, and *P. falciparum* [7–9].

In December 2019, a new severe acute respiratory syndrome coronavirus-2 (called SARS-CoV-2) emerged in China and led to the coronavirus-related pandemic in 2019 (COVID-19) [10]. The indiscriminate use of chloroquine and hydroxychloroquine as a first-line, adjuvant, or palliative drug(s) to treat victims of COVID-19 or to control new local outbreaks as a prophylactic [11, 12] emphasized the various longstanding clinical branches of drugs, including those against chronic disorders. Advantages such as low cost, long usage history, and market availability even in developing countries where malaria is endemic are reasons that explain, at least in part, the commercial triumph of these drugs, converting 4-aminoquinolines into "star drugs" for their reuse in the pharmaceutical industry. Then, we performed a review on the anti-tumor mechanisms of aminoquinolines, focusing on the responses and differences of histological tumor tissues and on the aspects of toxicity related to pharmacokinetics.

To carry out a comprehensive and consistent analysis, we use only primary and secondary materials, including research articles, reviews, books, and government publications written in English, Portuguese, or Spanish. The bibliographic research was performed in the scientific databases ScienceDirect, Scopus, PubMed, and Scielo. The descriptors "autophagy," "cell cycle," "apoptosis," "drug repurposing", and "anti-tumor" were combined with "aminoquinoline" for a narrative scientific exploration.

2. Main Text

2.1. Drug Repurposing for Anticancer Agents: Need or Pharmaceutical Business? Less toxic and more effective treatment designs are often the main reasons for redirections, considering previously recorded aspects of preclinical and clinical pharmacodynamics and toxicokinetics, making drug reuse faster [13–15].

Examples of reuse of effective anticancer drugs in advanced preclinical or clinical studies are almost immeasurable. As a typical example, thalidomide is a leading molecule that has been marketed in 1956 in West Germany, first as antiflu and in 1957 as an antiemetic for pregnancy, but has now been repurposed and approved for multiple myeloma [16, 17]; itraconazole, a triazole antifungal developed in the 1980s, showed anticancer activities in preclinical *in vitro* and *in vivo* models of pancreatic ductal adenocarcinoma derived from liver metastasis [18]; disulfiram, initially approved to mitigate alcoholism, has been investigated to treat radiation-resistant breast cancer stem cells [19]; nelfinavir, originally indicated for the treatment of HIV infection, also exhibits synergistic effects against human cervical cancer cells [20]; sildenafil, which failed in phase II clinical trials for angina disorders, has been redirected to the treatment of erectile dysfunctions and sensitizes prostate cancer cells to doxorubicin-mediated apoptosis [21]; mebendazole, a broad spectrum anthelmintic developed for the treatment of veterinary parasites, has advanced from the treatment of animals to the first clinical applications in humans, inhibiting the growth of adrenocortical carcinoma, gastric cancer, medulloblastoma, glioblastoma, leukemia and myeloma, and breast and prostate cancers [22]; metformin, a classic hypoglycemic medication for diabetes, has revealed a new identity as an antitumor activity by suppressing the mammalian target of rapamycin (mTOR) in human cervical cancer [20] and acute myeloid leukemia [23], and valproic acid, an anticonvulsant that has been considered in several clinical trials due to its epigenetic properties, inhibition of histone deacetylase, and induction of autophagy in neoplastic stomach cells [24].

In 1934, the first synthetized aminoquinoline—chloroquine [4-N-(7-chloroquinolin-4-yl)-1-N,1-N-diethylpentane-1,4-diamine]—was based on the quinine structure isolated from Cinchona officinalis barks in the 1800s. In 1946, hydroxychloroquine [2-[[(4S)-4-[(7-chloroquinolin-4-yl) amino]pentyl]-ethylamino]ethanol] was synthesized, and both molecules were developed as antimalarial tools (Figure 1), as well as extra 4- and 8-aminoquinolines (amodiaquine, tafenoquine, primaquine, mefloquine, quinacrine, quinine, quinidine, and 8-hydroxyquinoline and artemisinin) in an attempt to overcome resistance in *Plasmodium* species, and the side effects [8, 25, 26] seem similar to that of cancer therapy, whose initial successful single-target therapies have been replaced by more combined efficient protocols.

Currently, the aminoquinolines, chloroquine phosphate and hydroxychloroquine sulphate, have been the most

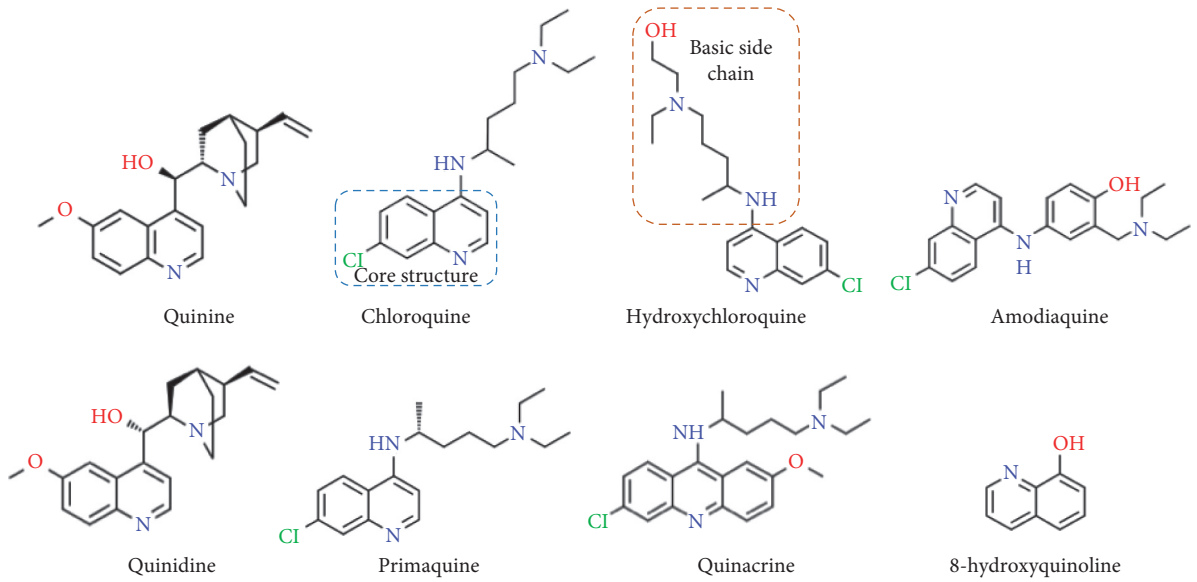

Figure 1: Structures of some common aminoquinolines in clinical use as antimalarials or anti-inflammatory drugs and under investigations as anticancer agents.

common salts used [27] as the first-line regimen for the radical cure of malaria by *P. vivax* in most regions [26] and to treat acute and chronic inflammatory conditions [9, 28–30], respectively, although primaquine and amodiaquine, when used alone or in combination with artemisinin, provide adequate efficacy against many chloroquine-resistant parasites [8, 26].

2.2. Antiproliferative Mechanism of Aminoquinolines. More than 50 years ago, chloroquine showed promising cytotoxicity of tumor cells *in vitro* [31], but only in the last two decades, studies with chloroquine, hydroxychloroquine, and related molecules demonstrated lysosomal-mediated cell death in cancer cells. The exact mechanism of cytotoxic action is not yet fully understood, but hypothesis have attempted.

These molecules can enter into endosomes/lysosomes by passive diffusion, or they can be taken up together with sodium in the exchange of protons, as demonstrated by specific inhibitors of eukaryotic membrane Na^+/H^+ exchangers (NHE) [32]. Both converge in the accumulation within endosomes/lysosomes, leading to the interference of the autophagic flux [33–35], disruption of several enzymes (e.g., acid hydrolases and cathepsin B and D lysosomal cysteine proteases) [36, 37], inhibition of antigen processing [38, 39], and post-translational modification of recently produced proteins [35, 40]. In addition, preclinical and clinical investigations are testing the effectiveness of quinines as inhibitors of the autophagy flux to overcome resistance when traditional chemotherapy drugs are used as monotherapy, since the induction of autophagy has been associated with resistance in the therapy of cancer [41, 42].

2.2.1. Brain Tumor Cells. Chloroquine decreases cell proliferation of p53 wild-type glioma lines more efficiently, indicating a key p53 responsibility for apoptotic cell death and cell cycle control through the HDM2, P21, PIG3, and *BAX* genes (Figure 2). Likewise, the induction of apoptosis *in vivo* was found in mice with U87MG glioma intracranially when treated with chloroquine [43].

On the other hand, chloroquine-induced neuronal cell death of normal neurons [44] indicates mitochondrial dysfunction as a result of p53-independent effects [43], but dependent on cathepsin D lysosomal cysteine proteases processing, proposing direct or indirect actions on the cathepsin D metabolism [37]. Moreover, chloroquine activation of ataxia telangiectasia-mutated (ATM)/ataxia telangiectasia and Rad3-related (ATR) kinase DNA injuries [45] seems unnecessary for caspases and p53 activation [37, 43, 44, 46–48], suggesting that aminoquinolines induce the death of glioblastoma cells, regardless of the p53 status [37].

The absence of DNA damage induced by chloroquine similar to DNA damage by direct ionizing radiation with consequent activation of p53 can be associated with its mechanism of interaction with DNA molecules, since chloroquine intercalates into DNA, but does not cause DNA damage directly [43, 49]; this does not exclude that caspase-3 activation is stronger in wild-type p53 glioma cells, proposing a clear contribution of p53 to chloroquine-induced apoptosis [43].

U251-MG brain cell line, orthotopic GL-261 gliomas, or rat brain-implanted C6 cells treated with suberoylanilide hydroxamic (histone deacetylase inhibitor, HDACi) and temozolomide (alkylating agent) in the presence of chloroquine 10–15 μM showed reduced cell viability, morphology changes, increase in the sub-G_1 population, Bax, cleaved-caspase-3, and cleaved-PARP1 [poly-(ADP-ribose)-polymerase 1], externalization of phosphatidylserine, and activation of caspase-3/7 (Table 1). Such events are features of apoptosis, but the time course curves showed that the

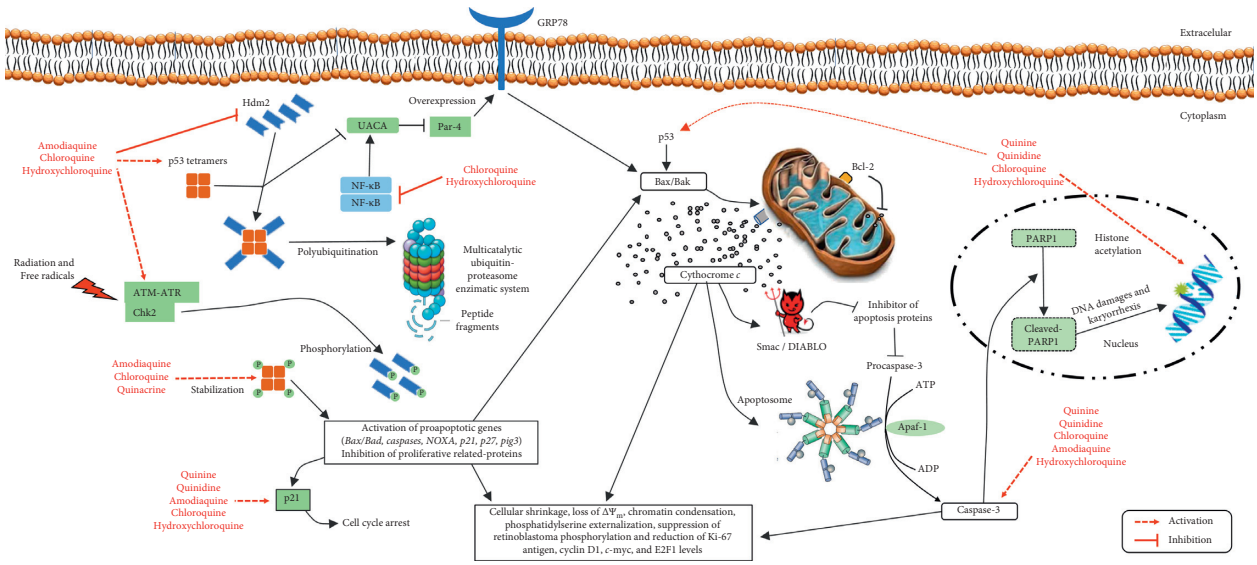

Figure 2: Pathways involved in general cytotoxicity and activation of apoptosis by 4-aminoquinolines. The transportation of both drugs is completely via passive diffusion (i.e., no transporters are involved). Bak and Bax are p53-induced proapoptotic members that constitute the apoptotic pore complex for the release of mitochondrial cytochrome c, leading to mitochondrial depolarization, activation of caspase-3, cleaving of poly-(ADP-ribose)-polymerase 1 (PARP-1), and nuclear DNA fragmentation. Aminoquinoline-dependent DNA damage activates p53 and its downstream gene p21, resulting in cell cycle arrest after a post-translational p53 activation by phosphorylation of the ataxia telangiectasia-mutated (ATM) protein, leading to ATM-dependent phosphorylation of p53 checkpoint protein kinase. Moreover, chloroquine, quinacrine, and amodiaquine trigger p53 stabilization in TP53-specific reporter human cancer cells and block the p53 ubiquitination properties of human double minute 2 (Hdm2) molecules, which in turn prevents p53 proteasome degradation. Stimulation of histone acetyltransferase (HAC) and inhibition of histone deacetylase (HDAC) are part of the rationale pattern of arresting growth. Chloroquine is linked to the activation of p53, inhibition of NF-κB (factor nuclear kappa B) and uveal autoantigen with coiled-coil domains and ankyrin repeats (UACA), which promotes secretion of prostate apoptosis response-4 (Par-4) and expression of glucose regulated protein 78 (GRP78) receptor on the cancer cell surface, and consequent apoptosis.

G_2/M arrest occurs with autophagy and before the apoptosis because the blocking of this response with autophagy inhibitors (3-methyladenine and chloroquine, for example) makes cells susceptible to temozolomide and suberoylanilide hydroxamic [54, 60].

2.2.2. Human Cervical Tumors. Human papilloma positive HeLa cells (p53 wild-type) are resistant to apoptosis-inducing effects of death receptors [64], but pretreatment with 75 μM chloroquine sensitized HeLa cells towards apoptosis mediated by Fas, as measured by TUNEL staining of DNA strand breaks [65], due to the disruption of mitogen-activated protein kinases (MAPK)/extracellular signal-regulated kinases (ERK)1/2, as found in cells treated with PD98059, a MEK1 inhibitor. Indeed, chloroquine and analogues appear to disable members upstream of the MAPK pathway (Figure 3), avoiding ERK phosphorylation and activation by a paradoxical Raf phosphorylation in specific residues, which possibly blocks the ERK activation by Akt activity [65].

HELa cells treated with 10–30 μg/mL of hydroxychloroquine presented an increase in lysosomal volume and cathepsin B release from lysosomes to the cytosol and the nucleus, resulting in cytoplasmic vacuolization, cellular shrinkage, exposure of phosphatidylserine, loss of mitochondrial transmembrane potential ($\Delta\Psi m$), release of cytochrome c, activation of caspase-3 (Figure 2), and condensation of chromatin. In particular, vacuolization was found before chromatin condensation and was accompanied by the signs of macroautophagy [36]. These effects were blocked by bafilomycin A1, which prevents degradation of LC3, induces its accumulation in autophagolysosomes [66] and acts as an inhibitor of the vacuolar-type H^+-ATPase, changing endosomal pH [67], showing that hydroxychloroquine activated apoptosis via lysosomes instead of other organelles (mitochondria or nuclei, for example).

The colorimetric MTT assay indicated that 3-methyladenine (3-MA) or chloroquine separately has no significant effects on the viability of HeLa cells, but both enhance the cytotoxic effects of cisplatin. The cotreatment also increased the expression of p62, the levels of cleaved caspase-3/-4, caused inhibition of autophagy downstream, and accumulation of ubiquitinated beclin-1 and LC3II misfolded proteins, and almost simultaneous apoptotic activation. Since cisplatin induces the generation of misfolded proteins, but increases autophagy, this would alleviate the physiological stress of endoplasmic reticulum by clearing the ubiquitinated proteins, which would trigger intrinsic apoptosis in HeLa cells [55]. The compound 3-MA is an inhibitor of phosphatidylinositol 3-kinases, which play an important role in controlling the activation of mTOR, a key regulator of autophagy [68].

2.2.3. Colorectal Cancers. As a pyrimidine analogue, 5-fluorouracil (5-FU) acts as an antimetabolite to inhibit DNA

Table 1: General mechanisms of chemosensitizing and radiosensitizing adjuvant actions of chloroquine, hydroxychloroquine, and analogues.

Treatment/Drug	Adjuvant actions	References
Phosphatidylinositol analogs, oligopeptides Akt-PH linkers, inhibitors of Akt-kinase, and blockers of ATP-binding site catalytic subunit	Mediated chemosensitization and enhanced cytotoxicity	[50]
All-trans retinoic acid	Reduction of Ki67-positive cells and clonogenicity, activation of histone acetyltransferase, and inhibition of histone deacetylase enzymes	[51]
5-Fluorouracil	Down-regulation of CDK-2 expression and cyclin E/CDK2 complex activity, arrest in G_0/G_1 phase, and enhancement of antiproliferative properties	[52]
Everolimus	Proliferative reduction, increase of p53 and $p21^{Cip1}$ levels, phosphorylation reduction at serine 2448 in mTOR proteins	[48]
Rapamycin	Blockade of autophagy and LC3-II degradation, cytotoxic chemosensitization and involvement of a caspase-independent mechanism	[53]
Cisplatin	Increase of caspase-3 activation, LC3 II ubiquitinated intracellular misfolded proteins, and intrinsic apoptosis	[54, 55]
Docetaxel	Enhanced cytotoxicity and stronger *in vivo* anti-tumor efficacy	[56]
Doxorubicin	Potentiated cytotoxicity upon coexposure	[57]
Oxilaplatin	Increased sensitivity under hypoxic conditions and p62 levels, delaying of tumor growth of HT-29 colon cancer xenografts	[58]
Sunitinib	Increase of the p62 level, reduction of blood vessel formation, CD-34 expression, microvessel density, and nitric oxide levels in tumor, and Ehrlich ascites carcinoma tumor growth reduction	[59]
Temozolomide	Cell viability reduction and intensification of cleaved-caspase-3, cleaved-PARP1, phosphatidylserine externalization, and caspase-3/7 activation	[54, 60]
Receptor-interacting protein kinase 3 (RIP3)	Upregulation of RIP3, accumulation of RIP3-p62 complexes and type II-LC3B, and efficiency on colon tumor-bearing mice	[61]
Bevacizumab	Weakening of the Akt-mTOR signaling pathway and recovering the tumor-suppressive effect of bevacizumab	[62]
Sertraline + erlotinib	Amplification of caspase-independent autophagic cell death and mouse survival in orthotopic non-small cell lung cancer mouse models	[63]

and RNA synthesis, but it also has radiosensitizing, immunosuppressive, and mutational properties and has been widely used to treat various solid tumors, including colorectal, breast, stomach, pancreas, ovary, bladder, and liver cancers [69]. The apoptotic effects of 5-FU on human colorectal adenocarcinoma HT-29 cells were also increased by chloroquine. The pretreatment of HT-29 cells with chloroquine suppressed CDK-2 expression and catalytic activity of cyclin E/CDK2 complexes (Figure 2), leading to the (G_0/G_1) arrest [52]. Such findings suppose autophagy as a protective route against the action of 5-FU, since autophagic inhibitors increase the antiproliferative properties of this fluoropyrimidine.

Murine cell lines showing endogenous upregulation of receptor-interacting protein kinase 3 (RIP3) were more sensitive to chloroquine [61] and presented cytosolic accumulation of RIP3-p62 complexes and LC3-II, which is commonly recruited to phagosome membranes. However, initial/executioner caspase levels are apparently not altered by chloroquine during necroptotic cell death in CT-26 cells [61].

Since the morphological and flow cytometric investigations of chloroquine-treated CT-26 cells showed dissolved nuclei, condensation, swelling of organelles, and rupture of the cell membrane, these findings suggested that, instead of apoptosis, RIP3-dependent necroptosis was probably a reason for $RIP3^+$-chloroquine-induced cell death [61, 70, 71].

The induction of tumor apoptosis *in vivo* exposed that apoptosis is not the only way by which chloroquine activates death cascade, as verified by TUNEL experiments and signals of necroptosis. In any case, mice with a CT-26-tumor xenograft showed tumor reduction after adjuvant treatments, whereas chloroquine alone showed a 45% reduction, and the combination with chemotherapies increased by up to 80% [61].

Chloroquine plus sunitinib, bevacizumab, and/or oxaliplatin increased intracellular levels of p62, indicating the accumulation and interruption of autophagic flux, increased caspase-3 activity and sensitivity under hypoxia conditions, and reduced blood vessel formation, expression of CD31,

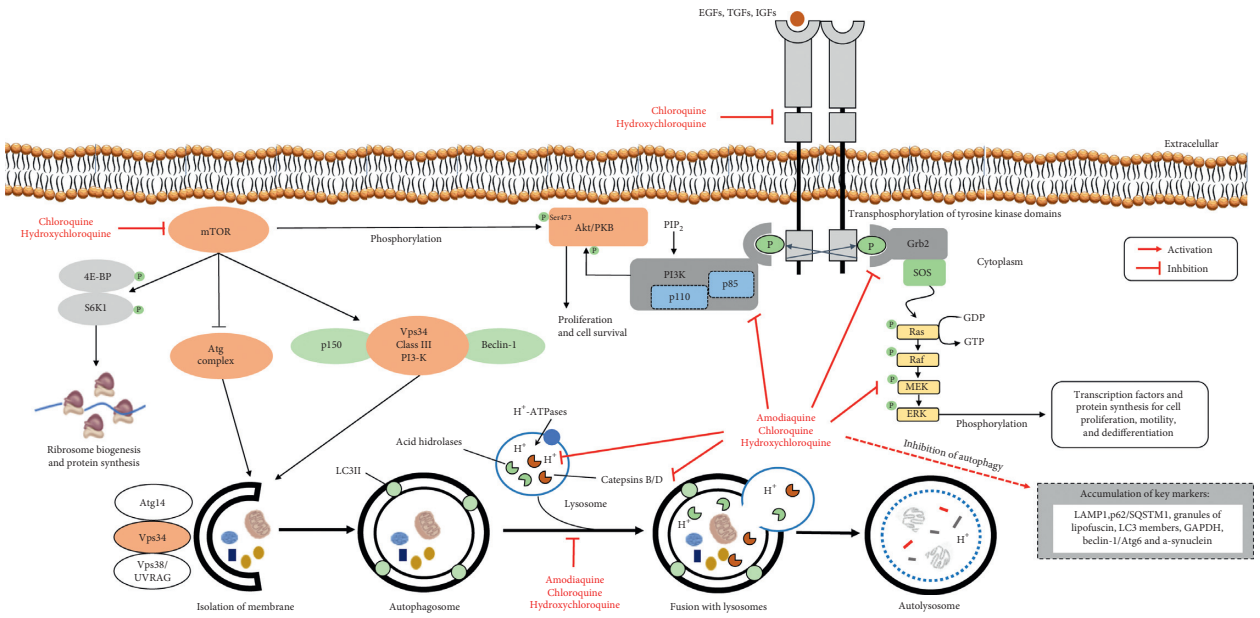

FIGURE 3: Molecular findings, which support the theory that chloroquine and analogues exerts, at least in part, antineoplastic effects altering the phosphorylation *status* of EGFR/PI3K/Akt/mTOR/Atg and p53 pathways, inhibiting directly PI3K-Akt and mTOR kinases, obstructing catalytic subunits in the ATP-binding site or altering the recycling of tyrosine kinase receptors, besides impairing or interfering in lysosomal and autophagosome functions. mTOR phosphorylates the eukaryotic initiation factor 4E-binding protein (4E-BP) and the p70S6 kinase1 (S6K1). Therefore, if specific drug inhibitors against mTOR kinase are used, this should not only have altered proliferation but also the protein synthesis rate. Vesicular protein sorting 34 (Vps34) complex I has Atg14p as an additional factor, which participates in the formation of autophagosomes, while complex II has Vps38, which is required for vacuolar protein sorting. These catalytic complexes work as ubiquitin-like conjugation systems for phagophore elongation and recruitment of other proteins to the self-digesting process, as seen with Vps34, a phosphatidylinositol serine-threonine kinase, its binding partner Beclin-1 (Atg6) and the protein kinase p150 in mammals (Vps15). Assembly of this complex is crucial for autophagy and it recruits other proteins to the phagophore assembly site (PAS). Therefore, the phagophore elongates into a cup-shaped structure and begins to engulf cellular material, sequestering the material in a double-membraned autophagosome. Both chloroquine and hydroxychloroquine block autophagy in initial phases, causing accumulation of acidic vesicle cell markers and appear to deactivate upstream members of mitogen-activated protein kinase (MAPK) pathway, preventing phosphorylation and activation of extracellular signal-regulated kinases (ERK)1/2 by a paradoxical phosphorylation of Raf at specific residues, which possibly blocks ERK activation by Akt activity.

microvessel density, and nitric oxide levels in colorectal cancers [58, 59]. The growth of HT-29 colon cancer xenografts in bevacizumab- and oxaliplatin-treated mice was postponed from 7.2 to 23 days when bevacizumab and oxaliplatin were coadministered with chloroquine [58].

In addition to acting as inhibitors of autophagy, chloroquine, quinacrine, and amodiaquine trigger p53 stabilization in TP53-specific reporter human cancer cells [59] and wild-type cell lines [49, 72] (Figure 2). Amodiaquine *in vitro* at 20 μM was specifically more efficient than chloroquine in inducing p53 stabilization by an independent ATM signaling pathway, interrupting cell proliferation of colorectal carcinoma cell lines (in addition to breast, hepatic, lung, sarcoma, and melanoma), decreasing the synthesis of a general ribosome precursor—47S rRNA—in U2OS cells, inducing the accumulation of LC3II autophagosome and lysosomal associated membrane protein 1 (LAMP1), and impairing translocation of the DDX21 nucleolar helicase to the nucleoplasma [49], the catalytic protein involved in the synthesis and processing of rRNA [73].

The nucleolar changes induced by amodiaquine were similar to those observed in cells treated with chloroquine and BMH-21l, a polymerase I inhibitor. Furthermore, amodiaquine inhibited the activity of ubiquitin ligase Hdm2's and thereby stabilized/activated p53 [49].

2.2.4. Breast Carcinomas. Quinidine [74–76], quinine [77], chloroquine [76, 77], and hydroxychloroquine [75] induced differentiation in MCF-7 cancer cells, as demonstrated by the accumulation of cells in the G_0 phase, intracellular milk fat globule membrane protein and lipid droplets (typical markers of differentiation), increased p21 and suppressed phosphorylation of retinoblastoma and expression of Ki-67 antigen, cyclin D1, *c*-myc, and E2F1 protein levels (Figure 2). While chloroquine was stronger in stimulating MCF-7 apoptosis, quinine was the most active in promoting differentiation [77].

Chloroquine or hydroxychloroquine + all-trans retinoic acid also reduced MCF-7 cells positive for Ki67, and their clonogenicity and hydroxychloroquine altered the acetylation *status* in the N-terminal lysines of the histones H3 and H4, epigenetic sites expected by the "zip": model of histone acetylation [51]. These observations indicate that, in association with all-trans retinoic acid, quinidine, quinine, chloroquine, or hydroxychloroquine regulates protein

acetylation events and the combination with all-trans retinoic acid stimulates histone acetyltransferase and inhibits HDAC enzymes in breast cancers (Figure 2). Nevertheless, the direct inhibition of the HDAC enzyme does not appear to be necessary for the differentiating activity of antimalarial quinolines [76].

Breast MCF-7 cells (wild-type for p53) presented 74% of cell cycle arrest in the G_1 phase after 24 h and 72 h of exposure to chloroquine 50 μM and everolimus [20 nM, 40-*O*-(2-hydroxyethyl)-rapamycin, an mTOR inhibitor], showing additive inhibitory effects when both drugs were added in 3-D cocultures. This proliferative reduction was confirmed by DNA quantification and increased levels of p53 and $p21^{Cip1}$ after the treatment of MCF-7 cells with chloroquine, but not everolimus, which indicates that G_1 arrest is mediated by tumor suppressor pathways p53 and p21 [48].

Loehberg et al. [46] detailed the dependency of p53 on the effects of chloroquine on BALB/c p53-null mammary epithelium cells and human mammary gland epithelial MCF10A line. Chloroquine-dependent DNA damage activates p53 and its downstream gene p21, resulting in the G_1 cell cycle arrest after a post-translation p53 activation by chloroquine-induced phosphorylation of ATM proteins, proving the existence of ATM-dependent phosphorylation of the p53 checkpoint (Figure 2). These molecular findings may explain the particular ability of chloroquine 3.5 mg/kg to reduce the growth rate and tumor incidence by 41% only in p53-wild-type BALB/c mice exposed to *N*-methyl-*N*-nitrosourea after 8 weeks of treatment. Since the TP53 is a mediator of hormone (estrogen/progesterone)-induced protection against chemical mammary carcinogenesis and no protection was observed in BALB/c p53-null mammary epithelium, it certainly shows that chloroquine can prevent breast cancer similar to estrogen/progesterone treatment and shows a p53 dependence [46].

As described before, autophagy is required for efficient growth of cells, and upon starvation chloroquine decreases LC3II lysosomal degradation [66, 73, 78, 79]. Therefore, 67-NR and 4-T1 mouse breast cell lines treated with chloroquine were sensitized preferentially in response to phosphoinositide 3-kinases or mTOR inhibitors, the route that directly regulates autophagy (Figure 3). Surprisingly, chloroquine sensitized 4-T1 and 67-NR cells to inhibit phosphoinositide 3-kinases or rapamycin even in *Atg12* gene nonfunctional cells, and the pan-caspase inhibitor zVAD-fmk (zVAD) did not increase cell survival, indicating that chloroquine should be able to sensitize even when autophagy has already been previously obstructed. Corroborating these findings, decreasing the cell viability involves a caspase-independent mechanism in which chloroquine but not bafilomycin A1 sensitizes cells to rapamycin-mediated cytotoxic actions, even though both of them block autophagy and LC3-II degradation [53].

2.2.5. Lung Cancers. Low concentrations of chloroquine (0.25–32 μM) up to 24 h exposure induced apoptosis of adenocarcinoma lung A-549 cells and vacuolation with increased volume of acidic compartments, but caused necrosis at 48 h and higher concentrations, as demonstrated by lactate dehydrogenase assays. Interestingly, in the presence of D609, a specific inhibitor of phosphatidylcholine-specific phospholipase C, only lower concentration effects were suppressed [80].

Hu et al. [50], using screening cytotoxic methods and absorbance assays, pointed out that the coculture of chloroquine and Akt inhibitors (phosphatidylinositol analogs, oligopeptides Akt-PH linkers, direct inhibitors of Akt-kinase activity, and blockers of catalytic subunit in the ATP-binding site) are more effective than either one alone. Such killing effects of chloroquine-mediated chemosensitization occurs at low concentrations as 10–20 μM and present specificity up to 120-fold for killing cancer than normal cells [50]. These findings indicate that chloroquine might significantly increase the therapeutic effects of some PI3K-Akt inhibitors with minor action on immortalized normal mammary gland epithelium 184B5 cells. Probably, chloroquine-mediated chemosensitization is related to the ability to block the formation of digestive vesicles, as those activated by tephrosin on cells, a natural rotenoid that induces endocytosis and subsequent degradation of human epithelial tyrosine kinase (HER-1 and 2) receptors [81].

2.2.6. Melanomas. A screening chemical library of antimalarial drugs against melanomas showed the endoperoxide-based redox antimalarial artemisinin-class members as inducers of apoptosis, while metastatic melanoma cells (A375, G361, and LOX) displayed a specific vulnerability to artemisinin and semisynthetic artemisinin-derivatives and NOXA-dependent apoptosis [82], a proapoptotic member of the Bcl2 family. Such sensitivity was corroborated by the upregulation of cellular oxidative stress, phosphatidylserine externalization, and cleavage of procaspase-3 [82]. Next, amodiaquine-exposed A-375 and G361 melanoma cells exhibited the formation of multivesicular single membrane-enclosed structures with electron-dense inclusions (indicative of lysosomal expansion), impairment of mitochondrial transmembrane potential, and accumulation of LAMP1, p62/SQSTM1, α-synuclein, lipofuscin, and LC3-II at concentrations as low as 1 μM [57], all accumulating autophagic proteins as a consequence of blocked autophagic-lysosomal flux (Figure 3). Such a blockade revealed a similar pattern of impaired lysosomal acidification in response to the treatment with either bafilomycin A1, amodiaquine, and chloroquine from a mechanistic point of view.

Intriguingly, a comparative analysis performed in A375 melanoma cells showed higher antiproliferative activity of amodiaquine when compared to chloroquine, which was confirmed by array analysis, revealing the modulation of gene expression antagonizing cell cycle progression (upregulation of *CDKN1A* and downregulation of *E2F1*) and modulation of the genes *TP53*, *CDKN1A*, *E2F1*, *CCND1*, and phosphorylated RB1. On the other hand, chloroquine failed to alter protein levels of TP53, E2F1, CCND1, and HSPA1A in A375 cells, demonstrating that the chloroquine treatment was not associated with the induction of cell cycle arrest, a finding extremely different from amodiaquine-induced melanoma cell cycle obstruction in the *S* phase [57].

Previous studies had already indicated amodiaquine as a more potent antimalarial molecule than chloroquine, a property attributed to a tropism targeting the acidic food vacuole of the plasmodium parasite [83]. Amodiaquine is a lysosomotropic 4-aminoquinoline-based tertiary amine as well, but it has a 1,4-aminophenol-pharmacophoric substituent capable of forming an electrophilic quinoneimine-metabolite under intracellular conditions of oxidation. Then, this reactive intermediate induces covalent protein adductions [57] and may contribute to higher potency.

2.2.7. Retinal Pigment Epithelial Cells. 10–250 μM chloroquine produced a persistent reduction in mTOR activity and intracellular calcium in retinal ARPE-19 cells, leading to the nuclear translocation of transcriptional factors for lysosomal biogenesis, expansion of lysosomes, severe suppression of autophagosome-lysosome fusion, and increased cytosolic levels of LAMP1, beclin-1, glyceraldehyde 3-phosphate dehydrogenase (GAPDH), and phospholipid intracellular content in 25-fold or greater [40, 84].

The inhibitors of endocytosis reduce endosomes and arrest a considerable amount of GAPDH into lysosomal cytosolic vesicles and cell membranes. On the other hand, its degradation is physiologically reduced or blocked as an adaptive reaction of lysosomes to retrieve normal functions, although accumulation of intracellular substrates, including p62, GAPDH, and phospholipids, are not entirely reestablished [84]. Anyway, chloroquine-induced protein accumulation indicates autophagy inhibition because p62 and GAPDH are degraded by lysosomes via autophagy and chaperon-mediated autophagy pathways, respectively [85].

GAPDH, an enzymatic 144-kDa tetramer expressed on the cell surface and secreted from cells leading to forward trafficking of active GAPDH out of cells, actively contributes to endosomal recruitment [85]. The versatility and promiscuity of functions and its interaction with multiple protein partners make GAPDH a vital tool for cell survival because it works as a scavenger agent to flush out misfolded molecules and activates inside processes during membrane trafficking and production of secretory lysosomes [86].

2.2.8. Mouse Embryonic Fibroblasts. In mouse embryonic fibroblasts (MEF), chloroquine and hydroxychloroquine confirmed their capacity to block autophagy in a concentration-dependent manner [87]. Indeed, $Bax^{-/-}$ and $Bak^{-/-}$ MEF cells were resistant against hydroxychloroquine-induced mitochondrial and plasma membrane permeabilization and hydroxychloroquine induced cathepsin B intracellular redistribution (Figure 3); besides, it was unable to cause mitochondrial depolarization, release of cytochrome *c*, or cell death when compared to wild-type MEF cells. Altogether, these data imply a specific sequence of subcellular alterations: (a) lysosomal accumulation resulting in the selective loss of mitochondrial potential and release of lysosomal enzymes, such as cathepsin B; (b) activation of Bax and mitochondrial permeabilization, and (c) caspase-3 activation, phosphatidylserine exposure, chromatin condensation, DNA loss, and apoptosis (Figure 2) [36]. Correspondingly, *in vivo* effects following 24 h or 48 h exposure of C57BL/6JOlaHsd mice to hydroxychloroquine 60 mg/kg showed Golgi changes and accumulation of LC3 [87].

These cells were also tested with a panel of approved-FDA drugs containing either quinoline or quinolone pharmacophores. Chloroquine caused the secretion of prostate apoptosis response-4 (Par-4) from wild-type p53 MEFs (Figure 2), as well as from normal human prostate stromal and lung fibroblast cells and their respective aminoquinoline derivatives, and induced Par-4 systemic secretion in C57BL/6 mice in a dose of 50 mg/kg body weight, and in patients from a clinical trial against cancer prior to surgery taking hydroxychloroquine [88]. As predictable, chloroquine caused the accumulation of LC-3II and p62/SQSTM1, but drug-induced secretion of Par-4 was not inhibited by zVAD, and differences in p62 levels have not been noticed after the treatment with wild-type Par-4 and $Par\text{-}4^{-/-}$ cells [88].

Par-4 is a tumor suppressor capable of inducing apoptosis selectively in most cancer cells without affecting normal/immortalized/nontransformed ones. The increase of Par-4 in the extracellular matrix causes cell death of tumor cells through binding to the overexpressing GRP78 receptor on the cell surface. Normal lines exhibit undetectable-to-low levels of this receptor [89], which protect them from the "friendly fire" though Par-4 is secreted by both normal and cancer tissues [89, 90]. Therefore, Par-4 secretion is not associated with apoptosis and does not affect autophagy in normal mouse embryonic fibroblasts. Meanwhile, the co-cultures of chloroquine-treated $Par\text{-}4^{+/+}$ MEFs plus H-460 lung $p53^{+/+}$ and H-1299, HOP92, and KP-7B lung or prostate PC-3 $p53^{-/-}$ cancer cells were sensitive to apoptosis, but not when cocultured with chloroquine-treated $Par\text{-}4^{-/-}$ MEFs, and chloroquine failed to induce Par-4 secretion in prostate cancer cells (LNCaP, C42B, DU-145, and PC-3) and lung cancer cells (H-460 and A-549). These discoveries indicate that chloroquine-induced Par-4 secretion from normal lines causes paracrine apoptosis in cancer cells [86], and such action increases the selective expression of Par-4 receptor GRP78 on the surface of cancer cells [91] (Figure 2).

In vivo related findings in C57BL/6 mice bearing LLC1 pulmonary tumors also showed systemic elevation of Par-4 regressed tumor growth and metastatic lung nodules in animals treated with chloroquine 25 mg/kg/days for 5 consecutive days [88, 90]. Once again, the antiproliferative activity of chloroquine is linked to the activation of p53 and inhibition of NF-κB because these events promote Par-4 secretion [88] because p53 regulates classical components of the secretory route (Figure 2). This relatively unknown Par-4 pathway adds new importance to the traditional DNA protection roles of normal *TP53* gene to manage the tumor suppressor.

2.3. We Need to Think Outside the Box

2.3.1. New Pharmacological Judgement. Traditional comprehension about the effects of chloroquine and analogues on the lysosomal physiology implies a specific sequence of subcellular alterations: (a) lysosomal accumulation resulting in the selective release of lysosomal enzymes, such as

cathepsin B and D; (b) activation of Bax/Bad and mitochondrial permeabilization; (c) loss of mitochondrial potential, and (d) activation of caspases, phosphatidylserine exposure, chromatin condensation, DNA loss, and apoptosis (Figure 2).

However, new pharmacological judgements have arisen and changed some scientific dogmas in this area. Higher lysosomal pH was observed after 4 h of treatment with known alkalinizer drugs (fluoxetine, imipramine, dimebon, tamoxifen, chlorpromazine, amitriptyline, and verapamil), including chloroquine. Considering their high lipophilic structures (clogP ranging from 3.49 to 6.24), this suggests suitable entry into target cells including osteosarcoma U2OS, adenocarcinoma cervical HeLa, embryonic rat cardiomyocytes H9C2, and the human retinal pigment epithelial ARPE-19 line. Indeed, among amodiaquine, artemisinin, mefloquine, piperaquine, primaquine, quinacrine, and chloroquine, two antimalarial compounds (mefloquine and quinacrine) were about 30- and 60-fold more potent autophagy inhibitors on U2OS cells than chloroquine, respectively [92].

However, higher pH values were sustained no more than the compound exposure time, and after 24 h, renewed acidic organelles with pH between 4-5 were detected, indicating restorage of pH, which was also confirmed by nuclear translocation of transcription factors involved in lysosomal biogenesis, bigger lysosomal volume, and returning of cathepsin levels in order to reestablish optimal conditions for enzyme digestion [84, 93, 94].

Most studies have also suggested that chloroquine- or hydroxychloroquine-induced cell death is initiated by the "type II programmed autophagic/lysosomal pathway," including sequestration of organelles into autophagosomes and cytoplasmic vacuolization (Figure 3), and these processes are followed by later signs of the "type I programmed death" [36, 40, 66], which traditionally display karyorrhexis, DNA fragmentation, release of mitochondrial cytochrome *c*, activation of Bcl-2 proapoptotic proteins and caspases, cellular shrinkage, and phosphatidylserine externalization (Figure 2). Additionally, although members of the 4-aminoquinoline family, including chloroquine, hydroxychloroquine, and Lys-05 (dimeric chloroquine) inhibit autophagy [68], it has been suggested that ribosome biogenesis stress found in treated cells is not a general consequence of autophagy inhibition and that amodiaquine stands out among the 4-aminoquinoline family as a compound functioning by 2 independent mechanisms in two distinct intracellular environments: cytoplasm, where autophagy inhibition occurs and nucleolus, for diminution/blockage of ribosome biogenesis [49], which demonstrate that amodiaquine but not chloroquine inhibits ribosome biogenesis, disrupts nucleolar structure, and triggers degradation of RNA polymerase I.

As endosomal trafficking, endosome-lysosome fusion, membrane stability, signaling pathways, and transcriptional activity are impaired by hydroxychloroquine and chloroquine, it was hypothesized that combining them with radiation would be a good adjuvant alternative [47]. Nevertheless, chloroquine sensitization of some breast cancer lines revealed to be independent of autophagy inhibition, since sensitization was not mimicked by the knockdown of *Atg12* or *Beclin 1* genes or following treatment with bafilomycin A1, and chloroquine-induced cell death occurred even in the absence of Atg12 [53], proposing that reducing autophagy does not affect drug cytotoxicity ubiquitously in all human cells. Meanwhile, studies have demonstrated that chloroquine has specific cell sensitization effects to particular antimitotic drugs, whereas primaquine and mefloquine can sensitize resistant cancer cells to all antimitotic drugs without preference [81].

In a similar way, most investigations indicate that chloroquine does not block all forms and steps of the endolysosomal system. Analysis showed that chloroquine/hydroxychloroquine inhibits autophagy in initial phases, causing accumulation of acidic vesicular organelles and break/discontinue autophagosome-lysosome fusions, but they do not alter the ability of lysosomes to digest target macromolecules as conventionally accepted. In another point of view, compounds that simply increase the upstream autophagic flux without altering downstream fusion and degradation steps may not provide therapeutic benefit [95]. This would explain why only chloroquine and hydroxychloroquine are officially recommended as autophagy inhibitors by the Food and Drug Administration (FDA).

If we recall a more integrated concept, considering the well-established details about the blockage of autophagic flux and the capacity to inhibit PI3K/Akt/mTOR pathways and trigger ATM/ATR/p53/p21 signaling, it is possible to visualize that they complement themselves to cause death of cancer cells. Once mTOR is commonly phosphorylated at position 2448 via the PI3K/Akt and has been inhibited when higher levels of $p15^{INK4B}$, $p16^{INK4A}$, $p21^{Cip1}$, $p27^{Kip1}$, p53, and other suppressor tumors are present under stress conditions, p21 obliges G_1 restriction by inhibitory binding to CDK2/cyclin E or other CDK/cyclin complexes [45]. These physiological aspects support the theory that chloroquine or hydroxychloroquine exhibits, at least in part, antineoplastic effects altering the phosphorylation status of EGFR/PI3K/Akt/mTOR/Atg and p53 pathways [43, 46, 48, 49, 57] due to the direct inhibition of PI3K-Akt kinases, obstruction of catalytic subunits in the ATP-binding site [80], and/or misregulation of signaling of epithelial growth factor receptors (EGFRs) during endocytosis because they seem to weaken receptor-mediated endocytic transfers of TKRs to degradative compartments [95] (Figure 3).

In this context, the inhibition of tyrosine kinase receptors and downstream pathways (Receptor/PI3K/Akt or Receptor/Grb2/Ras/Raf/MEK/ERK) are examples of suitable targets to select antitumor repurposing molecules [50, 80, 81] (Figure 3). Despite that tyrosine kinase inhibitors have demonstrated enhanced selectivity, extra effects on some kinases and beyond their target family show intrinsic polypharmacology often favorable for clinical efficacy [6]. Therefore, blocking the signaling pathways that maintain the stemness is thus a rational goal to avoid recurrence as well as to block tumor growth and metastasis. Metastatic cancer or surgically nonresectable tumors show five years mortality above 90% in aggressive cancers, e.g., pancreatic tumors and

acute myeloid leukemia. Hence, with a few exceptions, survival rates of aggressive cancer types are low, mainly due to therapeutic failure [15].

Instinctively, these new studies indicate that chloroquine does not increase lysosomal alkalinization in all cell types in a similar magnitude, and lysosomes may even maintain their competence (completely or not) to digest organic material, confirming that chloroquine inhibits the fusion between autophagosomes and lysosomes in a concentration-dependent way, but it does not change the lysosomal activity considerably [84, 87]. The extent of increase in lysosomal pH and how much time lysosomes demand to normalize after compound exposure can diverge a lot if we take into consideration cell specificities, doubling time, phagocyte capacity, and how efficiently the cells/lysosomes respond to the compound sequestration. In a cell point of view, autophagy responses constitute stress adaptation that can suppress apoptosis, but when autophagy is blocked either at earlier or later stages, it may lead to apoptosis as a result of the failure for adaptation to environmental changed states.

Overall, the precise mechanism by which quinines sensitizes cancer cells by PI3K-Akt or MEK/ERK inhibitors is unclear, but it is recognized that such signal pathways are overexpressed or upregulated in cancer rather than in normal cells, which opens a "window of opportunities" to design more target drugs and clinical trials based on the lysosomal blockade ability. It is very important to remember that patients with metastases present tumors with multiple molecular and cellular characteristics. Therefore, the heterogeneity of metastases, tumor advance, and cell selection becomes a common problem observed in tumor resistance during the first line chemotherapies [6]. Therefore, including sensitizers with antimutagenic action (such as chloroquine) reduces the extent of primary DNA rearrangements responsible for the appearance of mutant clones and may delay/inhibit tumor progression.

A generalized overview also emphasizes the most vulnerable issue: do the effects of aminoquinolines share a common mode of action or are they the products of a variety of distinct processes? Once their mechanisms remain uncertain, molecular and clinical lessons are indispensable to detail dose/concentration-response relationships and safety-related aspects to guide the development of new modulating autophagy therapies [30].

2.3.2. Pharmacokinetic-Related Toxicity. The most common adverse effects of chloroquine, hydroxychloroquine, amodiaquine, and other aminoquinolines in clinical use are nausea, abdominal/hypochondrial pain, changes in visual acuity (blurred vision), bitter taste in mouth, insomnia, weakness, arthralgia, back pain, pruritus (sensation of itching and stinging), diarrhea, and pale stools. Indeed, up to 50% of patients receiving hydroxychloroquine report some gastrointestinal effects. This is dose-dependent and most often occurs with loading doses >800 mg [96, 97], but 400–800 mg daily doses have been related to symptoms of psychosis, agitation, insomnia, confusion, hallucinations, paranoia, depression, catatonia, and suicides. These psychological/neurological effects may appear at any age, during acute or chronic use, and in patients with or without a history of psychiatric illness [98].

Poisoning with antimalarial drugs have also caused cardiovascular problems such as myocarditis, ventricular arrhythmias, cardiac arrest, and QTc prolongation due to the blockade of hERG potassium channels. Thereof, chloroquine, hydroxychloroquine, amodiaquine, and other derivatives should be used with caution in oncologic patients with cardiac diseases, history of ventricular arrhythmias, hypokalemia and/or hypomagnesemia, or bradycardia (˂50 bpm), and during concomitant administration of QT interval prolonging agents (e.g., macrolides and fluoroquinolones) [9, 99–101]. If cardiotoxicity is suspected, quick discontinuation of the QT interval prolonging agents may prevent life-threatening complications.

Severe hypoglycemia with the loss of consciousness in patients treated or not with antidiabetic medications have been observed [102], inspite of beneficial effects for the metabolic syndrome [103]. Therefore, patients presenting clinical symptoms of hypoglycemia during treatment should have their blood glucose checked and treatment reviewed when necessary. Additionally, rhabdomyolysis [99] and ototoxicity when they are used by pregnant women in the 3rd trimester and even irreversible deafness [104] were reported. Nonetheless, health guidelines have indicated the maintenance of treatment with hydroxychloroquine during pregnancy and breastfeeding in patients with autoimmune diseases since these aminoquinolines do not cross the placenta easily and low quantity is found in breast milk [105].

Chloroquine and hydroxychloroquine structures and modes of action are closely similar except for an additional hydroxyl moiety, which makes hydroxychloroquine less permeable to blood-retinal barrier, and it allows faster clearance from retinal pigment cell, suggesting minor risks and safer option since long-term clinical trials with hydroxychloroquine tolerates higher daily doses and revealed less drug-drug interactions [102]. Their therapeutic window is relatively narrow, and retinal damage is one of the most common side effects for long term use [106]. Around 20% of chloroquine users showed ocular injuries due to high doses and treatment frequency in 1980s [39], and, since 1974, it has been a prescribed medicine in Japan due to chloroquine-associated retinopathy [107]. Thus, ocular or color vision examinations of patients under antimalarial therapies is indispensable for the early detection of retinal toxicity at a stage in which it is still reversible once treatment is interrupted [39]. The initial development of retinal damages with a daily dose of 800 to 1200 mg of hydroxychloroquine has been detected using sensitive retinal screening tests [108].

The simultaneous use of tamoxifen—the most prescribed selective modulator of estrogen receptors to treat hormone-receptor-positive, early/advanced-stage or metastatic breast cancers after surgery to reduce the risk of recurring—with hydroxychloroquine increases the risk of eye toxicity owing to the synergistic block of lysosomal/autophagy steps in retinal epithelial cells and accumulation of potentially toxic ubiquitinated proteins [108]. Although retinopathy is more

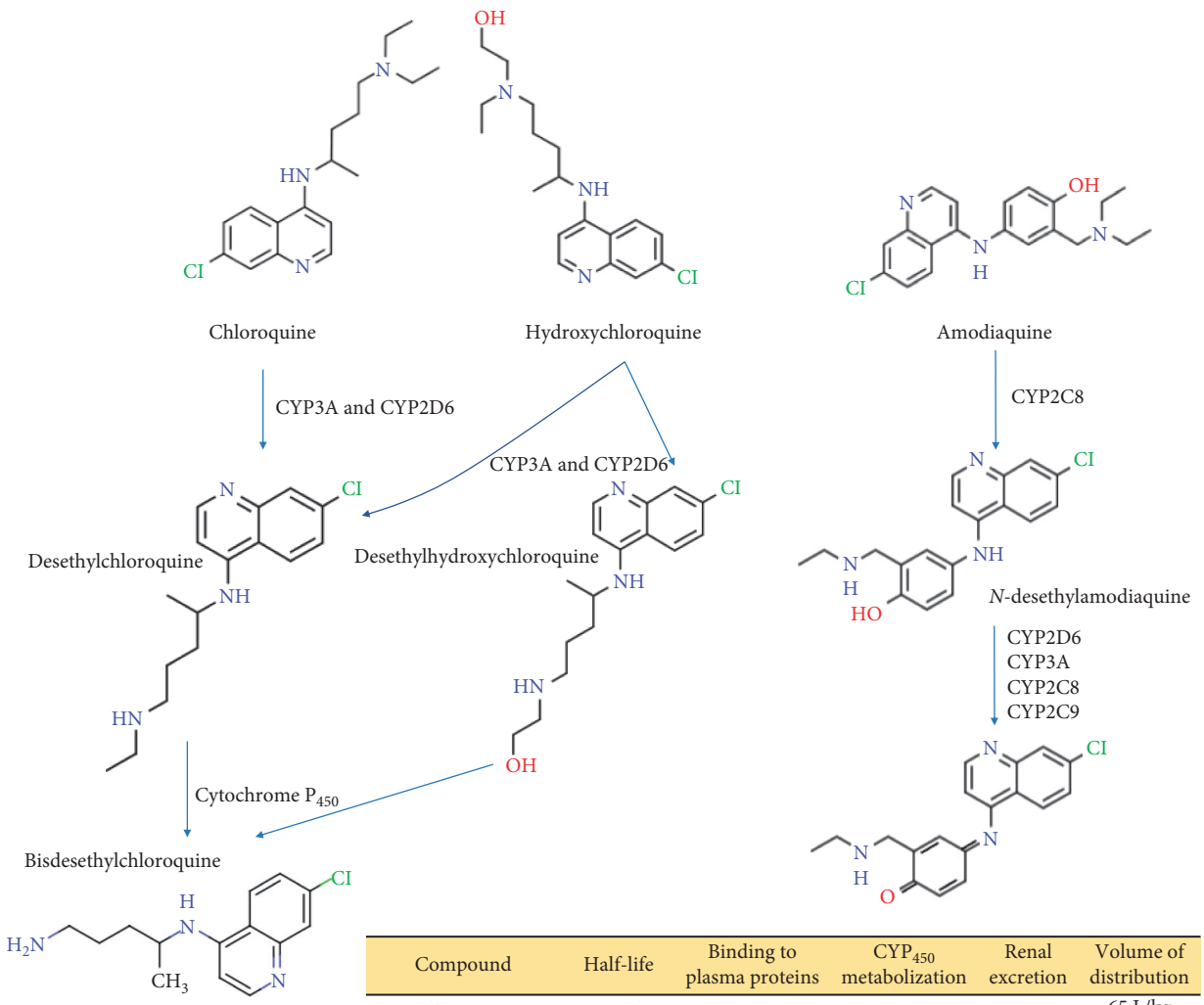

Compound	Half-life	Binding to plasma proteins	CYP_{450} metabolization	Renal excretion	Volume of distribution
Chloroquine	12-60 days	37-67 %	30-60 %	50-60 %	65 L/kg
Hydroxychloroquine	32-50 days				47.3 L/kg
Amodiaquine	5.3-7.7 h	90 %	70-80 %	20-30 %	39.2 L/kg
Primaquine	4-.7 h	45-65 %	90-99 %	0.54 %	2.9 L/kg

Figure 4: Metabolism of some aminoquinolines and pharmacokinetic features.

commonly correlated with chloroquine than with hydroxychloroquine, which might also be explained by the lower volume of distribution (Vd) for hydroxychloroquine (47.3 L) compared with chloroquine (65 L) (Figure 4). Ophthalmology guidelines have recommended comedication of tamoxifen plus hydroxychloroquine for up to 6 months, and a maximal daily dose of 5 mg/kg/day body weight of hydroxychloroquine not more than 5 years [30, 40, 106, 109].

Besides molecular similarities, chloroquine and hydroxychloroquine occur as enantiomers (R and S isomers), and *in vitro* and *in vivo* analyses have not shown important differences owing to the bioactivity [30], stereoselectivity of drug-drug interactions, and clinical consequences on toxicity due to the preferential metabolism of one enantiomer [105]. Both S(+)-chloroquine and -hydroxychloroquine present higher binding to albumin and α_1-acid glycoprotein, but hydroxychloroquine was enantioselective *in vivo* and in healthy volunteers, indicating the less protein-bound R(−)-enantiomer [110]. Then, the hydroxychloroquine binding degree to plasma proteins seems to control its distribution into cells, which can help explain how chloroquine have a larger Vd, since its R(−)-enantiomer is almost 2-fold less protein bound than the S(+)-enantiomer [105]. Notably, the S(+)-form of hydroxychloroquine is less taken up by rabbit ocular tissues [111], which suggests that the administration of the pure S(+)-enantiomer could offer better efficacy and lesser toxicity [105].

Experimental blockers such as 3-MA, bafilomycin A1, and short hairpin RNA (shRNA) knockdown of gene *Beclin* cause the deficiency of autophagy and increase tubular cell p53-dependent apoptosis during cisplatin treatment in kidney proximal tubular cells [112], supporting convincing

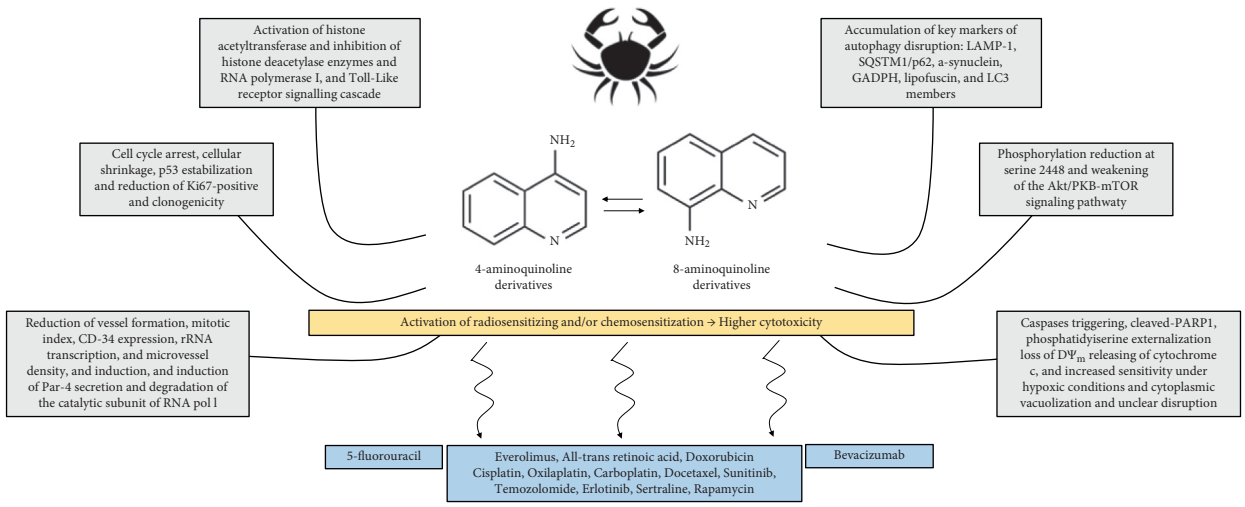

Figure 5: General properties of aminoquinolines on tumors.

data that autophagy is critical for renal cell survival. Hence, the concomitant exposure to anticancer agents and clinically available autophagy blockers (e.g., amodiaquine, primaquine, and analogues) also sensitizes normal tissues and can dramatically worsen renal function in patients with acute or chronic kidney illnesses. Under these circumstances, an impaired renal function increases the bioavailability of antimalarial drugs and comedications and the risk of adverse effects by pharmacological interactions.

In the pharmacokinetic context: (i) a single oral dose of chloroquine 300 mg can be detected in blood and urine from healthy volunteers up to 52 and 119 days postdose, respectively [113]; (ii) terminal elimination half-life of chloroquine, hydroxychloroquine, and their active metabolites (desethylchloroquine and desethylhydroxychloroquine, respectively, and finally, bisdesethyl chloroquine as a downstream metabolite of both drugs) varies from 20–60 days [30, 114]; (iii) both drugs can distribute to aqueous cellular and intercellular compartments, resulting in long mean residence times (about 1,300 h for hydroxychloroquine and 900 h for chloroquine) [114]; (iv) 30 to 50% of these antimalarial drugs are transformed by hepatic cytochromes P_{450}, mainly, CYP3A and CYP2D6 [115], and (v) about 37–67% of chloroquine/hydroxychloroquine bound to liver-derived plasma proteins [110, 116, 117]. Additionally, the half-life of amodiaquine is only 5.3–7.7 h, since it is subject to rapid first-pass metabolism and generate *N*-desethylamodiaquine, the principal route of disposition in humans, whose active metabolite has half-life >100 h and, therefore, amodiaquine can be considered a prodrug [118]. Thus, in contrast to amodiaquine, chloroquine and hydroxychloroquine are not highly bound to plasma proteins but have strong tissue binding.

It is also critical to ponder the coexistence of hepatic diseases (cancer-related or not), first pass metabolism, and comedications if the question is bioavailability or linked-side effects because elimination is significantly reduced in the presence of hepatic dysfunction, and nearly 50% of chloroquine is recovered in urine as unchanged drug. As background, a recent Brazilian study showed that the administration of hydroxychloroquine (400 mg twice daily for 7 days) without or with azithromycin (500 mg once a day for 7 days) caused a rise in liver-enzyme levels [119].

Indeed, clinical trials with anticancer purposes showed that adverse effects and toxicity of chloroquine and hydroxychloroquine are strongly dose-dependent (100–1200 mg/day). According to Common Terminology Criteria for Adverse Events version 3.0, toxicity was found with 100 to 200 mg/day [120–122]. Between 200 and 600 mg/day, the most common adverse effects were classified as grade 1 and 2, and include rash, visual blurring, sensitivity to light, nausea, diarrhea, fatigue, weight loss, vomiting, dyspepsia, anorexia, and dry skin [123–128]. The adverse effects of grade 3 or higher were detected from 600 to 1200 mg/day. Grade 4 toxicity was associated with myelosuppression at 800 mg/day of hydroxychloroquine [122]. Meanwhile, the combination of temsirolimus (25 mg/day, mTOR inhibitor) and hydroxychloroquine (200–1200 mg/day) was considered safe and tolerable, even at highest doses in patients with advanced solid tumors and melanoma [126]. Grade 2 or 3 adverse events were more common, resulting in a decrease of dosages after 2–3 months of treatment. Hydroxychloroquine and bortezomib, a proteasome inhibitor administered in patients with relapsed/refractory myeloma, cause grade 1 or 2 adverse events, mainly, but some patients experienced bone marrow suppression and grade 3 gastrointestinal toxicity [127]. At 1200 mg/day, hydroxychloroquine induced lymphopenia and an increase in serum alanine aminotransferase (grade 3/4) in patients with metastatic pancreatic cancer [128].

3. Conclusions

The mechanisms of sensitization attributed to aminoquinolines have a histological basis, but most of them are interconnected to the autophagic process. They express signals of autophagy disruption and cytotoxic-related action, including accumulation of key markers, predominantly,

LAMP1, p62/SQSTM1, LC3 members, GAPDH, beclin-1/Atg6, α-synuclein, and granules of lipofuscin.

Aminoquinolines act as lysosomal alkalinizers and take ownership during death-promoting mechanisms, which explain, at least in part, their chemotherapy and radiotherapy sensitizer effects when used as adjuvant option in clinical trials against solid tumors. They overturn lysosomal-related pathophysiological barriers, reduces uptake and drug distribution, avoid resistance, and improve cytotoxic activity response of weak-base clinical drugs, since they work as chemosensitizers under specific microenvironmental conditions, especially when acid lysosomal and inflamed tissues pH cause ion trapping and sequestering of chemotherapeutic drugs into protonated acidic endosomes. Additionally, they have also overwhelmed tumor resistance *in vivo*, suggesting that autophagy inhibition has antiangiogenic effectiveness as well. Therefore, in a mechanistic point of view, aminoquinolines induce ATM-ATR/p53/p21 signaling, caspase activation, and exhibit unspecific capacity for overlapping the apoptotic cascade to either upstream of caspase-3 activation and/or encompass nonp53/apoptotic/autophagy routes (Figure 5).

More specifically, two 4-aminoquinolines—chloroquine and hydroxychloroquine—accumulate slowly into cells and take time to develop cytotoxicity. Then, longer time exposure is believed to provide better antiproliferative effects, considering that they have a late onset but a prolonged action even after drug discontinuation. Moreover, no important differences have been found about the stereoselectivity of drug-drug interactions, clinical consequences on bioactivities, and additional pharmacokinetic-related toxicities. However, a continuous pharmacovigilance is required because these antimalarial molecules exhibit multiple cellular unspecific modes of action (undesired off-targets), relatively narrow therapeutic windows, recurrent adverse effects, and self-treatment-related poisoning. Retinopathy, mainly, has been more associated with chloroquine, and compromised renal and liver functions and increased the bioavailability of antimalarials and risk of adverse interactions. Therefore, their use must be under rigorous rules, ethical and medical prescription, and clinical and laboratory follow-ups.

Abbreviations

ATM-ATR: Ataxia telangiectasia-mutated/ataxia telangiectasia and Rad3-related kinases
Atg: Autophagy-related protein
CDK: Cyclin-dependent kinase
EGFR: Epithelial growth factor receptor
GAPDH: Glyceraldehyde 3-phosphate dehydrogenase
GRP78: Glucose regulated protein 78
LAMP1: Lysosomal associated membrane protein 1
MAPK: Mitogen-activated protein kinases, originally called ERK, extracellular signal-regulated kinases
LC3: Microtubule-associated protein 1A/1B-light chain 3
NF-κB: Factor nuclear kappa B
Par-4: Prostate apoptosis response-4
p53: Protein 53
p62: Protein 62
PARP1: Poly-(ADP-ribose)-polymerase 1
PI3K: Phosphatidylinositol 3-kinases
SQSTM1: Sequestosome 1
S6K1: p70S6 kinase1
TLR: Toll-like receptor
TKR: Tyrosine kinase receptor
UACA: Uveal autoantigen with coiled-coil domains and ankyrin repeats
Vps34: Vesicular protein sorting 34
4E-BP: 4E-binding protein
5-FU: 5-Fluorouracil
zVAD-fmk: Benzyloxycarbonyl-Val-Ala-Asp-fluoromethyl ketone.

Data Availability

The data used to support the findings of this study are cited as references.

Conflicts of Interest

The authors declare that they have no conflicts of financial interest or personal relationships that could influence this work and outcomes reported in this paper.

Authors' Contributions

PMPF planned the review and wrote about mechanisms of action and toxicokinetic findings. JROF collaborated in toxicity-related issues. DPB discussed about drug reuse with anticancer purposes. RWRS and GCGM analyzed *in vitro* mechanisms and revised the article. All authors have read and agreed to the published version of the manuscript.

Acknowledgments

Dr Paulo Michel Pinheiro Ferreira and Dr Daniel Pereira Bezerra are grateful to the public Brazilian agency "Conselho Nacional de Desenvolvimento Científico e Tecnológico" (CNPq) for their personal scholarships (303247/2019-3 and 313350/2018-3, respectively).

References

[1] M. Plummer, C. De Martel, J. Vignat, J. Ferlay, F. Bray, and S. Franceschi, "Global burden of cancers attributable to infections in 2012: a synthetic analysis," *The Lancet Global Health*, vol. 4, pp. e609–16, 2016.

[2] GBD Risk Factors Collaborators, "Global, regional, and national comparative risk assessment of 79 behavioural, environmental and occupational, and metabolic risks or clusters of risks, 1990–2015: a systematic analysis for the global burden of disease study 2015," *The Lancet*, vol. 388, pp. 1659–1724, 2016.

[3] World Health Organization (WHO), *Cancer. Fact Sheet*, World Health Organization, Geneva, Switzerland, 2018, https://www.who.int/news-room/fact-sheets/detail/cancer/.

[4] V. Srivastava, A. S. Negi, J. K. Kumar, M. M. Gupta, and S. P. S. Khanuja, "Plant-based anticancer molecules: a

chemical and biological profile of some important leads," *Bioorganic & Medicinal Chemistry*, vol. 13, no. 21, pp. 5892–5908, 2005.

[5] S. Sau, H. O. Alsaab, S. K. Kashaw, K. Tatiparti, and A. K. Iyer, "Advances in antibody-drug conjugates: a new era of targeted cancer therapy," *Drug Discovery Today*, vol. 22, no. 10, pp. 1547–1556, 2017.

[6] P. M. P. Ferreira and C. Pessoa, "Molecular biology of human epidermal receptors, signaling pathways and targeted therapy against cancers: new evidences and old challenges," *Brazilian Journal of Pharmaceutical Sciences*.vol. 53, pp. 1–17, 2017.

[7] V. Ferrari and D. J. Cutler, "Uptake of chloroquine by human erythrocytes," *Biochemical Pharmacology*, vol. 39, no. 4, pp. 753–762, 1990.

[8] M. A. Travassos and M. K. Laufer, "Resistance to antimalarial drugs: molecular, pharmacologic, and clinical considerations," *Pediatric Research*, vol. 65, pp. 64–70, 2019.

[9] S. D'Alessandro, D. Scaccabarozzi, L. Signorini et al., "The use of antimalarial drugs against viral infection," *Microorganisms*, vol. 8, p. 85, 2020.

[10] C. Huang, Y. Wang, X. Li et al., "Clinical features of patients infected with 2019 novel coronavirus in Wuhan, China," *The Lancet*, vol. 395, pp. 497–506, Article ID 10223, 2020.

[11] S. Arshad, P. Kilgore, Z. S. Chaudhry et al., "Treatment with hydroxychloroquine, azithromycin, and combination in patients hospitalized with COVID-19," *International Journal of Infectious Diseases*, vol. 97, pp. 396–403, 2020.

[12] Z. Wang, Q. Wang, T. He et al., "The combination of artesunate and carboplatin exerts a synergistic anti-tumour effect on non-small cell lung cancer," *Clinical and Experimental Pharmacology and Physiology*, vol. 47, no. 6, pp. 1083–1091, 2020.

[13] F. Pammolli, L. Magazzini, and M. Riccaboni, "The productivity crisis in pharmaceutical R&D," *Nature Reviews Drug Discovery*, vol. 10, no. 6, pp. 428–438, 2011.

[14] A. S. Brown and C. J. Patel, "A standard database for drug repositioning," *Scientific Data*, vol. 4, Article ID 170029, 2017.

[15] C. Mottini, F. Napolitano, Z. Li, X. Gao, and L. Cardone, "Computer-aided drug repurposing for cancer therapy: approaches and opportunities to challenge anticancer targets," *Seminars in Cancer Biology*, vol. 68, pp. 59–74, 2019.

[16] P. M. P. Ferreira, P. M. D. Costa, A. D. M. Costa et al., "Cytotoxic and toxicological effects of phthalimide derivatives on tumor and normal murine cells," *Anais da Academia Brasileira de Ciências*, vol. 87, no. 1, pp. 313–330, 2015.

[17] M. M. Kian, A. Haghi, M. Salami et al., "Arsenic trioxide and thalidomide combination induce autophagy along with apoptosis in acute myeloid cell lines," *Cell Journal*, vol. 22, pp. 193–202, 2020.

[18] F. Jiang, H. S. Xing, W. Y. Chen et al., "Itraconazole inhibits proliferation of pancreatic cancer cells through activation of Bak-1," *Journal of Cellular Biochemistry*, vol. 120, no. 3, pp. 4333–4341, 2019.

[19] T. Sun, W. Yang, S. M. Toprani et al., "Induction of immunogenic cell death in radiation-resistant breast cancer stem cells by repurposing anti-alcoholism drug disulfiram," *Cell Communication and Signaling*, vol. 18, no. 1, p. 36, 2020.

[20] C. Xia, R. Chen, J. Chen et al., "Combining metformin and nelfinavir exhibits synergistic effects against the growth of human cervical cancer cells and xenograft in nude mice," *Scientific Reports*, vol. 7, Article ID 43373, 2017.

[21] A. Das, D. Durrant, C. Mitchell, P. Dent, S. K. Batra, and R. C. Kukreja, "Sildenafil (Viagra) sensitizes prostate cancer cells to doxorubicin-mediated apoptosis through CD95," *Oncotarget*, vol. 7, no. 4, pp. 4399–4413, 2016.

[22] L. K. Rushworth, K. Hewit, S. Munnings-Tomes et al., "Repurposing screen identifies mebendazole as a clinical candidate to synergise with docetaxel for prostate cancer treatment," *British Journal of Cancer*, vol. 122, no. 4, pp. 517–527, 2020.

[23] F. Yuan, C. Cheng, F. Xiao, H. Liu, S. Cao, and G. Zhou, "Inhibition of mTORC1/P70S6K pathway by metformin synergistically sensitizes acute myeloid leukemia to Ara-C," *Life Sciences*, vol. 243, Article ID 117276, 2020.

[24] J. Sun, J. Piao, N. Li, Y. Yang, K.-Y. Kim, and Z. Lin, "Valproic acid targets HDAC1/2 and HDAC1/PTEN/Akt signalling to inhibit cell proliferation via the induction of autophagy in gastric cancer," *FEBS Journal*, vol. 287, 2019.

[25] J. P. Gil and S. Krishna, "Pfmdr1 (*Plasmodium falciparum* multidrug drug resistance gene 1): a pivotal factor in malaria resistance to artemisinin combination therapies," *Expert Review of Anti-infective Therapy*, vol. 15, no. 6, pp. 527–543, 2017.

[26] E. G. Tse, M. Korsik, and M. H. Todd, "The past, present and future of anti-malarial medicines," *Malaria Journal*, vol. 18, p. 93, 2019.

[27] World Health Organization (WHO), *World Health Organization Model List of Essential Medicines: 21st List*, World Health Organization, Geneva, Switzerland, 2019, https://apps.who.int/iris/handle/10665/325771/.

[28] D. J. Wallace, M. Linker-Israeli, S. Hyun, J. R. Klinenberg, and V. Stecher, "The effect of hydroxychloroquine therapy on serum levels of immunoregulatory molecules in patients with systemic lupus erythematosus," *Journal of Rheumatology*, vol. 21, pp. 375-376, 1994.

[29] I. Ben-Zvi, S. Kivity, P. Langevitz, and Y. Shoenfeld, "Hydroxychloroquine: from malaria to autoimmunity," *Clinical Reviews in Allergy and Immunology*, vol. 42, no. 2, pp. 145–153, 2012.

[30] E. Schrezenmeier and T. Dörner, "Mechanisms of action of hydroxychloroquine and chloroquine: implications for rheumatology," *Nature Reviews Rheumatology*, vol. 16, no. 3, pp. 155–166, 2020.

[31] S. Ohkuma and B. Poole, "Fluorescence probe measurement of the intralysosomal pH in living cells and the perturbation of pH by various agents," *Proceedings of the National Academy of Sciences*, vol. 75, no. 7, pp. 3327–3331, 1978.

[32] S. Wunsch, C. P. Sanchez, M. Gekle, L. Große-Wortmann, J. Wiesner, and M. Lanzer, "Differential stimulation of the Na^+/H^+ exchanger determines chloroquine uptake in *Plasmodium falciparum*," *Journal of Cell Biology*, vol. 140, no. 2, pp. 335–345, 1998.

[33] M. Wibo and B. Poole, "Protein degradation in cultured cells. II. The uptake of chloroquine by rat fibroblasts and the inhibition of cellular protein degradation and cathepsin B1," *Journal of Cell Biology*, vol. 63, no. 2, pp. 430–440, 1974.

[34] V. B. Randolph, G. Winkle, and V. Stollar, "Acidotropic amines inhibit proteolytic processing of flavivirus prM protein," *Virology*, vol. 174, no. 2, pp. 450–458, 1990.

[35] A. Savarino, J. R. Boelaert, A. Cassone, G. Majori, and R. Cauda, "Effects of chloroquine on viral infections: an old drug against today's diseases?" *The Lancet Infectious Diseases*, vol. 3, no. 11, pp. 722–727, 2003.

[36] P. Boya, R.-A. Gonzalez-Polo, D. Poncet et al., "Mitochondrial membrane permeabilization is a critical step of

lysosome-initiated apoptosis induced by hydroxychloroquine," *Oncogene*, vol. 22, no. 25, pp. 3927–3936, 2003.

[37] Y. Geng, L. Kohli, B. J. Klocke, and K. A. Roth, "Chloroquine-induced autophagic vacuole accumulation and cell death in glioma cells is p53 independent," *Neuro-Oncology*, vol. 12, pp. 473–481, 2010.

[38] J. A. Ratikan, J. W. Sayre, and D. Schaue, "Chloroquine engages the immune system to eradicate irradiated breast tumors in mice," *International Journal of Radiation Oncology, Biology, Physics*, vol. 87, no. 4, pp. 761–768, 2013.

[39] R. Thomé, S. C. P. Lopes, F. T. M. Costa, and L. Verinaud, "Chloroquine: modes of action of an undervalued drug," *Immunology Letters*, vol. 153, no. 1-2, pp. 50–57, 2013.

[40] Y. H. Yoon, K. S. Cho, J. J. Hwang, S.-J. Lee, J. A. Choi, and J.-Y. Koh, "Induction of lysosomal dilatation, arrested autophagy, and cell death by chloroquine in cultured ARPE-19 cells," *Investigative Opthalmology & Visual Science*, vol. 51, no. 11, pp. 6030–6037, 2010.

[41] V. R. Silva, S. P. Neves, L. D. S. Santos, R. B. Dias, and D. P. Bezerra, "Challenges and therapeutic opportunities of autophagy in cancer therapy," *Cancers*, vol. 12, no. 11, p. 3461, 2020.

[42] P. M. P. Ferreira, R. W. R. Sousa, J. R. O. Ferreira, G. C. G. Militão, and D. P. Bezerra, "Chloroquine and hydroxychloroquine in antitumor therapies based on autophagy-related mechanisms," *Pharmacological Research*, vol. 168, 2021.

[43] E. L. Kim, R. Wüstenberg, A. Rübsam et al., "Chloroquine activates the p53 pathway and induces apoptosis in human glioma cells," *Neuro-Oncology*, vol. 12, no. 4, pp. 389–400, 2010.

[44] A. U. Zaidi, J. S. McDonough, B. J. Klocke et al., "Chloroquine-induced neuronal cell death is p53 and Bcl-2 family-dependent but caspase-independent," *Journal of Neuropathology & Experimental Neurology*, vol. 60, no. 10, pp. 937–945, 2001.

[45] P. M. P. Ferreira, L. A. R. L. Rodrigues, L. P. D. A. Carnib et al., "Cruciferous vegetables as antioxidative, chemopreventive and antineoplastic functional foods: preclinical and clinical evidences of sulforaphane against prostate cancers," *Current Pharmaceutical Design*, vol. 24, no. 40, pp. 4779–4793, 2019.

[46] C. R. Loehberg, T. Thompson, M. B. Kastan et al., "Ataxia telangiectasia-mutated and p53 are potential mediators of chloroquine-induced resistance to mammary carcinogenesis," *Cancer Research*, vol. 67, no. 24, pp. 12026–12033, 2007.

[47] K. H. Maclean, F. C. Dorsey, J. L. Cleveland, and M. B. Kastan, "Targeting lysosomal degradation induces p53-dependent cell death and prevents cancer in mouse models of lymphomagenesis," *Journal of Clinical Investigation*, vol. 118, no. 1, pp. 79–88, 2008.

[48] C. R. Loehberg, P. L. Strissel, R. Dittrich et al., "Akt and p53 are potential mediators of reduced mammary tumor growth by chloroquine and the mTOR inhibitor RAD001," *Biochemical Pharmacology*, vol. 83, no. 4, pp. 480–488, 2012.

[49] J. A. Espinoza, A. Zisi, D. C. Kanellis et al., "The antimalarial drug amodiaquine stabilizes p53 through ribosome biogenesis stress, independently of its autophagy-inhibitory activity," *Cell Death & Differentiation*, vol. 27, no. 2, pp. 773–789, 2020.

[50] C. Hu, V. R. Solomon, G. Ulibarri, and H. Lee, "The efficacy and selectivity of tumor cell killing by Akt inhibitors are substantially increased by chloroquine," *Bioorganic & Medicinal Chemistry*, vol. 16, no. 17, pp. 7888–7893, 2008.

[51] R. Rahim and J. S. Strobl, "Hydroxychloroquine, chloroquine, and all-trans retinoic acid regulate growth, survival, and histone acetylation in breast cancer cells," *Anti-Cancer Drugs*, vol. 20, no. 8, pp. 736–745, 2009.

[52] K. Sasaki, N. H. Tsuno, E. Sunami et al., "Chloroquine potentiates the anti-cancer effect of 5-fluorouracil on colon cancer cells," *BMC Cancer*, vol. 10, no. 1, p. 370, 2010.

[53] P. Maycotte, S. Aryal, C. T. Cummings, J. Thorburn, M. J. Morgan, and A. Thorburn, "Chloroquine sensitizes breast cancer cells to chemotherapy independent of autophagy," *Autophagy*, vol. 8, no. 2, pp. 200–212, 2012.

[54] R. M. Gonçalves, J. P. Agnes, M. Delgobo et al., "Late autophagy inhibitor chloroquine improves efficacy of the histone deacetylase inhibitor SAHA and temozolomide in gliomas," *Biochemical Pharmacology*, vol. 163, pp. 440–450, 2019.

[55] Y. Xu, H. Yu, H. Qin et al., "Inhibition of autophagy enhances cisplatin cytotoxicity through endoplasmic reticulum stress in human cervical cancer cells," *Cancer Letters*, vol. 314, no. 2, pp. 232–243, 2012.

[56] X. Jiang, W. Lu, X. Shen et al. "Repurposing sertraline sensitizes non-small cell lung cancer cells to erlotinib by inducing autophagy," *JCI Insight*, vol. 3, no. 1, Article ID e98921, 2018.

[57] S. Qiao, S. Tao, M. Rojo de la Vega et al., "The antimalarial amodiaquine causes autophagic-lysosomal and proliferative blockade sensitizing human melanoma cells to starvation- and chemotherapy-induced cell death," *Autophagy*, vol. 9, no. 12, pp. 2087–2102, 2013.

[58] M. Selvakumaran, R. K. Amaravadi, I. A. Vasilevskaya, and P. J. O'Dwyer, "Autophagy inhibition sensitizes colon cancer cells to antiangiogenic and cytotoxic therapy," *Clinical Cancer Research*, vol. 19, no. 11, pp. 2995–3007, 2013.

[59] A. K. Abdel-Aziz, S. Shouman, E. El-Demerdash, M. Elgendy, and A. B. Abdel-Naim, "Chloroquine synergizes sunitinib cytotoxicity via modulating autophagic, apoptotic and angiogenic machineries," *Chemico-Biological Interactions*, vol. 217, pp. 28–40, 2014.

[60] A. Zanotto-Filho, E. Braganhol, K. Klafke et al., "Autophagy inhibition improves the efficacy of curcumin/temozolomide combination therapy in glioblastomas," *Cancer Letters*, vol. 358, no. 2, pp. 220–231, 2015.

[61] X. Hou, C. Yang, L. Zhang et al., "Killing colon cancer cells through PCD pathways by a novel hyaluronic acid-modified shell-core nanoparticle loaded with RIP3 in combination with chloroquine," *Biomaterials*, vol. 124, pp. 195–210, 2017.

[62] H. Huang, J. Song, Z. Liu, L. Pan, and G. Xu, "Autophagy activation promotes bevacizumab resistance in glioblastoma by suppressing Akt/mTOR signaling pathway," *Oncology Letters*, vol. 15, no. 2, pp. 1487–1494, 2018.

[63] D. Wang, J. Huang, X. Wang, Y. Yu, H. Zhang, Y. Chen et al., "The eradication of breast cancer cells and stem cells by 8-hydroxyquinoline-loaded hyaluronan modified mesoporous silica nanoparticle-supported lipid bilayers containing docetaxel," *Biomaterials*, vol. 34, no. 31, pp. 7662–7673, 2013.

[64] K. Wang, X. Wang, Y. Hou, H. Zhou, K. Mai, and G. He, "Apoptosis of cancer cells is triggered by selective cross-linking and inhibition of receptor tyrosine kinases," *Communications Biology*, vol. 2, no. 1, p. 231, 2019.

[65] S. M. Weber, J.-M. Chen, and S. M. Levitz, "Inhibition of mitogen-activated protein kinase signaling by chloroquine," *The Journal of Immunology*, vol. 168, no. 10, pp. 5303–5309, 2002.

[66] S. R. Yoshii and N. Mizushima, "Monitoring and measuring autophagy," *International Journal of Molecular Sciences*, vol. 18, no. 9, p. 1865, 2017.

[67] B. Pasquier, "Autophagy inhibitors," *Cellular and Molecular Life Sciences*, vol. 73, no. 5, pp. 985–1001, 2016.

[68] Y.-T. Wu, H.-L. Tan, G. Shui et al., "Dual role of 3-methyladenine in modulation of autophagy via different temporal patterns of inhibition on class I and III phosphoinositide 3-kinase," *Journal of Biological Chemistry*, vol. 285, no. 14, pp. 10850–10861, 2010.

[69] S. Christensen, B. Van der Roest, N. Besselink et al., "5-Fluorouracil treatment induces characteristic T>G mutations in human cancer," *Nature Communications*, vol. 10, no. 1, p. 4571, 2019.

[70] L. Sun, H. Wang, Z. Wang et al., "Mixed lineage kinase domain-like protein mediates necrosis signaling downstream of RIP3 kinase," *Cell*, vol. 148, no. 1-2, pp. 213–227, 2012.

[71] W. Chen, Z. Zhou, L. Li et al., "Diverse sequence determinants control human and mouse receptor interacting protein 3 (RIP3) and mixed lineage kinase domain-like (MLKL) interaction in necroptotic signaling," *Journal of Biological Chemistry*, vol. 288, no. 23, pp. 16247–16261, 2013.

[72] T. A. Sohn, R. Bansal, G. H. Su, K. M. Murphy, and S. E. Kern, "High-throughput measurement of the TP53 response to anticancer drugs and random compounds using a stably integrated TP53-responsive luciferase reporter," *Carcinogenesis*, vol. 23, no. 6, pp. 949–958, 2002.

[73] E. Calo, R. A. Flynn, L. Martin, R. C. Spitale, H. Y. Chang, and J. Wysocka, "RNA helicase DDX21 coordinates transcription and ribosomal RNA processing," *Nature*, vol. 518, no. 7538, pp. 249–253, 2015.

[74] Q. Zhou, M. A. McCracken, and J. S. Strobl, "Control of mammary tumor cell growth *in vitro* by novel cell differentiation and apoptosis agents," *Breast Cancer Research and Treatment*, vol. 75, no. 2, pp. 107–117, 2002.

[75] Z. K. Melkoumian, A. R. Martirosyan, and J. S. Strobl, "Myc protein is differentially sensitive to quinidine in tumor versus immortalized breast epithelial cell lines," *International Journal of Cancer*, vol. 102, no. 1, pp. 60–69, 2002.

[76] A. R. Martirosyan, R. Rahim-Bata, A. B. Freeman, C. D. Clarke, R. L. Howard, and J. S. Strobl, "Differentiation-inducing quinolines as experimental breast cancer agents in the MCF-7 human breast cancer model," *Biochemical Pharmacology*, vol. 68, no. 9, pp. 1729–1738, 2004.

[77] Q. Zhou, Z. K. Melkoumian, A. Lucktong, M. Moniwa, J. R. Davie, and J. S. Strobl, "Rapid induction of histone hyperacetylation and cellular differentiation in human breast tumor cell lines following degradation of histone deacetylase-1," *Journal of Biological Chemistry*, vol. 275, no. 45, pp. 35256–35263, 2000.

[78] G. Das, B. V. Shravage, and E. H. Baehrecke, "Regulation and function of autophagy during cell survival and cell death," *Cold Spring Harbor Perspectives in Biology*, vol. 4, Article ID 008813, 2012.

[79] R. Ciuffa, T. Lamark, A. K. Tarafder et al., "The selective autophagy receptor p62 forms a flexible filamentous helical scaffold," *Cell Reports*, vol. 11, no. 5, pp. 748–758, 2015.

[80] C. Fan, W. Wang, B. Zhao, S. Zhang, and J. Miao, "Chloroquine inhibits cell growth and induces cell death in A549 lung cancer cells," *Bioorganic & Medicinal Chemistry*, vol. 14, no. 9, pp. 3218–3222, 2006.

[81] S. Choi, Y. Choi, N. T. Dat, C. Hwangbo, J. J. Lee, and J.-H. Lee, "Tephrosin induces internalization and degradation of EGFR and ErbB2 in HT-29 human colon cancer cells," *Cancer Letters*, vol. 293, no. 1, pp. 23–30, 2010.

[82] C. M. Cabello, S. D. Lamore, W. B. Bair et al., "The redox antimalarial dihydroartemisinin targets human metastatic melanoma cells but not primary melanocytes with induction of NOXA-dependent apoptosis," *Investigational New Drugs*, vol. 30, no. 4, pp. 1289–1301, 2012.

[83] C. Obua, L. L. Gustafsson, C. Aguttu et al., "Improved efficacy with amodiaquine instead of chloroquine in sulfadoxine/pyrimethamine combination treatment of falciparum malaria in Uganda: experience with fixed-dose formulation," *Acta Tropica*, vol. 100, no. 1-2, pp. 142–150, 2006.

[84] S. Lu, T. Sung, N. Lin, R. T. Abraham, and B. A. Jessen, "Lysosomal adaptation: how cells respond to lysosomotropic compounds," *PLoS One*, vol. 12, no. 3, Article ID e0173771, 2017.

[85] A. S. Chauhan, M. Kumar, S. Chaudhary et al., "Trafficking of a multifunctional protein by endosomal microautophagy: linking two independent unconventional secretory pathways," *The FASEB Journal*, vol. 33, no. 4, pp. 5626–5640, 2019.

[86] P. Rawat, S. Kumar, N. Sheokand, C. I. Raje, and M. Raje, "The multifunctional glycolytic protein glyceraldehyde-3-phosphate dehydrogenase (GAPDH) is a novel macrophage lactoferrin receptor," *Biochemistry and Cell Biology*, vol. 90, no. 3, pp. 329–338, 2012.

[87] M. Mauthe, I. Orhon, C. Rocchi et al., "Chloroquine inhibits autophagic flux by decreasing autophagosome-lysosome fusion," *Autophagy*, vol. 14, no. 8, pp. 1435–1455, 2018.

[88] R. Burikhanov, N. Hebbar, S. K. Noothi et al., "Chloroquine-inducible Par-4 secretion is essential for tumor cell apoptosis and inhibition of metastasis," *Cell Reports*, vol. 18, no. 2, pp. 508–519, 2017.

[89] K. Kim, P. Araujo, N. Hebbar et al., "Development of a novel prostate apoptosis response-4 (Par-4) protein entity with an extended duration of action for therapeutic treatment of cancer," *Protein Engineering Design and Selection*, vol. 32, no. 3, pp. 159–166, 2019.

[90] Y. Zhao, R. Burikhanov, J. Brandon et al., "Systemic Par-4 inhibits non-autochthonous tumor growth," *Cancer Biology & Therapy*, vol. 12, no. 2, pp. 152–157, 2011.

[91] R. Burikhanov, T. Shrestha-Bhattarai, S. Qiu et al., "Novel mechanism of apoptosis resistance in cancer mediated by extracellular PAR-4," *Cancer Research*, vol. 73, no. 2, pp. 1011–1019, 2013.

[92] M. L. Goodall, T. Wang, K. R. Martin et al., "Development of potent autophagy inhibitors that sensitize oncogenic BRAF V600E mutant melanoma tumor cells to vemurafenib," *Autophagy*, vol. 10, no. 6, pp. 1120–1136, 2014.

[93] S. Nadanaciva, S. Lu, D. F. Gebhard, B. A. Jessen, W. D. Pennie, and Y. Will, "A high content screening assay for identifying lysosomotropic compounds," *Toxicology in Vitro*, vol. 25, no. 3, pp. 715–723, 2011.

[94] R. Logan, A. C. Kong, E. Axcell, and J. P. Krise, "Amine-containing molecules and the induction of an expanded lysosomal volume phenotype: a structure-activity relationship study," *Journal of Pharmaceutical Sciences*, vol. 103, no. 5, pp. 1572–1580, 2014.

[95] A. R. Choi, J. H. Kim, Y. H. Woo, H. S. Kim, and S. Yoon, "Anti-malarial drugs primaquine and chloroquine have different sensitization effects with anti-mitotic drugs in resistant cancer cells," *Anticancer Research*, vol. 36, no. 4, pp. 1641–1648, 2016.

[96] C. B. Braga, A. C. Martins, A. D. Cayotopa et al., "Side effects of chloroquine and primaquine and symptom reduction in malaria endemic area (Mâncio Lima, Acre, Brazil)," *Interdisciplinary Perspectives on Infectious Diseases*, vol. 2015, Article ID 346853, 7 pages, 2015.

[97] A. Srinivasa, S. Tosounidou, and C. Gordon, "Increased incidence of gastrointestinal side effects in patients taking hydroxychloroquine: a brand-related issue?" *Journal of Rheumatology*, vol. 44, p. 398, 2017.

[98] Spanish Agency of Drug and Health Products and Ministry of Health, "Chloroquine/hydroxychloroquine: precautions and vigilance of possible adverse reactions in patients with COVID-19," 2020, http://www.aemps.gob.es.

[99] M. G. S. Borba, F. F. A. Val, V. S. Sampaio et al., "Effect of high vs. low doses of chloroquine diphosphate as adjunctive therapy for patients hospitalized with severe acute respiratory syndrome coronavirus 2 (SARS-CoV-2) infection: a randomized clinical trial," *JAMA Network Open*, vol. 3, no. 4, Article ID e208857, 2020.

[100] J. M. Molina, C. Delaugerre, J. L. Goff et al., "No evidence of rapid antiviral clearance or clinical benefit with the combination of hydroxychloroquine and azithromycin in patients with severe COVID-19 infection," *Medecine et Maladies Infectieuses*, vol. 50, no. 4, p. 384, 2020.

[101] E. S. Rosenberg, E. M. Dufort, T. Udo et al., "Association of treatment with hydroxychloroquine or azithromycin with in-hospital mortality in patients with COVID-19 in New York state," *Journal of the American Medical Association*, vol. 323, no. 24, pp. 2493–2502, 2020.

[102] A. K. Singh, A. Singh, A. Shaikh, R. Singh, and A. Misra, "Chloroquine and hydroxychloroquine in the treatment of COVID-19 with or without diabetes: a systematic search and a narrative review with a special reference to India and other developing countries," *Diabetes & Metabolic Syndrome: Clinical Research Reviews*, vol. 14, no. 3, pp. 241–246, 2020.

[103] C. Rempenault, B. Combe, T. Barnetche et al., "Metabolic and cardiovascular benefits of hydroxychloroquine in patients with rheumatoid arthritis: a systematic review and meta-analysis," *Annals of the Rheumatic Diseases*, vol. 77, no. 1, pp. 98–103, 2018.

[104] M. C. Figueiredo, C. C. C. T. Atherino, C. V. Monteiro, and R. A. Levy, "Antimaláricos e Ototoxicidade," *Revista Brasileira de Reumatologia*, vol. 44, no. 3, pp. 212–214, 2004.

[105] J. Ducharme and R. Farinotti, "Clinical pharmacokinetics and metabolism of chloroquine. Focus on recent advancements," *Clinical Pharmacokinetics*, vol. 31, no. 4, pp. 257–274, 1996.

[106] A. Jorge, C. Ung, L. H. Young, R. B. Melles, and H. K. Choi, "Hydroxychloroquine retinopathy—implications of research advances for rheumatology care," *Nature Reviews. Rheumatology*, vol. 14, pp. 693–703, 2018.

[107] Y. Momose, S. Arai, H. Eto, M. Kishimoto, and M. Okada, "Experience with the use of hydroxychloroquine for the treatment of lupus erythematosus," *The Journal of Dermatology*, vol. 40, no. 2, pp. 94–97, 2013.

[108] L. S. Leung, J. W. Neal, H. A. Wakelee, L. V. Sequist, and M. F. Marmor, "Rapid onset of retinal toxicity from high-dose hydroxychloroquine given for cancer therapy," *American Journal of Ophthalmology*, vol. 160, pp. 799–805, 2015.

[109] M. F. Marmor, U. Kellner, T. Y. Y. Lai, R. B. Melles, and W. F. Mieler, "American academy of ophthalmology. recommendations on screening for chloroquine and hydroxychloroquine retinopathy (2016 revision)," *Ophthalmology*, vol. 123, no. 6, pp. 1386–1394, 2016.

[110] A. J. McLachlan, D. J. Cutler, and S. E. Tett, "Plasma protein binding of the enantiomers of hydroxychloroquine and metabolites," *European Journal of Clinical Pharmacology*, vol. 44, pp. 481–484, 1993.

[111] I. W. Wainer, J. C. Chen, H. Parenteau et al., "Distribution of the enantiomers of hydroxychloroquine and its metabolites in ocular tissues of the rabbit after oral administration of racemic hydroxychloroquine," *Chirality*, vol. 6, no. 4, pp. 347–354, 1994.

[112] S. Periyasamy-Thandavan, M. Jiang, Q. Wei, R. Smith, X.-M. Yin, and Z. Dong, "Autophagy is cytoprotective during cisplatin injury of renal proximal tubular cells," *Kidney International*, vol. 74, no. 5, pp. 631–640, 2008.

[113] L. L. Gustafsson, O. Walker, G. Alván et al., "Disposition of chloroquine in man after single intravenous and oral doses," *British Journal of Clinical Pharmacology*, vol. 15, no. 4, pp. 471–479, 1983.

[114] D. J. Cutler, A. C. MacIntyre, and S. E. Tett, "Pharmacokinetics and cellular uptake of 4-aminoquinoline antimalarials," *Basis for Variability of Response to Anti-Rheumatic Drugs*, vol. 24, pp. 142–157, 1988.

[115] K. P. Collins, K. M. Jackson, and D. L. Gustafson, "Hydroxychloroquine: a physiologically-based pharmacokinetic model in the context of cancer-related autophagy modulation," *Journal of Pharmacology and Experimental Therapeutics*, vol. 365, no. 3, pp. 447–459, 2018.

[116] O. Walker, D. J. Birkett, G. Alván, L. Gustafsson, and F. Sjoqvist, "Characterization of chloroquine plasma protein binding in man," *British Journal of Clinical Pharmacology*, vol. 15, no. 3, pp. 375–377, 1983.

[117] B. R. Moore, M. Page-Sharp, J. R. Stoney, K. F. Ilett, J. D. Jago, and K. T. Batty, "Pharmacokinetics, pharmacodynamics, and allometric scaling of chloroquine in a murine malaria model," *Antimicrobial Agents and Chemotherapy*, vol. 55, no. 8, pp. 3899–3907, 2011.

[118] S. L. Rawe and C. McDonnell, "The cinchona alkaloids and the aminoquinolines," in *Antimalarial Agents—Design and Mechanism of Action*, G. L. Patrick, Ed., Elsevier, Amsterdam, Netherlands, pp. 65–98, 2020.

[119] A. B. Cavalcanti, F. G. Zampieri, R. G. Rosa et al., "Hydroxychloroquine with or without azithromycin in mild-to-moderate COVID-19," *New England Journal of Medicine*, vol. 383, no. 21, 2020.

[120] J. Sotelo, E. Briceño, and M. A. López-González, "Adding chloroquine to conventional treatment for glioblastoma multiforme: a randomized, double-blind, placebo-controlled trial," *Annals of Internal Medicine*, vol. 144, no. 5, pp. 337–343, 2006.

[121] L. L. Rojas-Puentes, M. Gonzalez-Pinedo, A. Crismatt et al., "Phase II randomized, double-blind, placebo-controlled study of whole-brain irradiation with concomitant chloroquine for brain metastases," *Radiation Oncology*, vol. 8, no. 1, p. 209, 2013.

[122] M. R. Rosenfeld, X. Ye, J. G. Supko et al., "A phase I/II trial of hydroxychloroquine in conjunction with radiation therapy and concurrent and adjuvant temozolomide in patients with newly diagnosed glioblastoma multiforme," *Autophagy*, vol. 10, no. 8, pp. 1359–1368, 2014.

[123] S. B. Goldberg, J. G. Supko, J. W. Neal et al., "A phase I study of erlotinib and hydroxychloroquine in advanced non-small-cell lung cancer," *Journal of Thoracic Oncology*, vol. 7, no. 10, pp. 1602–1608, 2012.

[124] D. Mahalingam, M. Mita, J. Sarantopoulos et al., "Combined autophagy and HDAC inhibition: a phase I safety, tolerability, pharmacokinetic, and pharmacodynamic analysis of hydroxychloroquine in combination with the HDAC inhibitor vorinostat in patients with advanced solid tumors," *Autophagy*, vol. 10, no. 8, pp. 1403–1414, 2014.

[125] A. Arnaout, S. J. Robertson, G. R. Pond et al., "A randomized, double-blind, window of opportunity trial evaluating the effects of chloroquine in breast cancer patients," *Breast Cancer Research and Treatment*, vol. 178, no. 2, pp. 327–335, 2019.

[126] R. Rangwala, Y. C. Chang, J. Hu et al., "Combined MTOR and autophagy inhibition: phase I trial of hydroxychloroquine and temsirolimus in patients with advanced solid tumors and melanoma," *Autophagy*, vol. 10, no. 8, pp. 1391–1402, 2014.

[127] D. T. Vogl, E. A. Stadtmauer, K.-S. Tan et al., "Combined autophagy and proteasome inhibition: a phase 1 trial of hydroxychloroquine and bortezomib in patients with relapsed/refractory myeloma," *Autophagy*, vol. 10, no. 8, pp. 1380–1390, 2014.

[128] B. M. Wolpin, D. A. Rubinson, X. Wang et al., "Phase II and pharmacodynamic study of autophagy inhibition using hydroxychloroquine in patients with metastatic pancreatic adenocarcinoma," *The Oncologist*, vol. 19, no. 6, pp. 637-638, 2014.